

Modeling of the Midpalatal Suture during Maxillary Expansion Treatment
and its Implications towards Appliance Design

by

Daniel Logan Romanyk

A thesis submitted in partial fulfillment of the requirements for the degree of

Doctor of Philosophy

Department of Mechanical Engineering
University of Alberta

© Daniel Logan Romanyk, 2014

Abstract

Widening the maxilla, or upper jaw, is a common treatment in orthodontics used to generate additional room in the correction of tooth misalignments. Expansion is achieved through activation of an appliance inserted in the patients' upper jaw. Currently, appliances utilizing expansion screws, spring, magnets, or shape memory alloys are being used by clinicians. The unfused midpalatal suture, soft connective tissue between maxillary bones, is also widened during this procedure. In the literature concerning this treatment and its impact on patient response, little has been done to consider the suture's viscoelastic properties. Development of a viscoelastic model would allow for accurate prediction of suture response to the various expansion appliances and aid in guiding future appliance design and treatment protocols.

In the presented thesis research, complete viscoelastic creep-relaxation models are developed for the unfused midpalatal suture. First, nonlinear creep-strain models are established based on experimental data from the rabbit midsagittal suture. Then, interrelation techniques are utilized to generate subsequent stress-relaxation relations based on the previously obtained creep-strain constants. Development of an overall creep-relaxation model allows for prediction of suture response to expansion appliances that exert a constant or decaying force (springs, magnets, shape memory alloys) as well as step-wise increases in displacement (expansion screws).

In using developed creep-relaxation models to simulate the suture's response to expansion appliances, several key observations were made. In

regards to screw-activated appliances, it was found that stresses resulting from a single step-wise activation likely would not generate tissue failure; however, as few as two or three rapid activations may certainly do so. Additionally, stresses decayed rapidly to negligible values within minutes of screw activation. When considering appliances that exert a continuous force during expansion, it was determined that it is imperative to maintain as constant a force as possible; as the applied force decays over treatment, the amount of suture expansion generated closely follows this trend. Overall, it was found that an appliance able to generate a constant force throughout the entirety of treatment will be most effective in physiologically expanding the midpalatal suture. This in turn will decrease treatment time and improve overall results.

Preface

Chapter 2 of this thesis research was previously published as Romanyk DL, Lagravere MO, Toogood RW, Major PW, Carey JP. Review of maxillary expansion appliance activation methods: Engineering and clinical perspectives. *Journal of Dental Biomechanics*. 2010;2010:496906. As the lead author of this review, I was responsible for gathering relevant literature, analyzing the expansion appliances with respect to their treatment mechanics, and writing of the manuscript. Jason Carey and Roger Toogood assisted in the engineering analysis of relevant appliances while Manuel Lagravere and Paul Major provided clinical insight and expertise.

The literature review in Chapter 3 has been previously published as Romanyk DL, Collins CR, Lagravere MO, Toogood RW, Major PW, Carey JP. Role of the midpalatal suture in FEA simulations of maxillary expansion treatment for adolescents: A review. *International Orthodontics*. 2013;11:119-138. My responsibilities focused on guiding the literature review, analyzing relevant studies, development of the simplified maxilla complex model, and primary writing of the manuscript. Caroline Collins was responsible for gathering relevant literature, retrieving key values from studies, and writing the methodology section of the study. As in Chapter 2, Jason Carey and Roger Toogood contributed to the engineering discussion while Paul Major and Manuel Lagravere contributed to the clinical aspect of the study.

Chapter 4 of the presented thesis was previously published as Romanyk DL, Liu SS, Lipsett MG, Toogood RW, Lagravere MO, Major PW, Carey JP. Towards a viscoelastic model for the unfused midpalatal suture: Development and validation using the midsagittal suture in New Zealand white rabbits. *Journal of Biomechanics*. 2013;46:1618-1625. I was responsible for model development and validation, analysis of results, and constructing the manuscript. Sean Liu shared raw data from a previous unrelated study and provided clinical insight to the analysis. Mike Lipsett and Roger Toogood assisted in model development and evaluation, while Jason Carey shared his knowledge and expertise in the area of

tissue mechanics. Manuel Lagravere and Paul Major again contributed to the clinical discussion of results.

Chapter 5 has been published as Romanyk DL, Liu SS, Lipsett MG, Toogood RW, Lagravere MO, Major PW, Carey JP. Incorporation of stress-dependency in the modeling of midpalatal suture behavior during maxillary expansion treatment. *Proceedings of the ASME 2013 Summer Bioengineering Conference*. 2013;2013:SBC2013-14034. This publication has the same authorship as the manuscript presented in Chapter 4, with each author having the same roles.

Finally, Chapter 6 has been submitted to a peer-review journal as Romanyk DL, Liu SS, Long R, Carey JP. Considerations for determining relaxation constants from creep modeling of nonlinear suture tissue. *International Journal of Mechanical Sciences*. 14-page manuscript submitted September 4, 2013. My role as lead author included model development and evaluation, discussion of results, and writing of the manuscript. Sean Liu again shared his experimental data from an unrelated study and contributed to the clinical discussion in the manuscript. Rong Long and Jason Carey provided support and guidance with respect to the theoretical development of models, and contributed to the engineering discussion of results.

*“I remind myself every morning: Nothing I say this day will teach me anything.
So if I’m going to learn, I must do it by listening.”*
-Larry King

*“Life’s a dance you learn as you go
Sometimes you lead, sometimes you follow
Don’t worry about what you don’t know
Life’s a dance you learn as you go”*
-John Michael Montgomery

“It’s not that I’m so smart, it’s just that I stay with problems longer.”
-Albert Einstein

This work is dedicated to my wife, my family, and all the friends in my life for making me the person I am today. I would also like to dedicate this to family members who are no longer with us: Grandpa and Grandma Romanyk, Grandpa and Grandma Ramsey, and Aunt Cheryl.

Acknowledgements

There are so many people that I want to thank and acknowledge for their contributions throughout the course of my PhD. Some contributed directly to the research, some on a personal level, and many were both. Even though this thesis is a result of the research that I completed, it would not have been possible without the support of many people.

First and foremost, I must thank my supervisory committee: Drs. Jason Carey, Roger Toogood, and Paul Major. Dr. Major was instrumental in guiding the clinical aspect of this research and ensuring that it remained relevant for the clinician. The amount of respect I have for Dr. Toogood in regards to his engineering knowledge and mentorship in general cannot be overstated. He contributed greatly to the modeling aspect of my work and always provided excellent advice regarding career choices. Playing “Devil’s Advocate” to my research was always his favorite angle in challenging me, and it undoubtedly increased the quality of my thesis.

There is not enough that can be said about the impact that Jason has had on my personal and professional development over the years. From supervising me during my undergraduate research through to my graduate degree, he was a tremendous supporter and mentor. He always pushed me in my research endeavors as well as any other opportunities that would advance me as a professional. From sitting on student committees to teaching multiple courses, Jason always encouraged me to advance myself in many ways. I truly appreciate his guidance and mentorship over the years and know that he has helped in ensuring I have the necessary skills for my future career.

There are a number of other researchers outside of my supervisory committee that must be acknowledged for their contributions to my research. Dr. Manuel Lagravere was an excellent resource throughout my degree and answered many questions I had with regards to clinical orthodontics and maxillary expansion treatment. Dr. Sean Liu from Indiana University was instrumental in advancing my research through his open collaboration and sharing of data. Drs.

Mike Lipsett, Rong Long, and Peter Schiavone all provided tremendous support in the nonlinear modeling aspect of my research, especially with the mathematical framework. Finally, undergraduate researchers Lauren Brunette, Caroline Collins, and Brian Shim must be acknowledged for their contributions to this thesis.

Throughout my graduate studies I received financial support from a variety of sources allowing me to conduct my research. For that, I must acknowledge the University of Alberta, Department of Mechanical Engineering, Faculty of Medicine and Dentistry, ORMCO Corporation, NSERC, AITF, and the Burroughs Wellcome Fund. Furthermore, I must acknowledge the MecE shop, IT, and office staff. The machinists in the MecE shop are truly amazing for not only the work they do, but also in the way they help to train students. During my time as a student they always answered any question I had in a helpful manner, no matter how ridiculous. Also, the number of absurd computer questions I asked the IT staff over the years could never be tallied. I owe a big thanks to them, especially Dave and Virginia, for keeping my computer running over the years.

Thank you to all the lab-mates I have had over the years. Without the “good talks” with Cagri, or the excessive amount of coffee runs and “world problem solving sessions”, getting my degree wouldn’t have been nearly as fun.

Finally, absolutely none of this would have been possible without my friends and family. Friends have always helped in keeping a good work-life balance throughout my PhD helping to keep me grounded and relaxed. Joe and Joanna, while at times you may have made my life more challenging, I always knew you were there as supporters and would have done anything you could to help. Mom and Dad, you two always supported me in whatever decision I made and always pushed me to do my best. While I may have done the research in this thesis, you two gave me the opportunity to take this on and I could never thank you enough for that or repay you. Finally, to my wife Stacy, your support and patience, especially the latter, over the years has not gone unnoticed. Even though you didn’t always understand my research, you always listened to my

banter and did anything you could to me through this. You are a strong woman and knowing this has helped me to get through the difficult times of my thesis.

Table of Contents

1. INTRODUCTION	1
1.1. REFERENCES	4
<u>2. LITERATURE REVIEW: MAXILLARY EXPANSION APPLIANCES</u>	<u>6</u>
2.1. INTRODUCTION	7
2.2. METHODOLOGY	7
2.3. RESULTS	7
2.4. DISCUSSION	9
2.5. CONCLUSIONS	16
2.6. REFERENCES	17
<u>3. LITERATURE REVIEW: MODELING OF THE MIDPALATAL SUTURE</u>	<u>20</u>
3.1. INTRODUCTION	21
3.2. METHODOLOGY	22
3.3. RESULTS	25
3.4. DISCUSSION	29
3.4.1. ASSUMING NO MATERIAL	29
3.4.2. ASSUMING BONE PROPERTIES	31
3.4.3. ASSUMING SOFT TISSUE PROPERTIES	32
3.4.4. THE SUTURE AS A VISCOELASTIC MATERIAL	32
3.4.5. DISCUSSION OF THE MAXILLA COMPLEX AS A SYSTEM	34
3.5. CONCLUSIONS	38
3.6. REFERENCES	39
<u>4. DEVELOPING A CREEP MODEL FOR THE UNFUSED MIDPALATAL SUTURE USING EMPIRICAL DATA FROM THE MIDSAGITTAL SUTURE IN NEW ZEALAND WHITE RABBITS</u>	<u>43</u>
4.1. INTRODUCTION	44
4.2. METHODOLOGY	45
4.2.1. MODELING METHODS	45
4.2.2. EXPERIMENTAL DATA	48
4.2.3. EXPERIMENTAL DATA ASSUMPTIONS	51
4.2.4. CONSTANT DETERMINATION AND MODEL EVALUATION	53
4.3. RESULTS	54
4.3.1. MODEL CONSTANT DETERMINATION	54
4.3.2. MODEL VALIDATION	56
4.4. DISCUSSION	59

4.5. REFERENCES	61
<u>5. CREEP MODELING OF SUTURE BEHAVIOR USING A NONLINEAR BURGERS MODEL</u>	<u>65</u>
5.1. INTRODUCTION	66
5.2. METHODOLOGY	67
5.3. RESULTS	68
5.4. DISCUSSION AND CONCLUSIONS	70
5.5. REFERENCES	70
<u>6. INTERRELATING CREEP AND SUTURE MODELS FOR SUTURE VISCOELASTIC BEHAVIOR</u>	<u>72</u>
6.1. INTRODUCTION	73
6.2. METHODOLOGY	76
6.2.1. MODELING METHODS	76
6.2.2. EXPERIMENTAL DATA AND MODEL EVALUATION	80
6.3. RESULTS	82
6.4. DISCUSSION	85
6.5. CONCLUSIONS	90
6.6. REFERENCES	91
<u>7. SIMULATING SUTURE RESPONSE TO SCREW AND SPRING ACTIVATED MAXILLARY EXPANSION APPLIANCES</u>	<u>94</u>
7.1. INTRODUCTION	95
7.2. METHODOLOGY	95
7.2.1. SCREW ACTIVATED APPLIANCES	96
7.2.2. SPRING ACTIVATED APPLIANCES – CONSTANT FORCE	97
7.2.3. SPRING ACTIVATED APPLIANCES – DECAYING FORCE	98
7.3. RESULTS	98
7.4. DISCUSSION	101
7.5. CONCLUSIONS	104
7.6. REFERENCES	104
<u>8. CONCLUSIONS AND FUTURE WORK</u>	<u>107</u>
8.1. CONCLUSIONS	107
8.2. FUTURE WORK	109
<u>COMPLETE LIST OF REFERENCES</u>	<u>111</u>

List of Tables

Table 2-1: Categories of Activation Methods and Specific Examples	8
Table 3-1: List of Midpalatal Suture Material Properties used in FEA Simulations	26
Table 4-1: Cranial Suture Values for New Zealand White Rabbits as Determined by Radhakrishnan and Mao (2004) [23]	52
Table 4-2: Stress Values Used for Model Constant Determination and Validation	54
Table 4-3: Nominal, LB, and UB Constants for QLV	54
Table 4-4: Nominal, LB, and UB Constants for MST	55
Table 4-5: Nominal, LB, and UB Constants for Schapery's Method	55
Table 4-6: Nominal, LB, and UB Constants for Burgers Model	56
Table 4-7: Percentage Error between Average Experimental Validation Values and MST Model	60
Table 6-1: Average Values of Strain at each Measured Data Point for the Constant Determination and Validation Data (± 1 SD)	81
Table 6-2: Creep Model Constants for Each Load Set and their Corresponding Average (± 1 SD)	82
Table 6-3: Relaxation Function Model Constants Determined using the Creep Constants from Each Load Set as well as the Average Creep Constants	84
Table 7-1: Activation Stress Values at Varying Levels of Initial Displacement	99
Table 7-2: Comparison of Decaying Functions to 70% and 90% to a Constant Force Spring	101

List of Figures

Figure 1-1: A simplified schematic of the maxilla geometry and attachment to surrounding bones (left: frontal view of skull; right: inferior view of the maxilla) through sutures	1
Figure 1-2: Mirror view of the maxilla showing a typical maxillary expansion appliance and location of the midpalatal suture	2
Figure 2-1: Typical force-displacement characteristics for (a) linear and (b) viscoelastic materials	9
Figure 2-2: Typical force response to a stepwise and discrete generation of displacement for a viscoelastic material. Following each idealized step, the tissue relaxes, and observed force decreases	11
Figure 2-3: Typical force-expansion curves during treatment for (a) linear springs and (b) magnetic appliances	13
Figure 3-1: Flowchart describing inclusion/elimination of articles from systematic review	25
Figure 3-2: (a) Half-section of manufactured human skull and the model representation of the maxilla complex; (b) free body diagram of the model representation	36
Figure 4-1: Mirror view of a typical expansion appliance inserted in a patient's upper jaw	44
Figure 4-2: Spring-damper configuration of the Burgers model	48
Figure 4-3: (a) Sample image of the whole New Zealand white rabbit skull; (b) schematic of the rabbit skull highlighting the midsagittal suture; (c) enlarged image showing the midsagittal suture on the rabbit skull	49
Figure 4-4: Schematic representation of spring and MSI configuration around the midsagittal suture	50
Figure 4-5: Approximated dimensions of the midsagittal suture	51
Figure 4-6: Sample plot showing the fitting of model curves to experimental data	56
Figure 4-7: Model curves plotted against validation data using nominal constants for each respective load	57

Figure 4-8: Cross-validation sensitivity plots for the MST model	58
Figure 4-9: Model curves plotted against validation data using a single set of averaged model constants	58
Figure 5-1: (a) Typical maxillary expansion appliance; (b) Spring-damper schematic of the Burgers model	66
Figure 5-2: Model comparison at 0.49N of spring force	68
Figure 5-3: Model comparison at 0.98N of spring force	69
Figure 5-4: Model comparison at 1.96N of spring force	69
Figure 6-1: Model validation plots at 0.49N, 0.98N, and 1.96N load levels using the validation creep data from Liu et al. (2011) [16]	83
Figure 6-2: Relaxation plots for the 2TI, 3TS, 3TI, and ST models using the averaged creep constant values as described in Table 6-2 (Note: 1 hour $\approx 600 \cdot 10^{-5}$ weeks)	85
Figure 6-3: Creep and relaxation predictions using the single-term and three-term inseparable functions for data from Thornton et al [10]	89
Figure 7-1: (a) Plot of initial stress at varying levels of activation displacement; (b) Sample plot of stress-decay for the worst and best case scenarios (1 hour ≈ 0.006 weeks)	99
Figure 7-2: Suture strain response to exponentially, linearly, and inversely decaying springs and a constant force spring for: (a) 30% decrease in force; (b) 10% decrease in force	100

List of Common Symbols and Variables

- $\varepsilon(t)$ A general strain response to general stress input as a function of time
- $\varepsilon_c(t)$ The creep-strain response to a constant applied stress as a function of time
- ε_0 A constant applied strain during a stress-relaxation scenario
- $\sigma(t)$ A general stress response to general strain input as a function of time
- $\sigma_r(t)$ The stress-relaxation response to a constant applied strain as a function of time
- σ_0 A constant applied stress during a creep-strain scenario
- σ_L A decaying stress function used to simulate suture strain response resulting from a linearly decaying spring
- σ_E A decaying stress function used to simulate suture strain response resulting from an exponentially decaying spring
- σ_I A decaying stress function used to simulate suture strain response resulting from an inversely decaying spring
- $J(t), J(t,\sigma)$ “Creep function” associated with a general or creep-strain viscoelastic response; this may be a function solely of time, (t) , or stress and time, (t,σ) , respectively
- $J'(t)$ A “reduced creep function” whereby $J(t,\sigma)$ is separated into its time, $J'(t)$, and stress-dependent, $\varepsilon^e(\sigma)$, components; used in quasi-linear viscoelastic (QLV) theory
- $\varepsilon^e(\sigma)$ The “elastic strain response” whereby $J(t,\sigma)$ is separated into its time, $J'(t)$, and stress-dependent, $\varepsilon^e(\sigma)$, components; used in quasi-linear viscoelastic (QLV) theory
- $G(t), G(t,\varepsilon)$ “Relaxation function” associated with a general or relaxation viscoelastic stress response; this may be a function solely of time, (t) , or strain and time, (t,ε) , respectively
- $G'(t)$ A “reduced creep function” whereby $G(t,\varepsilon)$ is separated into its time, $G'(t)$, and strain-dependent, $\sigma^e(\varepsilon)$, components; used in quasi-linear viscoelastic (QLV) theory

$\sigma^e(\varepsilon)$ The “elastic stress response” whereby $G(t, \varepsilon)$ is separated into its time, $G'(t)$, and strain-dependent, $\sigma^e(\varepsilon)$, components; used in quasi-linear viscoelastic (QLV) theory

Glossary of Common Terms

- Active Phase** The phase of maxillary expansion treatment during which the appliance exerts an outwardly directed force or displacement to widen the maxilla (upper jaw; approximate region outlined in Figure 3-2)
- Creep-Strain or Creep** Continuous strain, or displacement, of a material during the application of a constant stress, or force
- FEA** Finite Element Analysis
- in-vitro*** Simulation of a process outside of a living organism or body
- in-vivo*** A process taking place inside a living organism or body
- Maxilla** The upper jaw, or palate; approximate region outlined in Figure 3-2
- ME** Maxillary Expansion: A common orthodontic treatment used to widen a patient's maxilla
- Midpalatal Suture** Soft connective tissue adjoining maxillary bones
- Retention Phase** The phase of maxillary expansion treatment during which the appliance is held inactive in the maxilla (upper jaw; approximate region outlined in Figure 3-2)
- Stress-relaxation or Relaxation** Decay of internal stress, or force, in a material during the application of a constant strain, or displacement
- SMA** Shape Memory Alloy
- Viscoelastic** A type of deformation exhibiting the mechanical characteristics of viscous flow and elastic deformation¹

¹ Callister WD. Glossary. In: Materials Science and Engineering: An Introduction. 6th ed. Hoboken NJ: John Wiley & Sons Inc.; 2003. P.790.

1. Introduction

The study of orthodontics from a biomechanics perspective has become a popular point of research in the literature. Methods for studying various treatment protocols include *in-vivo* [1,2] and *in-vitro* [3,4] experimental methods, finite element analysis (FEA) [5,6], and analytical modeling [7,8]. In using these scientific tools to investigate the mechanics of orthodontic treatments, researchers and clinicians are able to better understand the driving factors governing patient response. This in turn allows for methodical alteration of protocols and appliance designs to improve overall treatment results.

Maxillary expansion (ME) is a procedure used by orthodontists to widen the maxilla (Figure 1-1), upper jaw or palate, of a patient [9-11] which dates back as early as 1860 [9,10]. An orthodontic appliance such as that shown in Figure 1-2 is used to generate this expansion. The presented thesis will focus on ME treatment in a healthy adolescent with a normal palate. In such a case, clinicians use expansion to generate additional room with which to move teeth in correction of malocclusions. Expansion may also be used in the correction of other issues such as a cleft palate [12,13]; however, such scenarios are not considered in this study. There are a number of appliances available to clinicians as well as a variety of protocols and methodologies that may be employed for each appliance [14]. Additionally, definitive scientific evidence currently lacks from the literature which supports a specific appliance and/or protocol. This has led to differing opinions, and hence approaches, amongst clinicians with regards to ME treatment.

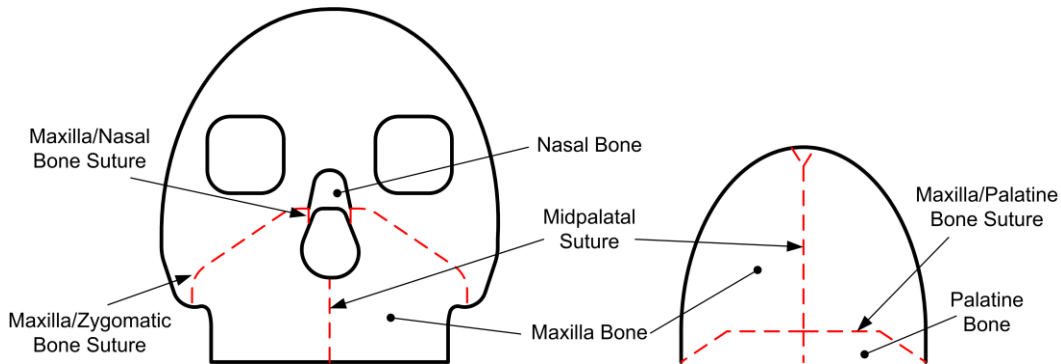


Figure 1-1: A simplified schematic of the maxilla geometry and attachment to surrounding bones (left: frontal view of skull; right: inferior view of the maxilla) through sutures

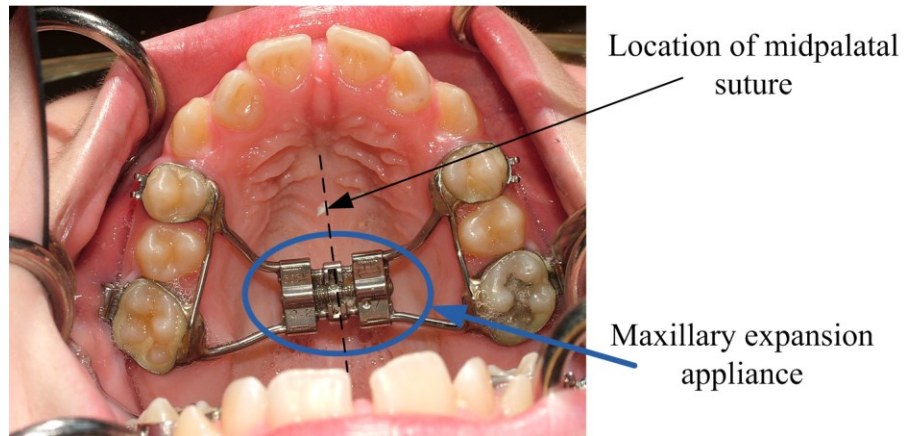


Figure 1-2: Mirror view of the maxilla showing a typical maxillary expansion appliance and location of the midpalatal suture

The midpalatal suture is the connective soft tissue located down the midline of the palate joining the maxilla bones (Figure 1-2). During ME this suture is exposed to a tensile loading and will widen throughout the course of treatment [6]. The importance of the midpalatal suture in terms of its load-bearing requirements during ME has been debated in the literature; however, it has also been shown in FEA simulations that variation of suture material properties will influence the instantaneous response of the skull to ME loading conditions [6].

Ideally, the active phase of ME treatment would be conducted as quickly as possible without damaging the midpalatal suture tissue. After this active phase, the appliance is typically left inactive in the palate to facilitate bone formation in the suture preventing relapse; a period known as the retention phase. It has been suggested that maintaining the integrity of suture tissue during activation can improve treatment time and overall results [15-17]. This is a result of bone formation in the suture as a consequence of continually applied traction. If the process of bone formation is facilitated throughout the active phase of ME, it will decrease the amount of time required for retention as bone has already been generated in the suture.

Current ME appliances available to clinicians include those using expansion screws, springs, magnets, and shape memory alloys (SMA's) as the active element [14]. As will be discussed in this thesis, each of these appliances

has unique advantages and disadvantages with regards to their impact on ME treatment and mechanics. With such a variety of appliances available to practicing clinicians, it is imperative that research be conducted to understand their impact on patient response during ME treatment.

A variety of studies simulating the patient response to ME have been conducted, many of which utilize FEA [6,18,19]. The research in this thesis will illustrate that these studies do provide useful information towards understanding expansion treatment; however, the literature's scope is limited as these studies treat the suture as a linear elastic material or neglect it completely during analysis. In reality, the suture behaves in a viscoelastic manner [19, 20].

Viscoelasticity is the nature of a material to exhibit creep, continuous deformation during a constant stress, and/or stress-relaxation, reduction of stress under a constant applied strain. Depending on the material, there could be a number of factors contributing to this type of behavior. In the case of the midpalatal suture, straightening of collagen fibers and fluid transfer throughout the tissue are driving forces behind its viscoelastic nature [19, 20]. When making conclusions/observations pertaining to the suture, or in the near vicinity, this viscoelastic behavior should be included depending on study goals/hypotheses. This is especially true when investigating response over a given timeframe as creep and/or relaxation phenomena would influence results.

The overall goal of the presented thesis is to investigate the effect of ME on midpalatal suture behavior. First, a review of the literature is conducted to study existing ME appliances and simulation techniques in Chapters 2 and 3, respectively. In Chapters 4-6, existing data from the midsagittal suture in New Zealand white rabbits will be used to construct and evaluate various applicable creep modeling methods. In order to fully study the suture's viscoelastic behavior during ME, it was necessary to convert appropriate creep models into a subsequent stress-relaxation form which is presented in Chapter 6. Using the developed creep-relaxation models along with a generalized strain-time relationship, the suture's response to existing ME appliances is studied in Chapter 7. This analysis focuses on the clinical impact of the thesis allowing for

knowledge translation to clinicians. Finally, the findings and conclusions from all Chapters are synthesized in Chapter 8 along with a discussion of future work.

1.1. REFERENCES

1. Sia S, Koga Y, Yoshida N. Determining the center of resistance of maxillary anterior teeth subjected to retraction forces in sliding mechanics: An in vivo study. *Angle Orthodontist*. 2007;77:999-1003.
2. Sander C, Huffmeier S, Sander FM, Sander FG. Initial results regarding force exertion during rapid maxillary expansion in children. *Journal of Orofacial Orthopedics*. 2006;67:19-26.
3. Fok J, Toogood RW, Badawi H, Carey JP, Major PW. Analysis of maxillary arch force/couple systems for a simulated high canine malocclusion: Part 1. Passive ligation. *Angle Orthodontist*. 2011;81:953-959.
4. Xia Z, Chen J. Biomechanical validation of an artificial tooth-periodontal ligament-bone complex for in vitro orthodontic load measurement. *Angle Orthodontist*. 2013;83:410-417.
5. Jayade V, Annigeri S, Jayade C, Thawani P. Biomechanics of torque from twisted rectangular archwires: A finite element investigation. *Angle Orthodontist*. 2007;77:214-220.
6. Lee H, Ting K, Nelson M, Sun N, Sung SJ. Maxillary expansion in customized finite element method models. *American Journal of Orthodontics and Dentofacial Orthopedics*. 2009;136:367-374.
7. Komatsu K, Sanctuary C, Shibata T, Shimada A, Botsis J. Stress-relaxation and microscopic dynamics of rabbit periodontal ligament. *Journal of Biomechanics*. 2007;40:634-644.
8. Romanyk DL, Melenka GW, Carey JP. Modeling stress-relaxation behavior of the periodontal ligament during the initial phase of orthodontic treatment. *Journal of Biomechanical Engineering*. 2013;135:0910071-8.
9. Angell EH. Treatment of irregularity of the permanent or adult teeth. Part 1. *Dental Cosmos*. 1860;1:540-544.
10. Angell EH. Treatment of irregularity of the permanent or adult teeth. Part 2. *Dental Cosmos*. 1860;1:599-560.

11. Haas AJ. Rapid expansion of the maxillary dental arch and nasal cavity by opening the midpalatal suture. *Angle Orthodontist*. 1961;31:73-90.
12. Trindade IEK, Castilho RL, Sampaio-Teixeira ACM, Trindade-Suedam IK, Silva-Filho OG. Effects of orthopedic rapid maxillary expansion on internal nasal dimensions in children with cleft lip and palate assessed by acoustic rhinometry. *Journal of Craniofacial Surgery*. 2010;21:306-311.
13. Yang CJ, Pan XG, Qian YF, Wang GM. Impact of rapid maxillary expansion in unilateral cleft lip and palate patients after secondary alveolar bone grafting: Review and case report. *Oral Surgery, Oral Medicine, Oral Pathology and Oral Radiology*. 2012;114:e428-430.
14. Romanyk DL, Lagravère MO, Toogood RW, Major PW, Carey JP. Review of maxillary expansion appliance activation methods: engineering and clinical perspectives. *Journal of Dental Biomechanics*. 2010;2010:496906.
15. Liu SS, Opperman LA, Kyung H, Buschang PH. Is there an optimal force level for sutural expansion? *American Journal of Orthodontics and Dentofacial Orthopedics*. 2011;139:446-455.
16. Zahrowski JJ, Turley PK. Force magnitude effects upon osteoprogenitor cells during premaxillary expansion in rats. *Angle Orthodontist*. 1992;62:197-202.
17. Storey E. Tissue response to the movement of bones. *American Journal of Orthodontics*. 1973;64:229-247.
18. Provatidis CG, Georgiopoulos B, Kotinas A, McDonald JP. Evaluation of craniofacial effects during rapid maxillary expansion through combined in vivo/in vitro and finite element studies. *European Journal of Orthodontics*. 2008;30:437-448.
19. Tanaka E, Miyawaki Y, Tanaka M, Watanabe M, Lee K, de Pozo R, Tanne K. Effects of tensile forces on the expression of type III collagen in rat interparietal suture. *Archives of Oral Biology*. 2000;45:1049-1057.
20. Herring SW. Mechanical influences on suture development and patency. *Frontiers of Oral Biology*. 2008;12:41-56.

2. Literature Review: Maxillary Expansion Appliances

The following chapter presents a detailed literature review of maxillary expansion appliances with respect to their activation methods. Specifically, appliances are analyzed from an engineering perspective regarding the manner in which they expand the maxilla. The loading scenarios discovered in this review are used in Chapter 7 when simulating the midpalatal suture's response to current expansion treatment protocols. A version of this chapter has been published as:

Romanyk DL, Lagravere MO, Toogood RW, Major PW, Carey JP. Review of maxillary expansion appliance activation methods: Engineering and clinical perspectives. *Journal of Dental Biomechanics*. 2010;2010:496906.

2.1. INTRODUCTION

Use of maxillary expansion (ME) to widen the midpalatal suture is a common orthodontic treatment. While there are a variety of methods for anchoring an expansion appliance to a patient [1,2], the following discussion will only be concerned with activation methods.

To date, all review publications on the subject are concerned with the clinical impact of expansion while none have reviewed appliances from a combined clinical and engineering perspective [3,4]. The purpose of this review is to analyze current ME devices using engineering principles in describing the clinical implications of the activation method, and suggest future areas of design improvement.

2.2. METHODOLOGY

Scopus and PubMed were used to retrieve literature regarding ME appliances. Keywords used in the databases are “maxillary expansion” and “palatal expansion”. Further result reduction was attained by adding “appliance”, “apparatus”, or “device” keywords. A sample search could be given as “maxillary expansion” AND “device”, thus allowing for a maximum number of relevant papers to be retrieved from the databases.

Canadian and U.S. patent searches were also conducted in addition to review of the academic literature. In the U.S., the patent classification number used was 433/7 which is defined under the heading of Orthodontics as, “By device having means to apply outwardly directed force (e.g., expander)”. In Canada, the current International Classification of A61C7/10 was used along with previous Canadian Classification 83-1.

2.3. RESULTS

Upon reviewing the literature, it was determined that the methods of activation could be broken down into four categories: screw, spring, magnetic, and Shape Memory Alloy (SMA) activation methods. Table 2-1 lists the general activation methods discussed in this paper along with specific examples from the literature.

Table 2-1: Categories of Activation Methods and Specific Examples

Activation Category	Specific Examples
Screw	Hyrax Car Jack Telescoping
Spring	Coil Wire Minne
Magnetic	Repulsion Magnets
Shape Memory Alloy	Coil Spring Wire Spring Screw

Screw activation includes any method that requires adjustment through manual rotation of a shaft to expand the appliance. The Hyrax screw (jackscrew), or expansion screw, is commonly seen in current appliances such as those presented by Haas (1961) [1] or Biederman (1968) [5]. Other expansion mechanisms include telescoping [2] and car-jack style [6] appliances. Whether by a key or wrench, these expanders require frequent patient or clinician adjustment to achieve expansion of the maxilla.

Any mechanism that deforms a body, and subsequently relies upon elastic restoration forces for ME, was classified as a spring type appliance. This would include devices that utilize coil or wire springs with representative examples being the Minne expander [7] and the appliance presented by Defraia *et al.* (2008) [8], respectively. Upon activation, these devices will exert a continuous force as the maxilla widens.

Expansion appliances that utilize magnets as the primary activation method have been reported [9]. Since a magnetic field has directionality, two magnets can be oriented such that they apply opposing forces to generate expansion.

SMA technology is the fourth maxillary expansion activation method. It was found that appliances made use of the super elastic nature of these alloys through coil springs [10], wire springs [11], or expansion screws [12]. While this type of appliance utilizes configurations already discussed (e.g. screw and spring),

they are considered separately due to the unique force-displacement (stress-strain) characteristic resulting from SMA material behavior.

2.4. DISCUSSION

Midpalatal suture structure is highly variable at different ages [13]. Additionally, fiber bundles found inside the suture will change orientation and fluid will transfer during treatment as a result of the expansion forces applied by the appliance [14]. This complicated structure and behavior greatly affects the mechanics of the maxilla complex during treatment. Computational models exist that study the mechanical response of the skull to maxillary expansion, but none incorporate the viscoelastic behavior of the sutures [15,16]. For instance, Lee *et al.* (2009) constructed a finite element analysis model to simulate maxillary expansion that used accepted linear elastic properties of the periodontal ligament for the sutures and not a viscoelastic model [16].

Typical engineering materials, such as steel or aluminum, have linear force-displacement, or stress-strain, relationships in their elastic range allowing for simple prediction of behavior [17]. Soft tissues exhibit non-linear viscoelastic force-displacement behavior as shown in Figure 2-1, which are difficult to predict as they are deformation and deformation-rate dependent; the latter produces larger force values at increased deformation rates as illustrated in Figure 2-1.

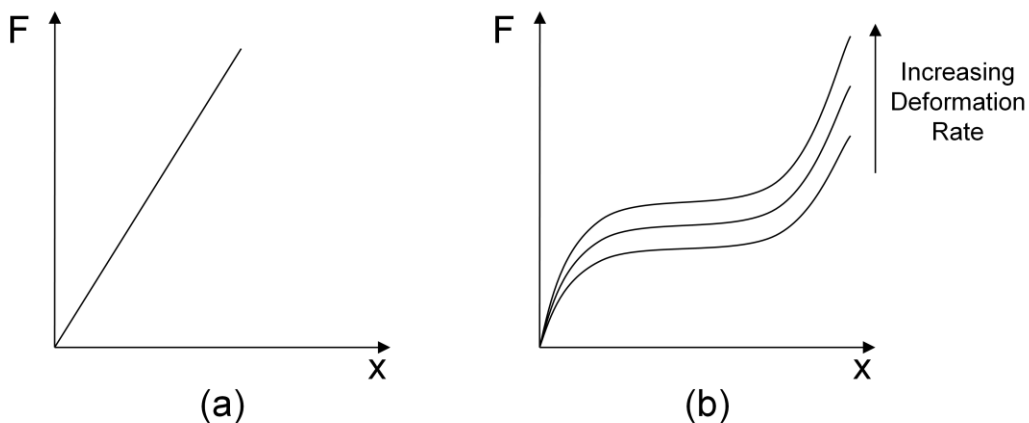


Figure 2-1: Typical force-displacement characteristics for (a) linear and (b) viscoelastic materials

Forces generated in the maxilla by a screw activated appliance, with respect to both time and displacement, are essentially a function of tissue properties of the patient. The appliance may undergo minor deformation, but it will be negligible compared to that of the maxilla. This is due to the fact that for the same applied force, the ratio of appliance-to-tissue deformation is inversely related to the ratio of their stiffness values, where the stiffness of the appliance will be much greater than that of the soft tissue. Force generation can be visualized by turning an expansion screw in a device that is not placed in a patient. No transverse force is generated as the appliance expands since there is no resistance to expansion other than the friction between screw threads. As such, it is impossible to predict the force that will be generated with respect to time or displacement without fully understanding the properties and geometry of the maxilla complex. This is supported by results in the literature that shows much variation in the forces generated by screw activated appliances for different patients [18-20].

Additionally, screw type appliances displace the maxilla in a manner that could be assumed as step-wise. That is, each displacement occurs approximately instantaneously and remains constant until the next activation. If an assumed step-wise displacement is applied to a viscoelastic material, the resultant force will spike and then begin to relax if the displacement is held constant [21]. The applied displacement is also assumed to be completely linear with no rotation. Though the biomechanics of maxillary expansion have been studied and it is shown that the maxilla halves rotate during treatment, this will be neglected for the purpose of this qualitative analysis [22]. This type of behavior is illustrated in Figure 2-2.

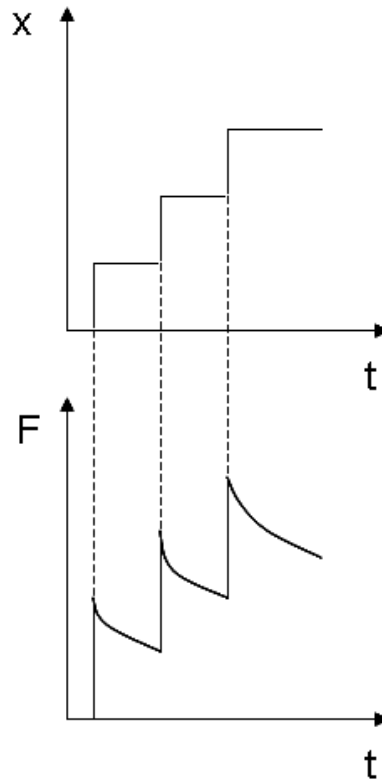


Figure 2-2: Typical force response to a stepwise and discrete generation of displacement for a viscoelastic material. Following each idealized step, the tissue relaxes, and observed force decreases

The relaxation behavior of the tissue can be modeled using a relationship known as the relaxation function [21]. This is an idealized function where a step-input in displacement is imposed on the tissue and is then held constant. The relaxation function describes the force-time, or stress-time, behavior of the tissue once the displacement is held. In order to be used as a predictive tool, mechanical properties of the tissue must be understood to accurately define function parameters.

The greatest advantage of screw activated appliances is arguably the simple and well understood mechanics. For a given amount of screw rotation there is a corresponding amount of thread-pitch dependent expansion. This allows clinicians to prescribe a given number of activations to achieve specific expansion between patient visits. Screw activated appliances are easily designed to be compact and light-weight which is a significant advantage.

While screw activation may be the most popular choice for clinicians, it also suffers from the greatest disadvantages of the methods considered. The maxilla is subjected to step-wise increments of the appliance which in turn causes rapid increases in forces. This may not only be uncomfortable for the patient, but it has also been suggested that high magnitude forces may result in less physiologic expansion of the suture [23,24]. Of all the activation methods, the screw activated appliances will produce the highest forces. Isaacson found that forces as high as 100 N were generated during treatment [18-20]. A possible way to decrease force magnitude is to decrease expansion rate as this would allow for greater tissue relaxation between activations; however, the rapid increase in force level at activation cannot be avoided.

The screw activation method requires the patient to activate the appliance. This is a substantial disadvantage as treatment success depends on patient compliance. If patients do not follow the prescribed activation protocol then expansion will not progress as intended, thus needlessly extending treatment time. Ideally, patient involvement in treatment protocols would be minimized or eliminated completely.

For the remaining activation methods, forces generated during treatment with respect to displacement can be predicted; however, the force with respect to duration of treatment, or time, still remains unknown. Screw activated appliances provide a known displacement, assuming appliance deformation is negligible, to the maxilla and the resistance of the tissue to this input causes the resulting force generation. Spring and magnetic activation methods themselves resist displacement, thus when an appliance utilizing one of these methods is compressed there are already forces present. From Newton's Third Law, which states that the reaction forces between two bodies will be equal and opposite, the forces imposed on the complex during expansion should theoretically be the same as forces produced by the activation method. This statement only holds true if the acceleration of the maxilla is neglected, which in our scenario is a fair assumption since in most cases it will only move approximately 1cm over the span of several weeks. A great advantage is provided here in that the forces generated during

expansion can be predicted and controlled. Typical curves for spring and magnetic activation methods are illustrated in Figure 2-3. The curve for the spring activation method is shown as linear while the magnetic curve is not. This arises from the fact that the force between two magnets used in repulsion is inversely proportional to the distance separating them squared, as illustrated in eq. (1). The relationship shown is only for two point charges, and as such is a simplification of the physical situation with two magnets which would involve more extensive analysis; however, it serves as an aid in understanding the force-displacement behavior between charged objects [25]. Linear springs will show a linear relationship between force and displacement as shown in eq. (2), and graphically in Figure 2-3. This may not always be the case as other nonlinear force-displacement spring relationships may be observed [26].

$$F = \frac{1}{4\pi\epsilon_0} \frac{(q_1q_2)}{x^2} \quad (1)$$

$$F = F_0 - kx \quad (2)$$

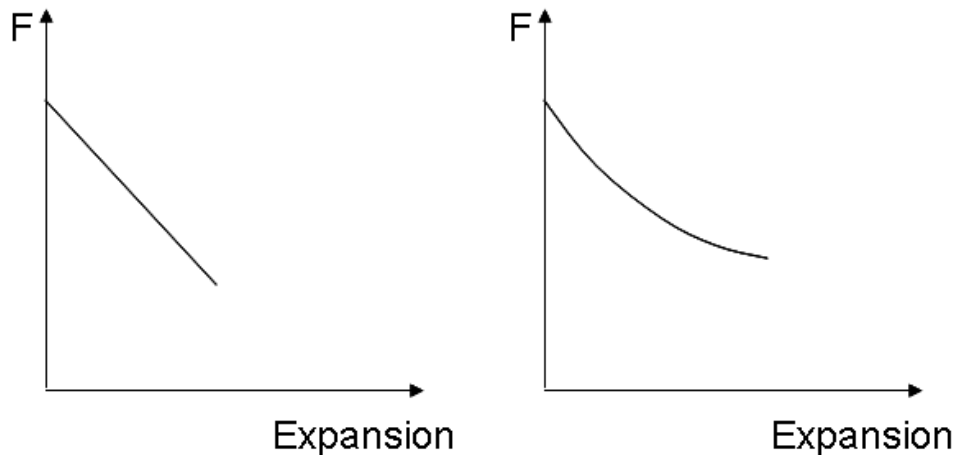


Figure 2-3: Typical force-expansion curves during treatment for (a) linear springs and (b) magnetic appliances

When considering force-time behavior during treatment, the general shape of the curves may not be the same as those in Figure 2-3. The rate at which the force decreases over time is entirely dependent on the resistance of the patient's

tissue to deformation. For a patient with very little resistance to expansion, or greater tissue relaxation, the force will decrease faster than if the tissue were to have a higher resistance. As such, accurate prediction of the force-time behavior will be highly patient-specific and will require knowledge of maxilla complex properties.

Continuous force application throughout treatment is an advantage of spring activation methods. This minimizes the number, and amplitude, of rapid force increases exerted on the tissue which may lead to more physiologic expansion and increased comfort. Also, force-displacement behavior can be predicted since it is not patient-specific and is governed by the spring. Lastly, patient involvement is eliminated which provides increased convenience and improves treatment results.

One disadvantage of typical spring activation methods is that the force output of the device is inversely proportional to expansion. As the deformation of the spring element decreases, the force output will also decrease. This may require intermediate activations to maintain the necessary force magnitude to cause expansion. The ideal situation would see an appliance that could induce expansion with a single low force activation, meaning that force would need to remain at least approximately constant during treatment.

Spring activated mechanisms can be structurally weak in the directions transverse to expansion. While the device is stable and predictable in the direction of expansion, these mechanisms in general lack the ability to resist forces in the other directions. This is more indicative of wire spring mechanisms than of coil springs, since the latter typically have an additional structural member providing support. If the spring undergoes unwanted deformation during treatment the outcome may be adversely affected.

SMA technology has only been implemented in screw and spring configurations [10-12]. As such, the force application trends that have been discussed for these methods will also apply to SMA appliances, differing only by force magnitude. Since the theory regarding SMA's is highly involved, only a brief discussion will be included here. It should be understood that in order to

harness the properties of SMA's, the material must be heated into the austenitic region from the martensitic to allow for interface movement, or twinning, of the materials structure [27]. The human mouth temperature can allow clinicians to take advantage of the twinning process that alters material stiffness. Since stiffness is defined as the force required for a unit displacement, the force magnitude applied during expansion will be different when using SMA's over conventional materials, such as stainless steel, when in the patient's mouth.

Though the SMA produces more physiologic forces, both in magnitude and in relation to displacement, these devices still suffer from some of the disadvantages of conventional springs. Wire spring devices lack structural stability in the directions transverse to the direction of expansion. Also, a device presented by Darendeliler and Lorenzon (1996), which used a Ni-Ti coil spring, showed that during expansion the force decreased from 7.85 N, to approximately 3.92 N [10]. Though this may not be as significant as the decrease seen with conventional materials, and may not be indicative of all potential SMA springs, it still shows a 50% decrease in force with displacement.

A device presented by Wichelhaus *et al.* (2004) utilizes Ni-Ti in a combined expansion screw and spring application [12]. The force-displacement curve shows an improvement from conventional screws as it does not involve the large force jumps seen previously; however, a tensile testing machine was used to gather data which does not accurately represent maxilla complex's compliance and viscoelastic behavior. As such, while results show promise compared to other screw appliances, future testing in a more physically representative environment would be necessary to show the true behavior during treatment. Again, as with all screw mechanisms, the patient is significantly involved in this treatment and must activate the screw themselves. Also, the force magnitude reached by this appliance shows forces ranging between 15-20N which are large compared to other Ni-Ti appliances [10].

The use of magnets for the purpose of expanding the maxilla is a technique that has been attempted [9]. When used in the repulsive configuration these types of appliances have many of the same advantages and disadvantages of

spring appliances. Magnets are able to produce a continuous force without any additional adjustments by the patient. One advantage that magnetic appliances have over springs, primarily wire spring devices, is that they can be made to be more structurally stable in all directions which will aid in preventing undesirable results.

When using magnets in repulsion, the force output will be inversely proportional to the distance-squared between the magnets. As the magnets move further apart during treatment the force will decrease in magnitude which may require intermediate adjustments. One pair of magnets may be used throughout the treatment, but in order to maintain a force level large enough to still produce expansion, the initial forces will need to be significant.

Ideal forces to achieve palatal expansion remain unknown. Isaacson and Ingram (1964) pointed out that RME appliance anchored to teeth should produce heavy forces designed to produce minimal tooth movement, while allowing bone repositioning [19]. Lower force magnitudes have been promoted as more physiologic, but when anchored to teeth may cause undesirable tooth movement. Bone anchored appliances may allow for lower, more physiologic, forces during midpalatal suture separation without unwanted tooth movement.

2.5. CONCLUSIONS

Through review of literature regarding ME appliances, the following conclusions can be drawn:

- Screw activation has the most disadvantages. It induces large magnitude discontinuous forces and requires patient activation.
- Spring appliances improve on screw activation in that they provide continuous force; however, the force level is typically dependent on the displacement of the expander and wire springs lack structural stability.
- Magnets can provide low-level forces that are continuous over the displacement. Unfortunately, the applied force decreases as the magnets displace further apart.
- SMA technology may provide more physiologic force-displacement characteristic than other methods; however, when used in conventional

ways such as with a screw or spring, the method still suffers from many of the disadvantages seen with conventional materials.

It is clear that there are more improvements that can be made to maxillary expansion activation methods. Methods that can provide lower levels of displacement-independent forces while requiring no patient involvement would be ideal. Future work should be concerned with determining an ideal force range for maxillary expansion, which would include modeling of the suture.

2.6. REFERENCES

1. Haas AJ. Rapid expansion of the maxillary dental arch and nasal cavity by opening the midpalatal suture. *Angle Orthodontist*. 1961;31:73-90.
2. Mommaerts MY. Transpalatal distraction as a method of maxillary expansion. *British Journal of Oral and Maxillofacial Surgery*. 1999; 37:268-272.
3. Lagravere MO, Major PW, Flores-Mir C, Orth C. Long-term dental arch changes after rapid maxillary expansion treatment: a systematic review. *Angle Orthodontist*. 2005;75:155-161.
4. Kilic N, Oktay H. Effects of rapid maxillary expansion on nasal breathing and some naso-respiratory and breathing problems in growing children: A literature review. *International Journal of Pediatric Otorhinolaryngology*. 2008;72:1595-1601.
5. Biederman W. A hygienic appliance for rapid expansion. *Journal of Practical Orthodontics*. 1968;2:67-70.
6. Koudstaal MJ, van der Wal KG, Wolvius EB, Schulten AJ. The Rotterdam Palatal Distractor: introduction of the new bone-borne device and report of the pilot study. *International Journal of Oral and Maxillofacial Surgery*. 2006;35:31-45.
7. Viazis AD, Vadiakis G, Zelos L, Gallagher RW. Designs and applications of palatal expansion appliances. *Journal of Clinical Orthodontics*. 1992;26: 239-243.
8. Defraia E, Marinelli A, Baroni G, Tollaro I. Dentoskeletal effects of a removable appliance for expansion of the maxillary arch: a postero-anterior cephalometric study. *European Journal of Orthodontics*. 2008;30: 57-60.

9. Darendeliler MA, Strahm C, Joho JP. Light maxillary expansion forces with the magnetic expansion device. A preliminary investigation. *European Journal of Orthodontics*. 1994;16:479-490.
10. Darendeliler MA, Lorenzon C. Maxillary expander using light, continuous force and autoblocking. *Journal of Clinical Orthodontics*. 1996;30:212-216.
11. Corbett MC. Slow and continuous maxillary expansion, molar rotation, and molar distalization. *Journal of Clinical Orthodontics*. 1997;31:253-263.
12. Wichelhaus A, Geserick M, Ball J. A new nickel titanium rapid maxillary expansion screw. *Journal of Clinical Orthodontics*. 2004;38:677-680.
13. Persson M. The role of sutures in normal and abnormal craniofacial growth. *Acta Odontologica Scandinavica*. 1995;53:152-161.
14. Tanaka E, Miyawaki Y, de Pozo R, Tanne K. Changes in the biomechanical properties of the rat interparietal suture incident to continuous tensile force application. *Archives of Oral Biology*. 2000;45:1059-1064.
15. Fang Y, Lagravere MO, Carey JPR, Major PW, Toogood RR. Maxillary expansion treatment using bone anchors: development and validation of a 3D finite element model. *Computation Methods in Biomechanics and Biomedical Engineering*. 2007;10:137-149.
16. Lee H, Ting K, Nelson M, Sun N, Sung SJ. Maxillary expansion in customized finite element method models. *American Journal of Orthodontics and Dentofacial Orthopedics*. 2009;136:367-374.
17. Popov EP, Balan TA. Chapter 2: Strain. In: *Engineering Mechanics of Solids*. 2nd ed. Upper Saddle River NJ: Prentice-Hall Inc.; 1998. p. 60-68.
18. Isaacson RJ, Wood JL, Ingram AH. Forces produced by rapid maxillary expansion: Part 1. Design of the force measuring system. *Angle Orthodontist*. 1964;34:256-260.
19. Isaacson RJ, Ingram AH. Forces produced by rapid maxillary expansion: Part 2. Forces present during treatment. *Angle Orthodontist*. 1964;34:261-270.
20. Zimring JF, Isaacson RJ. Forces produced by rapid maxillary expansion. Part 3. Forces present during retention. *Angle Orthodontist*. 1965;35:178-186.

21. Fung YC. Chapter 2: The meaning of the constitutive equation. In: Biomechanics: mechanical properties of living tissues. 2nd ed. New York NY: Springer Science+Business Media Inc.; 1993. p. 43-46.
22. Braun S, Bottrel JA, Lee KG, Lunazzi JJ, Legan HL. The biomechanics of rapid maxillary sutural expansion. *American Journal of Orthodontics and Dentofacial Orthopedics*. 2000;118:257-261.
23. Bell RA. A review of maxillary expansion in relation to rate of expansion and patient's age. *American Journal of Orthodontics*. 1982;81:32-37.
24. Storey E. Tissue response to the movement of bones. *American Journal of Orthodontics*. 1973;64:229-247.
25. Young HD, Freedman RA. Chapter 21: Electric charge and electric field. University Physics 11th ed. San Francisco CA: Pearson Education Inc.; 2004. p. 801.
26. Jutte CV, Kota S. Design of nonlinear springs for prescribed load-displacement functions. *Journal of Mechanical Design*. 2008; 130: 081403-1-081403-10.
27. Reed-Hill RE, Abbaschian R. Chapter 17: Deformation twinning and martensite reactions. In: Physical metallurgy principles. 3rd ed. Boston, MA: PWS Publishing Company; 1994. p. 584-585.

3. Literature Review: Modeling of the Midpalatal Suture

Chapter 3 presents a review of the literature surrounding modeling the midpalatal suture as a viscoelastic material and simulation of maxillary expansion treatment. The main intent of this review was to understand how the suture has been modeled in previous work regarding expansion treatment simulations and identify gaps in the literature which could be improved by advanced modeling. Additionally, a simplified model of the maxilla complex is generated using beam theory to illustrate the intricacies involved in predicting patient response even for a greatly simplified case. A version of this chapter has been published as:

Romanyk DL, Collins CR, Lagravere MO, Toogood RW, Major PW, Carey JP. Role of the midpalatal suture in FEA simulations of maxillary expansion treatment for adolescents: A review. *International Orthodontics*. 2013;11:119-138.

3.1. INTRODUCTION

The use of a maxillary expansion (ME) appliance to widen the upper jaw has become a widely accepted procedure amongst clinicians. Expansion screw appliances were among the first to be used [1,2] and are still arguably the most popular. More recent appliances include springs, magnets, or are constructed of a shape memory alloy (SMA) for the activation method [3]. While each of these appliances utilizes a different mechanism of activation, they all provide an outwardly directed force or displacement on the maxilla halves causing them to widen.

The field of orthodontics is moving towards prediction and simulation for various treatments, and ME is no different. Authors have begun using finite element analysis (FEA) as a tool to observe stresses, strains, and displacements as a result of orthodontic forces being applied to the maxilla [4-10]. It is hoped that one day clinicians will be able to predict treatment outcome for a specific patient and protocol; however, significant work remains before patient specific simulation is feasible.

One area that is still lacking in the literature is modeling of the midpalatal suture behavior resulting from an applied load. As has been shown in the past, the midpalatal suture behaves in a viscoelastic manner [11,12]. Tanaka *et al.* (2000) [13] used a Kelvin model, a linear viscoelastic method, to represent midpalatal suture behavior; however, past this study there has been little work completed to further our understanding of how this suture might respond to a given load. When considering the suture in FEA simulations authors have chosen to ignore the suture, consider it fused, or to assign properties indicative of soft tissues. Choosing to ignore the suture or consider it fused is only accurate when the simulation concerns cases where the suture has been surgically removed or has completely ossified, respectively. If the simulation is to represent ME in adolescent patients where the suture remains unfused, the three aforementioned methods are inaccurate.

The purpose of this review is to highlight research that has been conducted with regards to modeling of the midpalatal suture as well as ME treatment

simulations. Only cases of unfused midpalatal suture, as in the case of an adolescent, are considered. This review has been completed in order to highlight research towards midpalatal suture modeling and ME treatment simulations, and provide insight towards future work in this area. While there are many influential factors in ME treatment such as bone-bending, tipping of anchorage teeth, or differential between anterior and posterior expansion, these topics are outside the scope of this review. Only the suture's material response to loading is considered here.

3.2. METHODOLOGY

A systematic review was conducted to find studies considering the stress-strain or force-displacement relationship in the unfused midpalatal suture during ME. The review targeted analyses that either developed a predictive model for these relationships or performed a FEA involving ME. The interest of this review was for expansion in human adolescents with normal palates; thus, studies involving only adults or cleft palate patients were not considered. Also, since ME induces bending in the maxilla walls, a sufficient portion of the skull must be included for acceptance in this review. At minimum, the maxilla bone must be included up to the approximate region of the zygomatic suture.

The search was restricted to English language, online journal articles from three databases: Pubmed, Scopus, and Biosis. To find relevant articles, a broad search was used to find articles with any link to the midpalatal suture or palatal expansion in conjunction with articles containing predictive models or FEA. Search terms were developed using keywords specific to each database. Both PubMed and Scopus use Medical Subject Headings (MeSH), while Biosis tags fields based on major concepts. The specific terms were searched in combination as keywords as well as in all fields to determine the combination which had the greatest number of search results. There were some exceptions to this strategy, as "Cranial Sutures", a MeSH term, was only searched as a MeSH term because articles containing the phrase "cranial sutures" without any of the other search terms were not of interest.

All search terms relating to maxillary expansion were combined with “or” and all search terms relating to a predictive model or FEA study were combined with “or” as well. These two groups of search terms were then combined with “and”. The MeSH terms relating to maxillary expansion were “Cranial Sutures”, “Palatal Expansion Technique”, “Tissue Expansion Devices”, “Tissue Expansion”, “Maxillofacial Abnormalities”, “Maxilla”, and “Palate”. Additional keywords that were searched were “midpalatal suture”, “mid-palatal suture”, and combinations including the roots palat*, maxill*, and expan*. The most results were found when using the keywords “maxillary expansion” and “palatal expansion” as specific statements. The midpalatal suture is also called the median palatine suture, therefore combinations including (medi* SAME palat*) were also searched; however, these combinations did not add to the results. The MeSH terms concerning the modeling of the suture were found to be “Models, Theoretical”, “Models, Anatomic”, “Models, Biological”, “Models, Structural”, and “Computer Simulation”. The other important keyword used was “Finite Element”.

The final search terms in PubMed were “((("Cranial Sutures"[MeSH] OR "Palatal Expansion Technique"[Mesh] OR "Tissue Expansion Devices"[Mesh] OR "Tissue Expansion" OR "Tissue Expansion"[Mesh]) OR ("Maxilla"[Mesh] OR "Palate"[Mesh] OR "Maxillofacial Abnormalities"[Mesh] OR “maxillary expansion” OR “palatal expansion”)) AND ("Models, Theoretical"[Mesh] OR "Models, Anatomic"[Mesh] OR "Models, Biological"[Mesh] OR "Computer Simulation" OR "Computer Simulation"[Mesh] OR "Models, Structural"[Mesh] OR “Finite Element Analysis”[MeSH] OR "Finite Element"))”. A similar process was followed with Scopus, but different keywords were successful in this database. The final search terms were (INDEXTERMS("Palatal Expansion Technique" OR "Tissue Expansion Devices" OR "Maxilla" OR "Palate" OR "Maxillofacial Abnormalities" OR "cranial sutures") OR "Tissue Expansion" OR (maxilla* PRE/2 expan*) OR (palat* PRE/2 expan*)) AND (INDEXTERMS("Models, Theoretical" OR "Models, Anatomic" OR "Models,

Biological" OR "Models, Structural") OR "Computer Simulation" OR "finite element" OR "FEA" OR "FEM").

Biosis followed a different cataloguing system. None of the major concepts specifically related to the midpalatal suture or ME, as such related keywords were searched as topics. Both major concepts and topics were included in the search terms for the numerical model. The final search terms in Biosis were (TS=(maxilla* SAME expan*) OR TS=(palat* SAME expan*) OR TS=(midpalatal sutur*) OR TS=(mid-palatal sutur*)) AND (MC=("Information Studies" OR "Models and Simulations" OR "Mathematical Biology" OR "Computer Applications") OR TS=("Finite Element")).

Articles were then screened based on their titles and abstracts. Any reviews, editorials, or similar that were not full articles were removed. As well, studies that dealt specifically with only maxillary protraction, Le Fort I osteotomies, dental implants, craniosynostosis, and other topics unrelated to ME were removed.

Eligibility criteria used during the full text assessment excluded articles that ultimately provided no simulation or predictive model for maxillary expansion based on force, expansion, or stress. Also, articles that only involved combinations of ME with other forces such as protraction were removed. Based on the criteria for a model of ME in adolescents with a normal palate, models solely considering cleft palates, surgically assisted maxillary expansion, and expansion in adults were also removed. Finally, studies that did not incorporate the maxilla walls in their model were rejected. This acceptance/rejection process is illustrated in Figure 3-1.

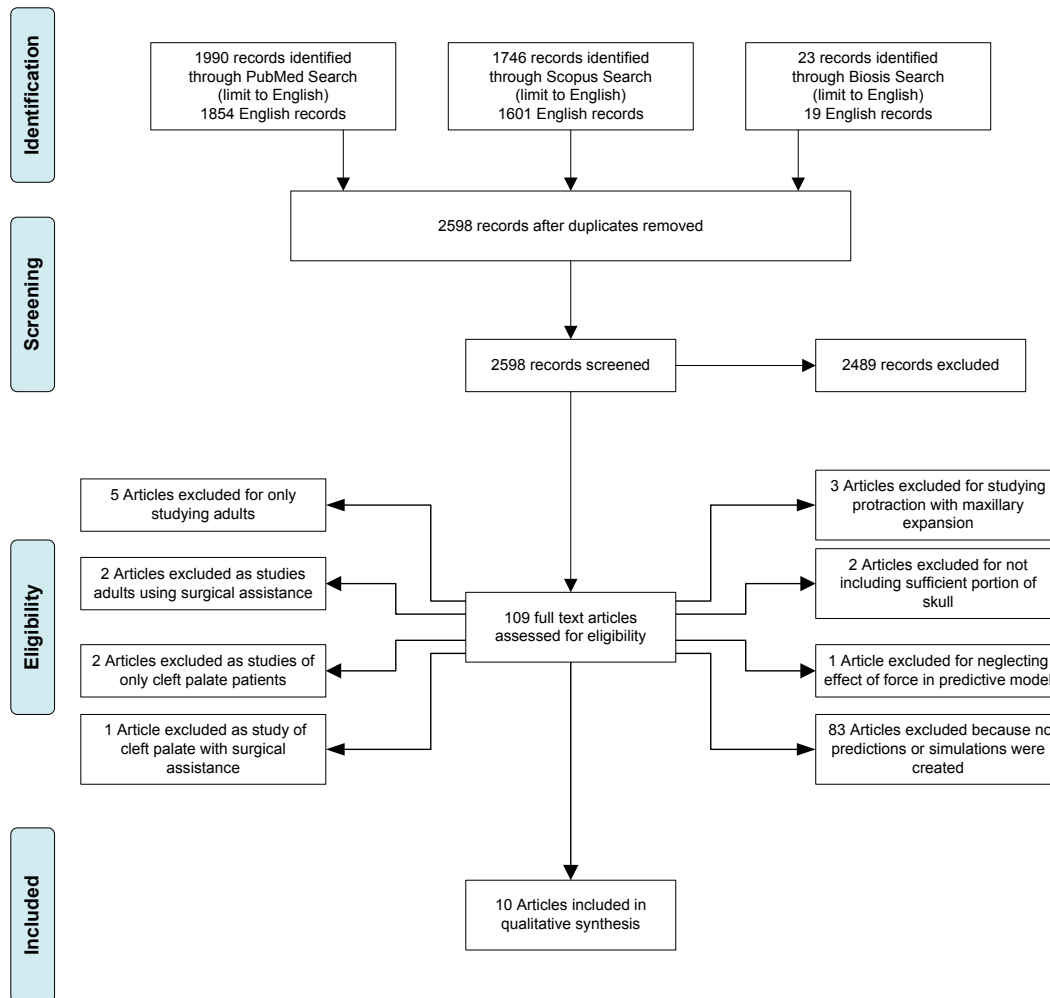


Figure 3-1: Flowchart describing inclusion/elimination of articles from systematic review

3.3. RESULTS

Together, the three databases yielded 3,474 articles in English. After duplicates were removed, the number decreased to 2,598. One hundred and nine full text articles were retrieved and assessed for eligibility. Ten articles were ultimately included. As the midpalatal suture was the focus of this review, data involving this suture was extracted. Specifically, assumptions made about the suture and material properties used in the model are recorded in Table 3-1.

Table 3-1: List of Midpalatal Suture Material Properties used in FEA Simulations

Author (Year)	Model Assessed	Assumptions Made	Suture Properties Used Elastic Modulus	Poisson's Ratio
Lee (2009)	Solid (same material properties throughout model)	linear elastic homogeneous isotropic	1.37×10^3 kg/mm ²	0.3
	Fused (separate properties for suture)	linear elastic homogeneous isotropic suture properties equivalent to PDL	6.8×10^{-2} kg/mm ²	0.49
	Patent (no suture)		0 kg/mm ²	--
Provatidis (2008)	unossified (suture has minimal properties)	linear elastic homogeneous isotropic	1 MPa	0.3
	partly ossified (suture has properties of some significance)	linear elastic homogeneous isotropic	500 MPa	0.3
	fully ossified (same properties throughout)	linear elastic homogeneous isotropic	13 700 MPa	0.3
Gautam (2007)	observed von Mises stresses in sutures as a result of ME		vacant	--
Holberg (2007)	suture properties the same as bone	linear homogeneous isotropic	13 700 MPa	0.3
Provatidis (2007)	sutures "open"	linear elastic homogeneous isotropic	1 MPa	0.3
	sutures "closed" (same properties as bone)	linear elastic homogeneous isotropic	13 700 MPa	0.3

Author (Year)	Model Assessed	Assumptions Made	Suture Properties Used	
			Elastic Modulus	Poisson's Ratio
Provatidis (2006)	circummaxillary, midsagittal, median palatine sutures open; all others same as bone	linear elastic homogeneous isotropic	1 MPa	unspecified
	circummaxillary, midsagittal, median palatine sutures open; all others same as bone used stress relaxation	linear elastic homogeneous isotropic	1 MPa	unspecified
	all sutures unossified/open	linear elastic homogeneous isotropic	1 MPa	unspecified
	all sutures ossified	linear elastic homogeneous isotropic	13 700 MPa	unspecified
	only midsagittal and median palatine suture unossified	linear elastic homogeneous isotropic	1 MPa	unspecified
Jafari (2003)	sutures have same properties as bone		vacant	--
Iseri (1998)	majority of sutures given properties of bone, but midpalatal suture vacant		vacant	--
Culea (2009)	suture has properties of bone	linear elastic homogeneous isotropic	9 600 MPa	0.3
Provatidis (2003)	ME device applies load in single step	“sutures: of small elastic modulus”	unspecified	unspecified
	ME device applies load in small increments and assumes residual stresses become zero between loads	“sutures: of small elastic modulus”	unspecified	unspecified

From the articles included in this review it was found that the midpalatal suture material properties were assigned in one of three ways: the suture was

removed from the analysis, was assumed to have the same linear elastic properties as surrounding bone, or was assigned linear elastic properties indicative of soft tissues. Each of the cases was found a total of five times in accepted literature. Several of the included studies considered multiple modeling approaches. In instances where both accepted and rejected models were discussed, only cases relevant to this review were considered.

Studies by Holberg (2005) [14] and Holberg and Rudzki-Janson (2006) [15] that have been rejected require further discussion. While all of these articles include models that target simulation of ME in adolescents, they do not incorporate the maxilla bones. These studies were concerned with the effects of ME on the sphenoid and cranial base, respectively. In Holberg (2005) [14] only the sphenoid was modeled in the FEA while Holberg and Rudzki-Janson (2006) [15] considered the sphenoid, frontal bone, occipital bone, and both temporal bones. A focal point of this review is discussing the amount of load carried by bending of the maxilla walls compared to the tensile load on the midpalatal suture. As such, any model must have included both structures in order to be accepted. Both Lee *et al.* (2009) [5] and Holberg *et al.* (2007) [8] consider models of the skull that are not entirely complete, but in both instances the maxilla bones and midpalatal suture are included. This is sufficient to provide valuable information for this review even though the entire skull was not modeled.

An individual model that requires further attention is the partially ossified model presented by Provatidis *et al.* (2008) [4]. In this model the authors hypothesized that the partially fused suture would have an elastic modulus of 500 MPa compared to the fused modulus of 13700 MPa and the unfused value of 1 MPa. It is evident that for a partially fused suture the elastic modulus will be somewhere between fused and unfused values; however, exactly what the true value should be will depend on degree of ossification. Experimental work surrounding bone [16] and soft tissues, such as the periodontal ligament [17], is widely available in the literature, while little is understood about material properties for a partially ossified midpalatal suture. As such, this particular case

will not be considered. While this is a very interesting topic, and one that should be considered in the future, it is not yet understood well enough to be included here.

The discussion of papers chosen for this review will be qualitative in nature, focusing on the choice of material properties for the midpalatal suture. While it is desirable in many reviews to numerically analyze results of the accepted studies, typically through statistical analysis, it does not make sense in this instance. Model geometry, element choice, and load application differ amongst studies making direct comparison of results impractical. In order to directly compare results it would require that all parameters be the same for different cases. For instance, a study by Lee *et al.* (2009) [5] considered various suture properties using the same geometry which allows for comparison amongst the models; however, cross-study comparison when different geometries have been used cannot be accomplished. Although quantitative comparison may not be accomplished, a qualitative approach will still provide valuable insight into the state of FEA for ME treatment and the direction for future work.

3.4. DISCUSSION

Each of the aforementioned assumptions for the midpalatal suture in FEA simulations carries specific advantages and disadvantages which will now be considered. Included in this discussion will be a simplified analysis of the maxilla complexes response to an applied load. This model is not meant to be taken as a highly accurate representation of the true situation, but rather to serve as a discussion point for directing future research. Even after dramatic simplification, it is evident that the maxilla's response to ME is highly complex and further investigation is required to better understand its behavior.

3.4.1. Assuming No Material

In five studies [5-7,9,10] at least one of the models presented in each case assumed the midpalatal suture material to be vacant. In the case of Culea and Bratu (2009) [6] and Lee *et al.* (2009) [5], the suture elements themselves were entirely removed from the model. A different approach to removing the suture from the FEA was taken by Jafari *et al.* 2003 [10], Iseri *et al.* (1998) [9], and

Gautam *et al.* (2007) [7]. In these studies the authors assigned bone material properties to the suture but left nodes on the central plane of symmetry unconstrained, allowing for free motion. Even though bone properties were assigned, the midpalatal suture will not provide resistance. Thus, the three previously mentioned studies were classified as assuming a vacant suture [7,9,10].

When considering models that have removed material from the midpalatal suture it is expected that the overall cranial structure will become less stiff during ME. That is, when a given force is applied to a skull lacking midpalatal suture material larger displacements will be observed than if the skull had material present. The work by Lee *et al.* (2009) [5] considers cases of no material as well as having bone and soft tissue properties. While no numerical displacement results are directly reported in the study, deformed fringe plots in the lateral view for all three cases are provided. When visually inspecting these it appears that the “patent model”, FEA without the midpalatal suture, shows larger displacements than the others. Without numerical results no firm observations can be made, but solely based on visual inspection this appears to be the case. A study that focuses on displacements of different cases in the future would certainly be of interest.

Besides the expected differences in displacement, it can also be postulated that the stress distribution will differ from the true case especially at the interface between the suture and surrounding bone. Assuming that the bone and suture remain attached, for static equilibrium it is necessary for the force acting on the suture to be equal and opposite of that acting on the bone at their interface. Thus, how the suture responds to loading will influence the stresses determined in the suture and in the local region surrounding it. By removing the suture its influence on stress and strain is lost. Lastly, by removing material from the midpalatal suture an artificial discontinuity is generated in the analysis. The normal stress, traction, on a free surface must vanish. A direct consequence of this is that there can be no traction on the inside surface of the midpalate when the suture material has been removed. In reality this of course is not the case. When inspecting the results from Lee *et al.* (2009) [5], and comparing stresses without the suture to

those where suture material was present, substantial discrepancies, some in excess of 50%, were noted.

3.4.2. Assuming Bone Properties

Work by Lee *et al.* (2009) [5], Holberg *et al.* (2007) [8], and Provatidis *et al.* [4,18,19] all utilized FEA where the midpalatal suture was assumed to have the same properties as surrounding bone. In all cases the Poisson's Ratio was assigned a value of 0.3 with elastic moduli of $1.37 \times 10^3 \text{kg/mm}^2$ (13440MPa) [5] or 13700MPa [4,8,18,19] being used. As previously mentioned, if the suture was assigned bone material properties but nodes on the central plane of symmetry were left unconstrained, then the model was classified as leaving the suture vacant. The five models considered here both assigned bone properties and constrained the central nodes of the suture.

Assuming the midpalatal suture to have the same properties as bone would lead one to believe that the model will be stiffer than the true case where the suture has not completely fused. In general, the elastic modulus of soft tissues, say the periodontal ligament, is on the order of MPa (10^6 Pa) [17] while that of bone is approximately 1000 times larger on the scale of GPa (10^9 Pa) [16]. With such a large discrepancy in properties it would be expected to see less deformation when bone properties have been used instead of soft tissue properties, and certainly less than when the midpalatal suture is vacant. Again, Lee *et al.* (2009) [5] considered all three cases but a lack of numerical data for displacements prevents any strong conclusions from being drawn.

By including material in the location of the midpalatal suture there is no longer a discontinuity that will influence stress distribution. The issue now moves to the relevance of the material model and properties. The elastic modulus of soft tissue can be significantly different from that of bone. With respect to FEA, selecting an inappropriate elastic modulus will influence displacements which are then used to calculate stresses. It has been found that suture ossification is still relatively low, less than 15%, even for adults well into their twenties and thirties [20]; thus, using bone properties for the midpalatal suture in adolescents is inaccurate. In addition, the studies included here are all linear elastic models

when in fact sutures are viscoelastic, non-linear, behaving materials [11,21]. When evaluating stresses and/or strains in the suture region it will be necessary to accurately represent the suture, as will be discussed in a forthcoming section.

3.4.3. *Assuming Soft Tissue Properties*

Five models from literature accepted in this review considered the midpalatal suture to have properties indicative of soft tissue [4,5,18,19,22]. Elastic moduli ranged from $6.8 \times 10^{-2} \text{kg/mm}^2$ (0.667MPa) [5] to 1MPa [4,18,19] and Poisson's ratios of 0.3 [4,18,19] and 0.49 [5] were utilized. A value of 0.5 for the Poisson's ratio means that the material is incompressible and will undergo no volume change when deformed [23,24]. Materials with a ratio less than 0.5 indicate a level of compressibility under deformation. For example, a Poisson's ratio of 0.3 is in the range of materials such as steel [25] or bone [26].

Of all the models considered in this review, using soft tissue properties is the closest to reality. Elastic properties used for the midpalatal suture in accepted studies have been based off of properties for the periodontal ligament, as in Lee *et al.* (2009) [5], or those used in a past study [4,18,19]. The previous study cited by Provatidis *et al.* [4,18,19] considered FEA of the dog skull [27] and had no experimental data at their disposal when assigning properties to the suture. As a result, they were arbitrarily chosen. Tanaka *et al.* (2000) [12] found that the relaxed elastic modulus of the unexpanded interparietal suture in rats ranged from 0.64 MPa at low strain to 4.51 MPa at higher strain. The studies considered here all used values inside this range, thus it is likely that they at least provided a reasonable approximation of the sutures elastic properties. All models were for linear elastic behavior, and as will be discussed in the following section it would be advantageous to consider the viscoelasticity of the suture in future FEA studies.

3.4.4. *The Suture as a Viscoelastic Material*

All studies that have been accepted in this review utilized linear elastic properties for the midpalatal suture. In certain instances this may be an acceptable simplification of the suture; however, incorporating the viscoelastic behavior of the suture would lead to a more robust model with wider applicability.

The advantages and disadvantages of both will be discussed here in detail as they pertain to FEA simulations of ME.

Using linear elastic, homogeneous, and isotropic (LEHI) models in FEA is desirable for a number of reasons. First, the model is easily implemented as only two elastic constants are required. Typically the Poisson's ratio and elastic modulus are used, but so long as two of the three constants are known then the third, shear modulus in this case, may be determined [23]. Not only is this model simple to use, it is also the best option for computational time and effort. Avoiding nonlinear numerical methods shortens solution time and uses less computational memory. Essentially, LEHI assumptions will allow for easier setup of a FEA model and a faster solution.

A viscoelastic material is one that exhibits phenomena such as creep and stress-relaxation. Creep is the continuous deformation of a material under a constant force, and the reduction in stress while a deformation is held constant is known as stress-relaxation. Incorporating a viscoelastic model into the FEA would increase simulation accuracy as it is a more physically representative model. The disadvantage is that the analysis becomes more complex and will increase computational effort and time.

The type of material model to use for the midpalatal suture should depend largely on the study goals. For instance, if the initial response of the skull to a known applied force is desired, then the suture's viscoelastic nature may not be necessary to obtain sufficiently accurate results. On the other hand if a transient analysis is considered (e.g. the response over time), then the viscoelastic behavior should be incorporated. Linear elastic models may be used in time-dependent analyses, but they are not able to represent creep and/or stress-relaxation which may be present. It would be ideal in the future to conduct a FEA simulation of ME from the very beginning of treatment to completion. To obtain the most accurate and physically representative results, it will be necessary to incorporate the viscoelastic behavior of the midpalatal suture. This is especially true when investigating results near, or inside, the suture.

Future experimental work that focuses on stress-strain behavior of the midpalatal suture, and subsequent theoretical modeling of the data, would make a valuable contribution to this field. Provatidis *et al.* [18,19] presents a “pseudoviscoelastic” FEA model where loading is accomplished in several steps. At the beginning of each load-step the residual stresses are set to zero while keeping displacements from the previous step in an attempt to model the skull’s stress-relaxation behavior. This is a reasonable first step towards modeling the viscoelastic response of the skull during ME, but in reality residual stresses everywhere would not vanish to zero [28]. If a detailed model for the suture were developed it could be utilized along with viscoelastic modeling of bone [16,29] to perform a more accurate FEA. This would prevent researchers from making arbitrary assumptions such as forcing residual stresses to zero.

Incorporating the viscoelastic behavior of the midpalatal suture into FEA studies will also allow for more accurate prediction of suture failure. Under a rapid displacement there will be a sudden spike in force, or stress, followed by the subsequent relaxation if the displacement is held constant. During ME it is ideal to widen the maxilla halves without tearing the midpalatal suture [30-32]. By experimentally studying failure criteria of the midpalatal suture and implementing a viscoelastic model, it would allow researchers to observe if a given treatment protocol is likely to cause suture tearing. Linear elastic models are unable to account for strain-rate dependency of the tissues response which is critical to investigating failure.

3.4.5. Discussion of the Maxilla Complex as a System

A simplified model of the maxilla complex will now be presented to aid in illustrating its response to expansion loads. This model is not to be taken as a detailed and highly accurate representation of the true scenario, only as a tool for discussion. By considering the simplified geometry here it will become evident as to where, and why, more investigation of ME and FEA will be advantageous in the future.

First, consider all cranial sutures to be fused except the midpalatal suture. This forms the extreme scenario where the remainder of the maxilla complex is at

its stiffest compared to the midpalatal suture. Also, consider the suture to act as a linear spring with an effective stiffness, k_{eff} . There are many sources of resistance inside the suture, all with their own value of stiffness. For simplicity k_{eff} will be used to account for all possible influences (e.g. collagen, elastin, etc.). Steady-state analysis is considered here to neglect any rate-dependency of bone or soft tissue. In reality both the suture and bone exhibit viscoelastic behavior but this will not be considered here. Finally, a 2D rectangular beam model will be utilized. Using a 3D model with the true geometry would unnecessarily complicate this analysis beyond the current objective of exploring bone flexure and midpalatal suture resistance.

Taking into account the aforementioned assumptions, and using beam theory [33], the overall system is modeled in two parts: a cantilevered beam with elastic modulus, E_B , and moment of inertia, I_B , representing the bone and fused sutures; the midpalatal suture given an effective stiffness k_{eff} . The expansion force, F_{exp} , is applied at a distance L from the point where the maxilla bone attaches to the rest of the skull. The force of the midpalatal suture, modeled as a spring force, is denoted as F_s and is equal to the effective stiffness, k_{eff} , times the displacement evaluated at the springs y -location, $x(y=L-s)$. The system representation and resulting free body diagram are shown in Figure 3-2. As noted in the free body diagram, the coordinate system has been chosen such that the x -direction is positive to the left and y -direction is positive downwards. By right-hand coordinate system convention this leads to moments being positive in the counter-clockwise direction. The resultant force in the x -direction and bending moment are denoted as R and M , respectively.

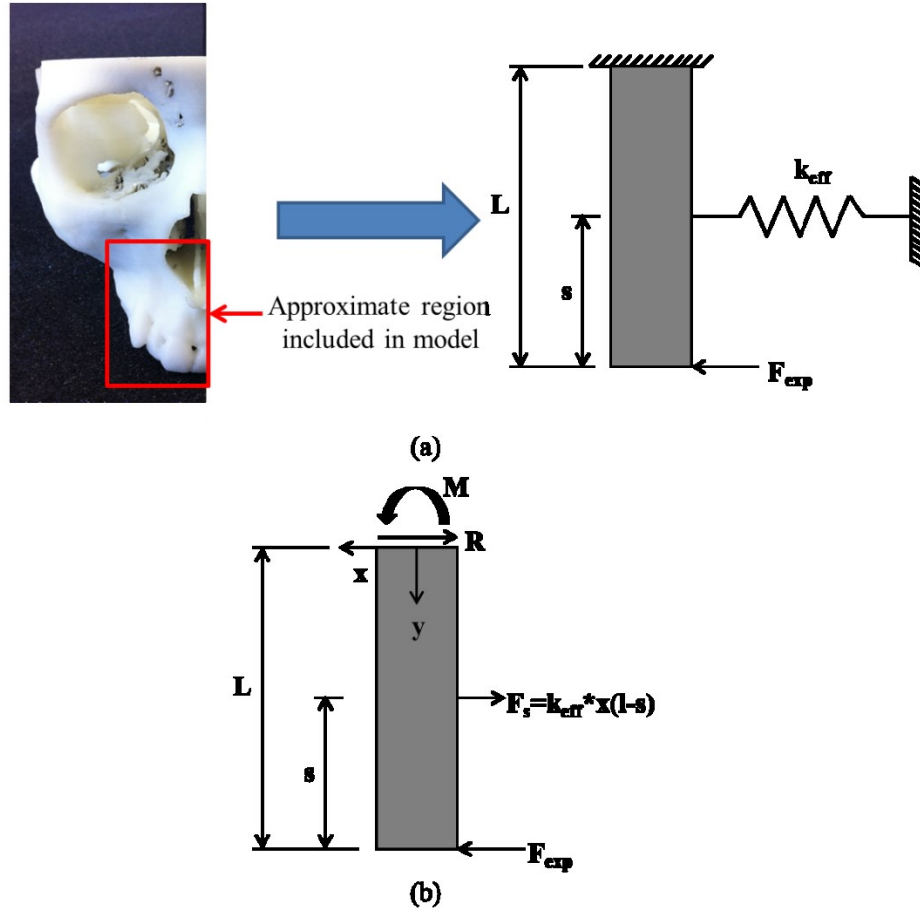


Figure 3-2: (a) Half-section of manufactured human skull and the model representation of the maxilla complex; (b) free body diagram of the model representation

In order to better understand how this system will behave as a result of F_{exp} , beam theory and singularity functions are used to obtain a relationship for displacement in terms of M , F_{exp} , E , I , k_{eff} , L , and s . A detailed discussion of the process will not be given here, but references [33-35] along with most textbooks relating to strength of materials may be consulted for more information. The following relationships are obtained for displacement at the point of force application, $x(y=L)$, and at the midpalatal suture, $x(y=L-s)$:

$$x(y=L) = \frac{1}{(EI)_B} \left[\frac{k_{eff} * x(y=L-s) * (L^3 - s^3)}{6} - \frac{F_{exp} * L^3}{6} - \frac{M * L^2}{2} \right] \quad (1)$$

$$x(y = L - s) = \frac{1}{(E * I)_B - \left[\frac{k_{eff} * (L^3 - s^3)}{6} \right]} \left[\frac{M * (L - s)^2}{2} - \frac{F_{exp} * (L - s)^3}{6} \right] \quad (2)$$

Equation (2) may be rearranged in order to isolate for the bone bending moment in terms of other variables as:

$$M = \frac{2}{L^2} \left[\frac{k_{eff} * x(y = L - s) * (L^3 - s^3)}{6} - \frac{F_{exp} * L^3}{6} - (E * I)_B * x(y = L) \right] \quad (3)$$

Inspecting eq. (1) – (3) there are several qualitative observations that can be made about how this system will behave under application of an expansion force. First, the idea that bone bending is the source of greatest resistance to expansion will be considered. From eq. (3) it can be seen that the magnitude of M will depend on several variables. Considering only material or geometric properties, the value of moment will decrease as k_{eff} increases and/or the difference $L^3 - s^3$ increases. Moment will also decrease as the displacement $x(y=L-s)$ increases. That is, the first term inside the bracket of eq. (3) will oppose the other two. This occurs as the difference between $(E * I)_B$ and $[k_{eff} * (L^3 - s^3)]/6$ decreases. On the other hand, as the stiffness of bone or its moment of inertia increases the moment will increase. Being that the magnitude of M depends on many factors, not just k_{eff} or E_B , it is necessary to further investigate this system with an accurate representation of the midpalatal suture. Observations from such an analysis would then allow researchers to accurately state how much of the expansion load is resisted through bone bending compared to tension in the midpalatal suture.

Changes in the displacement $x(y=L)$ will now be considered as a result of either neglecting the suture or considering it to have the same properties as surrounding bone. If k_{eff} is removed entirely from Equation (1) then the displacement at $y=L$ will artificially increase. Conversely, if k_{eff} is assumed to have the same properties as bone then $x(y=L)$ will decrease as the $k_{eff} * x(y=L-s) * (L^3 - s^3)/6$ term increases. Thus, based on this analysis, it can be seen that for the most accurate results the midpalatal suture should be included in the analysis;

furthermore, accurate properties indicative of the unfused suture should be used as not to under-predict displacements. This analysis supports the suggestions made in previous sections regarding assignment of suture material properties in FEA studies.

As previously mentioned, bone is typically much stiffer than soft tissue; however, it would be premature to simply neglect the sutures contributions during ME solely due to this fact. The moment of inertia of the maxilla bone as well as the distance to the suture will also play a role. Further to this, the analysis completed here is for a simplified, static, 2D case. If the actual physical situation is considered the system becomes even more complicated. This is especially true of the time-dependent viscoelastic properties of the midpalatal suture. It is not being suggested that the suture will necessarily have a significant influence on system behavior during treatment. Instead, it is the opinion of the authors that further research into maxilla complex behavior during ME needs to be conducted before the suture can simply be neglected from the analysis. The system is inherently complex and more factors other than elastic modulus will contribute to the suture's resistance.

3.5. CONCLUSIONS

Utilization of FEA in simulating ME treatment for adolescents has proven to be a useful tool available for researchers. From this review it has been found that authors have made valuable contributions to the literature; however, substantial work remains. Depending on the research objective it may be ideal to incorporate an accurate, viscoelastic model of the midpalatal suture. An example of such an instance would include an analysis that is primarily focused on stresses or strains near the suture. If researchers wish to move towards simulation of ME over the entire treatment period, then it will be necessary to incorporate a viscoelastic model. By their very definition, linear elastic models cannot account for time-dependent behavior while a viscoelastic model can. This would provide researchers with a more robust model that could be used in both static and transient analyses.

In the future it will be necessary to further investigate ME treatment in adolescents using a more accurate model of the midpalatal suture. As illustrated by the simplified analysis, the maxilla complex is an intricate system and its response will depend on several variables. If one component of the system is neglected or described inaccurately it can have a resounding effect throughout. Research to this point has made important and necessary steps in moving towards the ultimate goal of whole-treatment simulation. One of the next important steps will be further investigation of the midpalatal suture and its influence on ME treatment in adolescents.

3.6. REFERENCES

1. Angell EH. Treatment of irregularity of the permanent or adult teeth. Part 1. *Dental Cosmos*. 1860;1:540-544.
2. Angell EH. Treatment of irregularity of the permanent or adult teeth. Part 2. *Dental Cosmos*. 1860;1:599-560.
3. Romanyk DL, Lagravère MO, Toogood RW, Major PW, Carey JP. Review of maxillary expansion appliance activation methods: engineering and clinical perspectives. *Journal of Dental Biomechanics*. 2010;2010:496906.
4. Provatidis CG, Georgiopoulos B, Kotinas A, McDonald JP. Evaluation of craniofacial effects during rapid maxillary expansion through combined in vivo/in vitro and finite element studies. *European Journal of Orthodontics*. 2008;30:437-448.
5. Lee H, Ting K, Nelson M, Sun N, Sung SJ. Maxillary expansion in customized finite element method models. *American Journal of Orthodontics and Dentofacial Orthopedics*. 2009;136:367-374.
6. Culea L, Bratu C. Stress analysis of the human skull due to the insertion of rapid palatal expander with finite element analysis (FEA). *Key Engineering Materials*. 2009;399:211-218.
7. Gautam P, Valiathan A, Adhikari R. Stress and displacement patterns in the craniofacial skeleton with rapid maxillary expansion: a finite element method study. *American Journal of Orthodontics and Dentofacial Orthopedics*. 2007;132:5 e1-11.

8. Holberg C, Holberg N, Schwenzer K, Wichelhaus A, Rudzki-Janson I. Biomechanical analysis of maxillary expansion in CLP patients. *Angle Orthodontist*. 2007;77:280-287.
9. Iseri H, Tekkaya AE, Oztan O, Bilgic S. Biomechanical effects of rapid maxillary expansion on the craniofacial skeleton, studied by the finite element method. *European Journal of Orthodontics*. 1998;20:347-356.
10. Jafari A, Shetty KS, Kumar M. Study of stress distribution and displacement of various craniofacial structures following application of transverse orthopedic forces--a three-dimensional FEM study. *Angle Orthodontist*. 2003;73:12-20.
11. Herring SW. Mechanical influences on suture development and patency. *Frontiers of Oral Biology*. 2008;12:41-56.
12. Tanaka E, Miyawaki Y, de Pozo R, Tanne K. Changes in the biomechanical properties of the rat interparietal suture incident to continuous tensile force application. *Archives of Oral Biology*. 2000;45:1059-1064.
13. Tanaka E, Miyawaki Y, Tanaka M *et al.*. Effects of tensile forces on the expression of type III collagen in rat interparietal suture. *Archives of Oral Biology*. 2000;45:1049-1057.
14. Holberg C. Effects of rapid maxillary expansion on the cranial base--an FEM-analysis. *Journal of Orofacial Orthopedics*. 2005;66:54-66.
15. Holberg C, Rudzki-Janson I. Stresses at the cranial base induced by rapid maxillary expansion. *Angle Orthodontist*. 2006;76:543-550.
16. Fung YC. Chapter 12: Bone and cartilage. In: *Biomechanics: Mechanical properties of living tissues*. 2nd ed. New York, NY: Springer-Verlag; 1993.p. 510-513.
17. Fill TS, Carey JP, Toogood RW, Major PW. Experimentally determined mechanical properties of, and models for, the periodontal ligament: critical review of current literature. *Journal of Dental Biomechanics*. 2011;2011: 312980.
18. Provatidis C, Georgiopoulos B, Kotinas A, MacDonald JP. In vitro validated finite element method model for a human skull and related craniofacial effects

- during rapid maxillary expansion. *Proceedings of the Institution of Mechanical Engineers. Part H: Journal of Engineering in Medicine.* 2006;220:897-907.
19. Provatidis C, Georgiopoulos B, Kotinas A, McDonald JP. On the FEM modeling of craniofacial changes during rapid maxillary expansion. *Medical Engineering and Physics.* 2007;29:566-579.
 20. Knaup B, Yildizhan F, Wehrbein H. Age-related changes in the midpalatal suture. A histomorphometric study. *Journal of Orofacial Orthopedics.* 2004;65:467-474.
 21. Popowics TE, Herring SW. Load transmission in the nasofrontal suture of the pig, *Sus scrofa.* *Journal of Biomechanics.* 2007;40:837-844.
 22. Provatidis C, Georgiopoulos B, Kotinas A, McDonald JP. In-vitro validation of a FEM model for craniofacial effects during rapid maxillary expansion *Proceedings of the IASTED International Conference on Biomechanics; 2003 June 30-July 2; Rhodes, Greece: Acta Press; 2003: p. 68-73.*
 23. Hibbeler RC. Strain transformation. In: *Mechanics of materials. SI Edition.* Singapore: Prentice Hall Inc.; 2004. p. 512-515.
 24. Callister WD. Mechanical properties of metals. In: *Materials Science and Engineering: an introduction. 6th ed.* Hoboken, NJ: John Wiley & Sons Inc.; 2003. p. 121-123.
 25. Norton RL. Appendix C: Material Properties. In: *Machine Design: an integrated approach. 3rd ed.* Upper Saddle River, NJ: Pearson Prentice Hall; 2006. p. 943-950.
 26. Shahar R, Zaslansky P, Barak M, Friesem AA, Currey JD, Weiner S. Anisotropic Poisson's ratio and compression modulus of cortical bone determined by speckle interferometry. *Journal of Biomechanics.* 2007;40:252-264.
 27. Verrue V, Dermaut L, Verheghe B. Three-dimensional finite element modelling of a dog skull for the simulation of initial orthopaedic displacements. *European Journal of Orthodontics.* 2001;23:517-527.

28. Isaacson RJ, Ingram AH. Forces produced by rapid maxillary expansion. II. Forces present during treatment. *Angle Orthodontics*. 1964;34:261-270.
29. Johnson TP, Socrate S, Boyce MC. A viscoelastic, viscoplastic model of cortical bone valid at low and high strain rates. *Acta Biomaterialia*. 2010;6:4073-4080.
30. Storey E. Tissue response to the movement of bones. *American Journal of Orthodontics*. 1973;64:229-247.
31. Bell RA. A review of maxillary expansion in relation to rate of expansion and patient's age. *American Journal of Orthodontics*. 1982;81:32-37.
32. Liu SS, Opperman LA, Kyung HM, Buschang PH. Is there an optimal force level for sutural expansion? *American Journal of Orthodontics and Dentofacial Orthopedics*. 2011;139:446-455.
33. Popov EP, Balan TA. Symmetric beam bending. In: *Engineering Mechanics of Solids*. 2nd ed. Upper Saddle River, NJ: Prentice Hall; 1998. p. 325-367.
34. Popov EP, Balan TA. Beam statics. In: *Engineering mechanics of solids*. 2nd ed. Upper Saddle River, NJ: Prentice Hall; 1998. p. 267-313.
35. Norton RL. Load determination. In: *Machine design: an integrated approach*. 3rd ed. Upper Saddle River, NJ: Pearson Prentice Hall; 2006. p. 73-126.

4. Developing a Creep Model for the Unfused Midpalatal Suture using Empirical Data from the Midsagittal Suture in New Zealand White Rabbits

This chapter discusses the experimental data transformations and assumptions required for fitting a variety of viscoelastic creep models to previously obtained rabbit midsagittal suture data. A total of four creep modeling approaches are explored and their ability to replicate suture creep data over three applied loads is evaluated. This work forms the basis of suture viscoelastic modeling upon which Chapters 5, 6, and 7 expand. A version of this chapter has been published as:

Romanyk DL, Liu SS, Lipsett MG, Toogood RW, Lagravere MO, Major PW, Carey JP. Towards a viscoelastic model for the unfused midpalatal suture: Development and validation using the midsagittal suture in New Zealand white rabbits. *Journal of Biomechanics*. 2013;46:1618-1625.

4.1. INTRODUCTION

Maxillary expansion (ME), or widening of the upper jaw, is a procedure used to increase palatal width in adolescent patients via insertion of an appliance into the patient's maxilla [1,2]. An active element in the appliance then generates expansion by applying outwardly directed transverse forces or displacements to the palate. Figure 4-1 shows a typical appliance inserted in the upper jaw.



Figure 4-1: Mirror view of a typical expansion appliance inserted in a patient's upper jaw

Predicting patient response to ME has become a topic of interest, especially through use of finite element analysis (FEA) [3-5]. In adolescents the midpalatal suture will exist as soft connective tissue, at least for the most part, and behave as a viscoelastic material [6]. Yet, authors in FEA studies have assumed the suture behaves in a linear elastic manner or they have removed it completely from the analysis [7]. Modeling the suture as a viscoelastic material would allow for improved fidelity of time-dependent simulations.

Viscoelastic modeling of the suture in available literature is sparse. Tanaka *et al.* (2000) [8] used a Kelvin model to describe stress-strain behavior of the interparietal suture in rats, which was then incorporated into a FEA model of suture and surrounding parietal bone. Provatidis *et al.* [4,5] developed a “pseudo-viscoelastic” whole-skull FEA model whereby expansion loads were applied in steps, and the residual stresses were forced to zero at the beginning of each load-step. While these approaches are steps in the right direction, there is more work

that may be done to improve suture modeling. Utilization of more physically representative spring-damper models or advanced nonlinear approaches may provide a better fit to experimental data and should be explored.

The primary goal of this chapter was to conduct preliminary work towards development of an accurate viscoelastic creep model for the human midpalatal suture. Four viscoelastic models were evaluated: Burgers, quasilinear viscoelastic (QLV), modified superposition (MST), and Schapery's model. These models were selected based on their nonlinear description (QLV, MST, and Schapery's models) or because of the physically representative spring-damper configuration (Burgers model). Model parameter determination and validation was accomplished using displacement-time data, at a constant force, from the literature for the midsagittal suture in juvenile New Zealand white rabbits. It was hypothesized, and justified in the following discussion, that the midsagittal suture would behave in a similar manner to the midpalatal suture.

4.2. METHODOLOGY

4.2.1. Modeling Methods

In a first attempt at the detailed modeling of the sutures' creep behavior, literature was consulted to identify relevant existing modeling methods. A total of four methods were selected for evaluation in their current form. Upon identifying a suitable model for predicting suture behavior, future work will focus on altering the chosen model to include specific phenomena (e.g. permanent deformation).

4.2.1.1. QLV Method

One popular way to model the behavior of soft tissues is the quasi-linear viscoelastic (QLV) method proposed by Fung (1993a) [9]:

$$\varepsilon(t) = \int_0^t J'(t-\tau) \frac{d\varepsilon^{(e)}[\sigma(\tau)]}{d\sigma} \frac{d\sigma}{d\tau} d\tau \quad (1)$$

where $J'(t)$ is the reduced creep function and $\varepsilon^{(e)}(\sigma)$ is the elastic strain response. In a study by Yoo *et al.* (2011) [10], creep behavior of bovine extraocular muscles was studied using the QLV method and the following reduced creep function:

$$J'(t) = C_1 t + \frac{C_2 \sinh(C_3 t) - C_4 \cosh(C_3 t)}{C_5 \exp(C_6 t)} + C_7 \quad (2)$$

where C_1 to C_7 represent model constants to be determined experimentally. Substituting (2) into (1) and using a step-input for the stress, with a magnitude of σ_0 , the QLV creep formulation explored in this study is given as:

$$\varepsilon_c(t) = \sigma_0 J'(t) = \sigma_0 \left[C_1 t + \frac{C_2 \sinh(C_3 t)}{C_5 \exp(C_6 t)} - \frac{C_4 \cosh(C_3 t)}{C_5 \exp(C_6 t)} + C_7 \right] \quad (3)$$

4.2.1.2. MST Model

The MST approach is similar to the QLV model with the exception that the MST model considers the creep function inseparable [11]:

$$\varepsilon(t) = \int_0^t J[t - \tau, \sigma(\tau)] \frac{d\sigma(\tau)}{d\tau} d\tau \quad (4)$$

Delgadillo *et al.* (2012) [12] used the MST method to model creep of asphalt binders and proposed the following formulation:

$$\varepsilon_c(t) = \sum_{i=1}^n k_i t^{m_i} \sigma_0^{p_i} \quad (5)$$

where k_i , m_i , and p_i are model constants. If (5) is expanded to $n=2$, and σ is set to σ_0 , then the resulting creep formulation is given as:

$$\varepsilon_c(t) = \sigma_0 J(\sigma, t) = C_1 t^{C_2} \sigma_0^{C_3} + C_4 t^{C_5} \sigma_0^{C_6} \quad (6)$$

C_1 to C_6 represent model coefficients to be determined using experimental data. While asphalt binders are not necessarily related to suture tissue, it is the goal of this study to investigate a variety of viscoelastic models with different qualities, hence its selection.

4.2.1.3. Schapery's Method

Schapery's method is a viscoelastic model based on thermodynamic principles, given as [13,14]:

$$\varepsilon(t) = g_0 D_0 \sigma(t) + g_1 \int_0^t \varphi(\xi_\sigma - \xi'_\sigma) \frac{dg_2 \sigma(\tau)}{d\tau} d\tau \quad (7)$$

$$\xi_{\sigma} = \int_0^t \frac{ds}{a_{\sigma}[\sigma(s)]} \quad (7.1)$$

$$\xi'_{\sigma} = \int_0^{\tau} \frac{ds}{a_{\sigma}[\sigma(s)]} \quad (7.2)$$

where, in general, g_0 , g_1 , g_2 , and a_{σ} are functions of stress, D_0 is the time-independent compliance, and $\varphi(t)$ is the creep compliance. Derombise *et al.* (2011) [15] considered creep of aramid fibers using an adaptation of Schapery's method. Even though aramid fibers differ greatly from suture tissue, the modeling approach used by Derombise *et al.* (2011) [5] is of interest for a general exploration of viscoelastic models. These authors considered irreversible strain in their study; however, this is not a phenomenon that will be considered for the suture at this point. As such, the applicable portion of their creep model reduces to:

$$\varepsilon_c(t) = C_1\sigma_0 + C_2\sigma_0 \log_{10}(t+1) \quad (8)$$

$$C_1 = g_0D_0 \quad (8.1)$$

$$C_2 = g_2D_1 \quad (8.2)$$

where D_1 represents creep rate.

4.2.1.4. Burgers Model

While there are a variety of spring-damper formulations used to model viscoelastic materials [16,17], the Burgers model with constant coefficients was deemed most suitable for preliminary analysis. It was selected due to its instantaneous elastic response, viscous flow, and delayed elasticity; furthermore, it can also model permanent deformation. While permanent strain will not be considered in this study, it is important for future work. The Burgers model is a four-parameter configuration which consists of two springs and dampers as shown in Figure 4-2. The governing equation, eq. (9), and subsequent creep formulation, eq. (10), for the model are given as:

$$\sigma + \left(\frac{C_2}{C_1} + \frac{C_2}{C_3} + \frac{C_4}{C_3} \right) \dot{\sigma} + \frac{C_2C_4}{C_1C_3} \ddot{\sigma} = C_2 \dot{\varepsilon} + \frac{C_2C_4}{C_3} \ddot{\varepsilon} \quad (9)$$

$$\varepsilon_c(t) = \sigma_0 \left\{ \frac{1}{C_1} + \frac{t}{C_2} + \frac{1}{C_3} \left[1 - \exp\left(\frac{-C_3}{C_4} t\right) \right] \right\} \quad (10)$$

where C_1 through C_4 are all constant values.

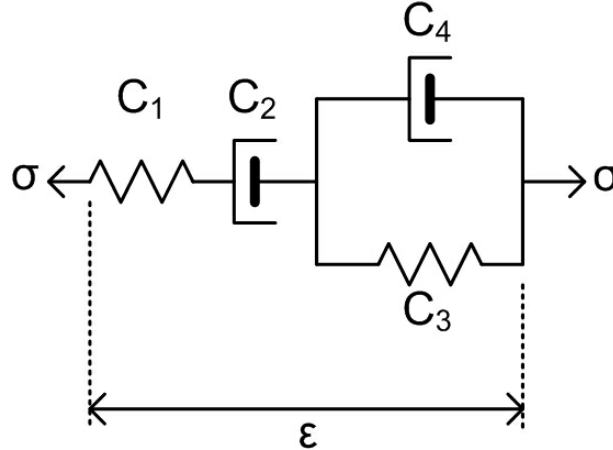


Figure 4-2: Spring-damper configuration of the Burgers model

4.2.2. Experimental Data

As sufficient experimental data for the midpalatal suture in humans or other animals was unavailable to the authors, raw data from Liu *et al.* (2011) [18] for the midsagittal suture (Figure 4-3) in New Zealand white rabbits was used. Sutures were exposed to a nearly constant force magnitude through Sentalloy[®] coil springs (GAC International, Bohemia, NY) at levels of 0.49N (50g), 0.98N (100g), and 1.96N (200g), with displacement(mm)-time(weeks) data being recorded. Mini-screw implants (MSIs) were set at a distance of approximately 4mm on either side of the midsagittal suture (Figure 4-4), to which the compressed springs were attached. Measurements were made using both calipers and radiographs at two-week intervals up to, and including, week six.

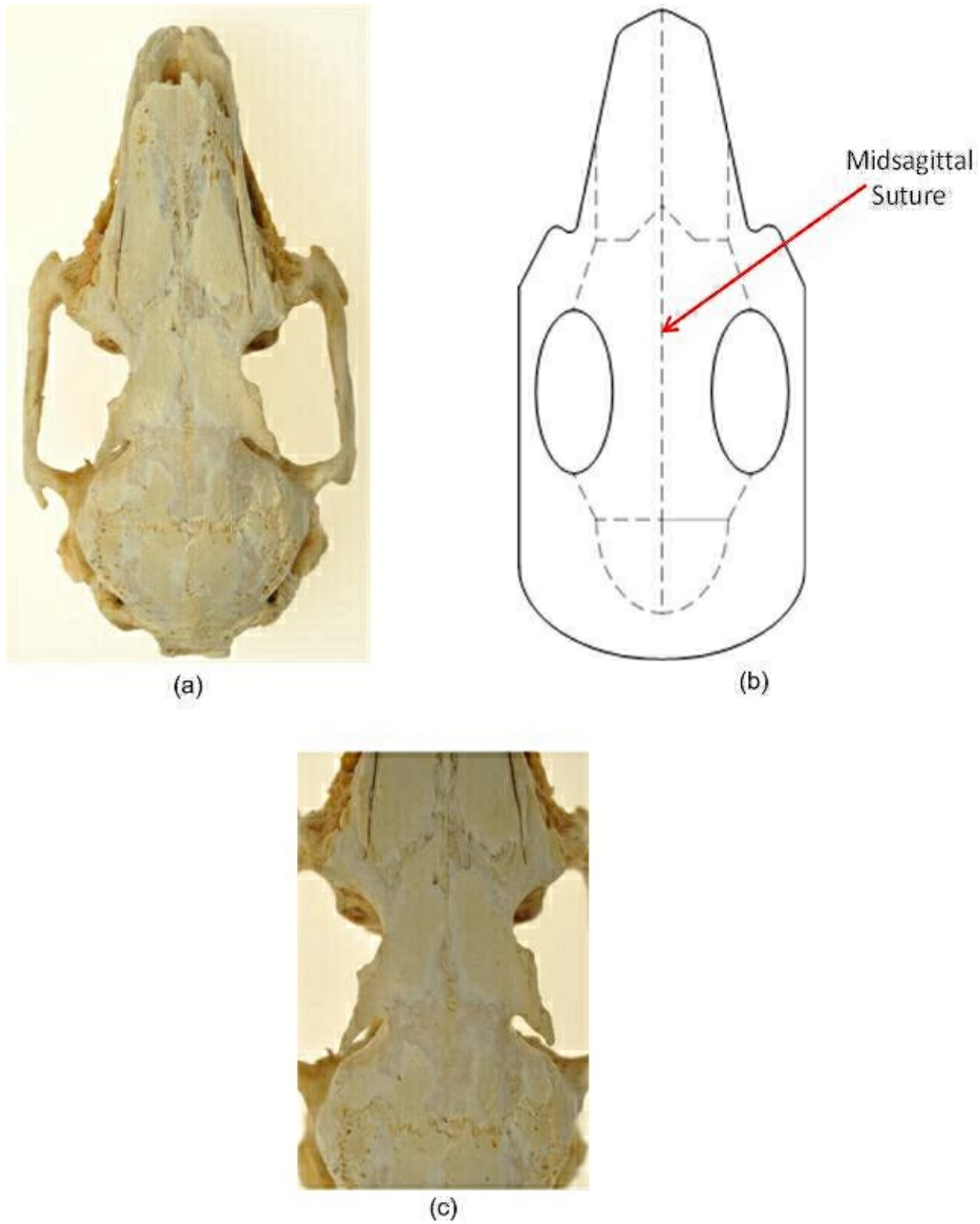


Figure 4-3: (a) Sample image of the whole New Zealand white rabbit skull; (b) schematic of the rabbit skull highlighting the midsagittal suture; (c) enlarged image showing the midsagittal suture on the rabbit skull

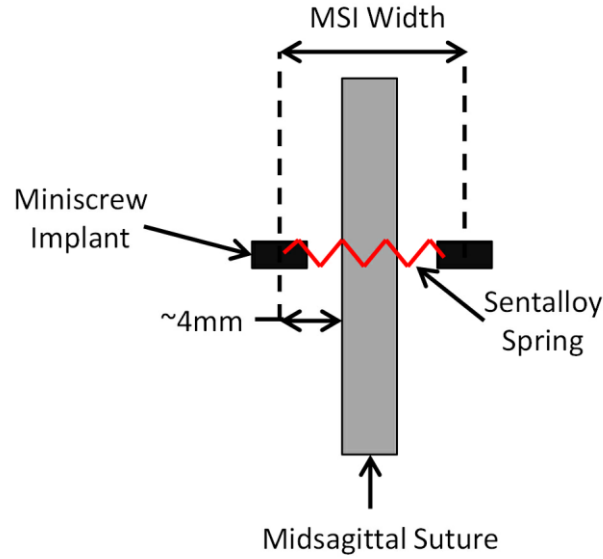


Figure 4-4: Schematic representation of spring and MSI configuration around the midsagittal suture

The original sample size consisted of 37 specimens. Upon removing any unsuccessful expansions (e.g. failed appliance, missed measurement, etc.) and the control group, which were not exposed to any load, the sample population was 26: 8 exposed to 0.49N, 9 at 0.98N, and 9 at 1.96N. Control specimens may be used in the future to incorporate growth into the model, but this was not considered here.

This data from Liu *et al.* (2011) was converted from force-displacement to stress-strain for modeling purposes. In order to minimize the effect of MSI tipping during experiments, strain was calculated using measurements made from radiographs (MSIr) as:

$$\varepsilon = \frac{W(t) - W_0}{W_0} \quad (11)$$

where $W(t)$ is the MSIr width at a given time and W_0 is the original MSIr width.

Stress in the suture was determined using:

$$\sigma = \frac{F}{A_0} \quad (12)$$

Calculating the original cross-sectional area, A_0 , of the suture in the sagittal plane required approximations from existing studies. Suture depth was obtained by

measuring a sample image provided in Liu *et al.* (2011) for the control group and was assumed representative of the population. A study conducted by Burrows *et al.* (1999) [19] utilized radiographs and Euclidean distance matrix analysis to obtain measurements for various markers of the New Zealand white rabbits' skull. From their study, the distance between markers 2 and 9 gives the approximate length of the midsagittal suture. A representation of the suture and dimensions assigned to it is provided in Figure 4-5.

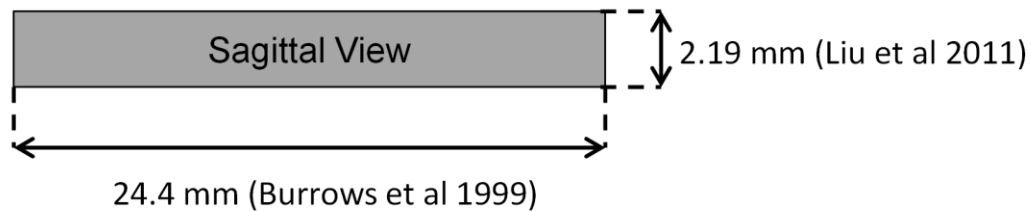


Figure 4-5: Approximated dimensions of the midsagittal suture

4.2.3. Experimental Data Assumptions

To be able to use the empirical data, several assumptions were required with respect to the data, experiment, and the materials involved, namely:

- Springs applied the manufacturer's specified force at a constant magnitude during treatment allowing for creep formulations of proposed models to be used. While the Sentalloy[®] springs used do not provide a perfectly constant force, they are sufficiently constant [20,21] to meet the goal of conducting preliminary work towards viscoelastic modeling of the suture.
- Since it has been reported that the elastic modulus of bone is on the order of 10 to 20GPa [22] while that of cranial sutures is on the order of 1 to 2MPa [23] - over three orders magnitude difference – it is assumed that all deformation as a result of the applied load occurs in the suture. That is, bone between MSIs and the suture will not deform.
- Deformation will be assumed entirely uniaxial in a direction parallel to the spring.
- Though a rabbit midsagittal suture is used in experiments and not the human midpalatal suture, it is expected that empirical data between the two will exhibit similar trends. As the structure of sutures' constituents (e.g.

orientations of fibers) has been found to be function-dependent [6,24], and the midsagittal suture is being loaded in the same way the midpalatal suture would be during ME, it can be suggested they will behave similarly. Rabbit soft tissues have also been used in the literature towards human applications [18,25,26]. Lastly, it was observed by Liu *et al.* (2011) [18] that the midsagittal suture expanded more anteriorly than posteriorly which is a characteristic of ME treatment in humans. Their study was in large part working towards ME treatment which further reinforces the use of rabbit suture data for the purpose of model validation as a natural progression to their work.

- The initial elastic response of the sagittal suture following spring activation had to be estimated since it was not measured directly by Liu *et al.* (2011). The initial strain was determined as:

$$\varepsilon_0 = \frac{\sigma_0}{E_0} \quad (13)$$

where ε_0 , σ_0 , and E_0 are the initial strain, stress, and elastic modulus, respectively. The initial elastic modulus was estimated from data published by Radhakrishnan and Mao (2004) for pre-maxillomaxillary, nasofrontal, and zygomaticotemporal cranial sutures in New Zealand white rabbits as listed in Table 4-1 [23]. An average value of 1.27MPa was selected for this study to give an estimation of the sagittal sutures' initial elastic modulus.

Table 4-1: Cranial Suture Values for New Zealand White Rabbits as Determined by Radhakrishnan and Mao (2004) [23]

Suture	Average Elastic Modulus (MPa)
Pre-maxillomaxillary	1.46
Nasofrontal	1.16
Zygomaticotemporal	1.20
Average	1.27

These assumptions are all justifiable within the scope of preliminary work towards detailed modeling of the suture. The analysis will still allow for

meaningful conclusions to be drawn with respect to selection of a suitable model for future development.

4.2.4. Constant Determination and Model Evaluation

All model constants were determined at each load level using MATLAB[®] (MathWorks[®], Natick, Massachusetts, U.S.A.). Specifically, the 'lsqcurvefit' command with default settings was used to obtain the best strain-time fit for models in a least-squares sense via a trust-region-reflective algorithm [27,28]. The aforementioned strain-time data [18] was used for four specimens at the 0.49N level and five specimens for both the 0.98N and 1.96N loads. All specimens were randomly selected using the 'randperm' command in MATLAB[®]. Remaining specimens were used to validate models at each nominal load by inspecting their fits with respect to the means and standard deviations.

A sensitivity analysis was conducted to consider whether a slight variation in spring load resulting from a non-constant application would dramatically alter model constants. Forces above and below the nominal suggested values were used to re-calculate constants. These bounds were determined from data in a study by Manhartsberger and Seidenbusch (1996) [20] that considered force-displacement behavior of Sentalloy[®] coil springs also used by Liu *et al.* (2011). It was claimed that the springs produce a constant force from 3mm of activation up to 12mm of activation. From this it was determined that a reasonable lower-bound (LB) could be approximated by averaging the load values at 3, 4, and 5mm, where the true force is actually lower than claimed [20]. Similarly, upper-bounds (UB's) were determined by averaging the loads at 10, 11, and 12mm of activation where reported forces are larger than nominal.

Additionally, cross-validation sensitivity analyses were conducted for promising approaches to determine if a single set of model constants could replicate data at all load levels. ME treatment may involve a variety of appliances and applied loads. Thus for predictive capabilities it would be advantageous to have a model that can be used with confidence irrespective of the applied load. This was done by using model constants determined at two load levels (e.g. 0.98N and 1.96N) for validation data at the remaining level (e.g. 0.49N).

4.3. RESULTS

4.3.1. Model Constant Determination

Using the aforementioned protocol, it was first necessary to determine model constants using nominal spring loads. The Lagrangian stresses assumed for given spring loads are provided in Table 4-2, and determined model constants are detailed in Table 4-3 through Table 4-6. A sample figure is provided to illustrate the fitting of a model curve to experimental data in Figure 4-6.

Table 4-2: Stress Values Used for Model Constant Determination and Validation

Nominal Spring Load (g)	Nominal Force (N)	Nominal Stress (MPa)	Upper-Bound Stress (MPa)	Lower-Bound Stress (MPa)
50	0.491	0.009	0.012	0.006
100	0.981	0.018	0.026	0.017
200	1.962	0.037	0.044	0.032

Table 4-3: Nominal, LB, and UB Constants for QLV

Spring Force (N)	C ₁ (1/MPa*s)	C ₂ /C ₅ (1/MPa)	C ₃ (1/s)	C ₄ /C ₅ (1/MPa)	C ₆ (1/s)	C ₇ (1/MPa)
0.49	9.5030	2.6376	1.0005	-0.6377	1.0005	4.2753
0.49 LB	14.2544	2.2027	1.1299	-0.1591	0.8698	3.3147
0.49 UB	7.1272	2.1449	1.0003	-0.1449	1.0003	3.2898
0.98	7.7134	2.6266	1.0005	-0.6266	1.0005	4.2532
0.98 LB	8.1671	2.7418	1.0005	-0.7419	1.0005	4.4838
0.98 UB	5.3400	2.0235	1.0003	-0.0236	1.0003	3.0471
1.96	3.9258	2.0833	1.0003	-0.0833	1.0003	3.1666
1.96 LB	4.5392	2.3046	1.0004	-0.3047	1.0004	3.6092
1.96 UB	3.3012	1.8579	1.0002	0.1421	1.0002	2.7158

Table 4-4: Nominal, LB, and UB Constants for MST

Spring Force (N)	C_1 (1/wk ^{C2} *MPa ^{C3})	C_2	C_3	C_4 (1/wk ^{C5} *MPa ^{C6})	C_5	C_6
0.49	1.0981	0.5777	0.5211	1.0981	0.5777	0.5211
0.49 LB	1.0982	0.5777	0.4798	1.0982	0.5777	0.4798
0.49 UB	1.0971	0.5777	0.5548	1.0971	0.5777	0.5548
0.98	1.1275	0.5077	0.4634	1.1275	0.5077	0.4634
0.98 LB	1.1272	0.5076	0.4568	1.1272	0.5076	0.4568
0.98 UB	1.1283	0.5077	0.5103	1.1283	0.5077	0.5103
1.96	1.1481	0.3883	0.4837	1.1481	0.3883	0.4837
1.96 LB	1.1477	0.3883	0.4632	1.1477	0.3883	0.4632
1.96 UB	1.1481	0.3883	0.5105	1.1481	0.3883	0.5105

Table 4-5: Nominal, LB, and UB Constants for Schapery's Method

Spring Force (N)	C_1 (1/MPa)	C_2 (1/MPa)
0.49	0.0157	66.0907
0.49 LB	0.0616	102.0822
0.49 UB	0.0290	51.0437
0.98	0.6584	56.1281
0.98 LB	0.6972	59.4298
0.98 UB	0.4558	38.8579
1.96	1.3207	29.1044
1.96 LB	1.5271	33.6519
1.96 UB	1.1106	24.4741

Table 4-6: Nominal, LB, and UB Constants for Burgers Model

Spring Force (N)	C ₁ (MPa)	C ₂ (MPa*wk)	C ₃ (MPa)	C ₄ (MPa*wk)
0.49	1.1903	1.0437	0.0160	0.0543
0.49 LB	0.8322	0.6719	0.0107	0.0362
0.49 UB	1.4495	1.3667	0.0214	0.0727
0.98	1.3381	449.1831	0.0184	0.0554
0.98 LB	1.2568	421.0937	0.0174	0.0523
0.98 UB	2.2795	718.5224	0.0266	0.0794
1.96	1.2798	0.6329	0.0666	0.0746
1.96 LB	1.1068	0.5474	0.0576	0.0645
1.96 UB	1.5219	0.7526	0.0792	0.0887

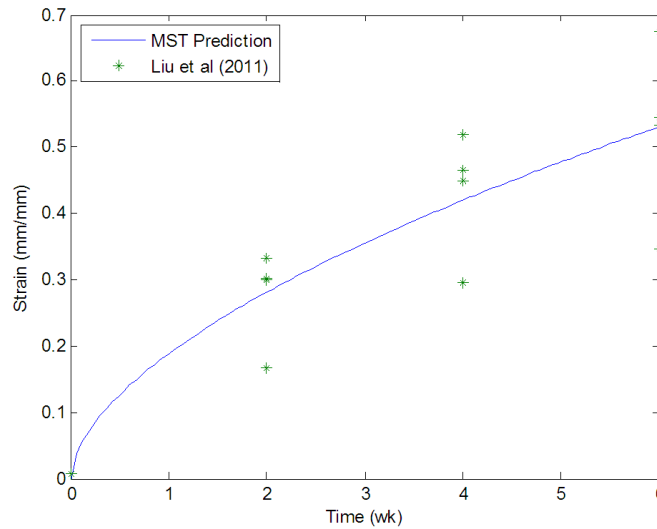


Figure 4-6: Sample plot showing the fitting of model curves to experimental data

4.3.2. Model Validation

The means and standard deviations were calculated for remaining experimental data at each measurement. Models were plotted against this data to observe if they could predict suture response within plus/minus one standard deviation. The results of this analysis, for all load levels, are presented in **Figure 4-7**.

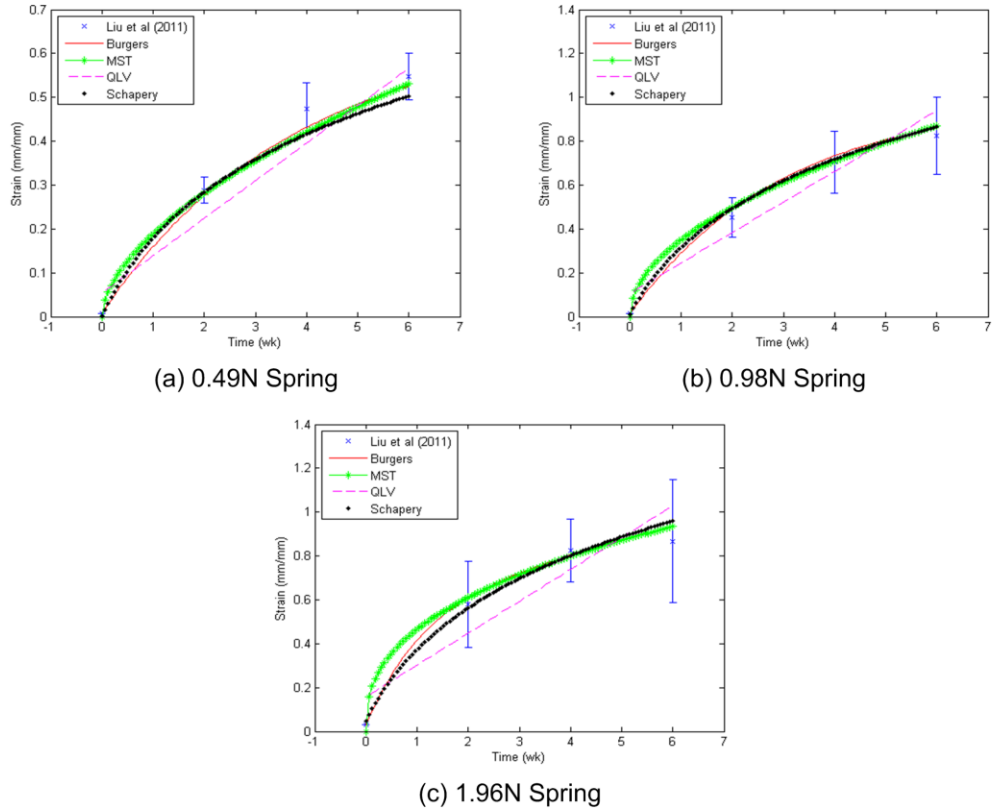
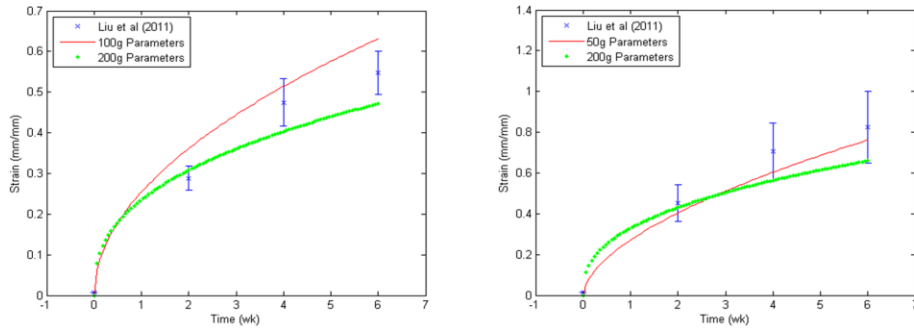


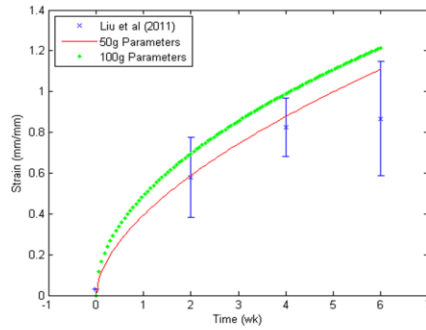
Figure 4-7: Model curves plotted against validation data using nominal constants for each respective load

Since it was able to represent experimental data well (Figure 4-7) and the determined model constants showed little variation as a function of applied load (Table 4-4), the MST model was explored further. Other models either provided a poor fit to the validation data, or showed a large variance with respect to constant values. In an effort to determine whether a single set of parameters could be used to represent data for the midsagittal suture, the aforementioned cross-validation sensitivity analysis was conducted for the MST. In a second analysis the nominal constants from Table 4-4 were averaged, and this single set of parameters was used for all data. All of the models are presented in this analysis to show the poor fit of the remaining three models (QLV, Burgers, and Schapery) to the data. Results of these analyses are provided in Figure 4-8 and Figure 4-9.



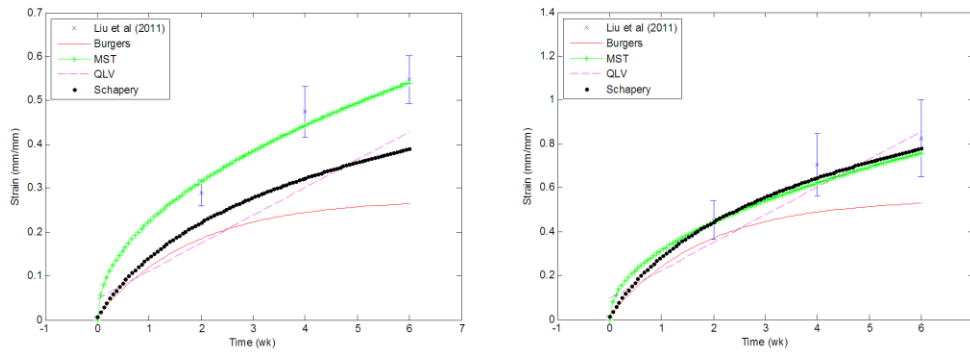
(a) 0.49N Spring

(b) 0.98N Spring



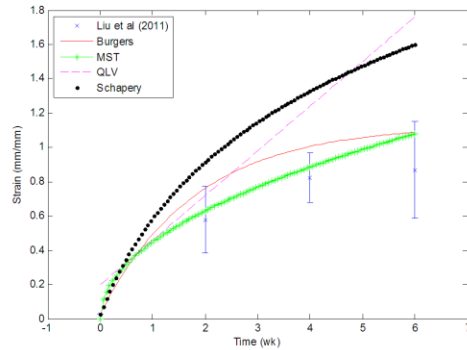
(c) 1.96N Spring

Figure 4-8: Cross-validation sensitivity plots for the MST model



(a) 0.49N Spring

(b) 0.98N Spring



(c) 1.96N Spring

Figure 4-9: Model curves plotted against validation data using a single set of averaged model constants

4.4. DISCUSSION

From analyses conducted here it was found that the QLV, Schapery's, and Burgers models did not meet desired specifications. The QLV approach showed a wide variation in parameter values, C_1 at 0.49N was nearly triple the value at 1.96N (Table 4-3), and showed a poor fit to validation data (Figure 4-7 and Figure 4-9). Experimental data was non-linear but the QLV predicted a nearly linear trend. While the Schapery's and Burgers models showed a reasonable fit to data at individual load levels, the parameters obtained were load-dependent.

Conversely, MST predictions showed a good fit to experimental data at all load levels, and also provided a reasonable fit when a single, averaged, set of parameters was used. MST model curves at all loads using average parameters fell within one standard deviation of data from Liu *et al.* (2011) [18]. This provides a substantial level of confidence in the model going forward to predict suture response during ME treatment. Interestingly, corresponding constants of the two-term expansion were equivalent. That is, $C_1 = C_4$, $C_2 = C_5$, and $C_3 = C_6$. This would imply that a single-term expansion would have been sufficient in describing suture behavior, and that the model can actually be reduced to a separable form. Due to a small sample size, statistical analysis would not provide meaningful results; however, an error comparison between MST predictions and validation data is given in Table 4-7. Initial error is not presented since the MST model presented here inherently predicts zero initial strain. Error results in Table 4-7 reinforce the observation that MST predictions accurately represent suture data. Liu *et al.* (2011) noted disruption and stretching of the collagen fibers in images of 0.98N and 1.96N samples [18]. This tissue failure is most likely the source of increasing errors at larger loads, especially the 1.96N level.

Table 4-7: Percentage Error between Average Experimental Validation Values and MST Model

Week	50g % Error	100g % Error	200g % Error
2	9.34	2.23	8.84
4	6.56	11.74	7.55
6	1.26	7.91	24.54

Though the Burgers model was disregarded, a discussion surrounding determined parameters at 0.98N is required. It was observed that the first damper, C_2 , had a significantly different value than at other load levels. Upon further investigation it was determined that C_2 has minimal influence on creep response in this study. As such, when computationally finding a solution for the Burgers model a wide variation of C_2 values could be selected with little consequence on the end solution. In fact, the maximum number of iterations considered in the ‘lsqcurvefit’ algorithm had to be increased to allow for a converged solution. C_2 becomes critical when investigating permanent strain upon removal of the applied load. This phenomenon will be investigated once additional experimental data is available.

Unlike the previous work completed by Tanaka *et al.* (2000) [8], the model developed here was based on a variety of load curves. In doing so, the generated MST model here proved to replicate suture strain-time data well over a variety of applied loads; however, the Burgers model was unable to accurately represent data using a single set of parameters. While the Kelvin spring-damper model used by Tanaka *et al.* (2000) differs from the Burgers model used here, the findings from this study do suggest that spring-damper models with constant coefficients is not the ideal method for modeling suture behavior.

The major impact of the developed MST model will come through the implementation in future simulations for patient response to ME treatment. As previously mentioned, FEA studies in literature do not consider the sutures’ viscoelastic nature. In the study performed by Lee *et al.* (2009) [3], while there

was no numerical results provided, FEA fringe plots showed visible differences in results as the suture properties were varied. This fact certainly points towards the necessity for further investigation with appropriate viscoelastic models. Upon transformation of the MST model developed here to a generalized stress input and stress-relaxation formulation, it may be used in FEA studies for further investigation. This will prevent the necessity for arbitrary assumptions regarding suture response such as those made in the “pseudo-viscoelastic” model used by Provatidis *et al.* [4,5].

In Chapters 6 and 7, the suture response to general loading conditions will be considered. With regards to ME treatment, not all appliances provide a constant load. It will be important to further develop the MST model to account for other input stress and strain functions. Further work with the Burgers model is considered in Chapter 5 by utilizing stress-dependent spring and damper parameters instead of the constant values used here.

The primary goal of this study was to investigate the ability of four viscoelastic models to represent suture creep data, and select at least one for future consideration. Overall, this study has shown that the MST modeling approach, considering aforementioned assumptions, provides a promising method of predicting suture creep response during ME treatment.

4.5. REFERENCES

1. Bell RA. A review of maxillary expansion in relation to rate of expansion and patient's age. *American Journal of Orthodontics*. 1982;81:32-37.
2. Haas AJ. Rapid expansion of the maxillary dental arch and nasal cavity by opening the midpalatal suture. *Angle Orthodontics*. 1961;31:73-90.
3. Lee H, Ting K, Nelson M, Sun N, Sung SJ. Maxillary expansion in customized finite element method models. *American Journal of Orthodontics and Dentofacial Orthopedics*. 2009;136:367-374.
4. Provatidis C, Georgiopoulos B, Kotinas A, MacDonald JP. In vitro validated finite element method model for a human skull and related craniofacial effects during rapid maxillary expansion. *Proceedings of the Institution of*

- Mechanical Engineers, Part H: Journal of Engineering in Medicine.* 2006;220:897-907.
5. Provatidis C, Georgiopoulos B, Kotinas A, McDonald JP. On the FEM modeling of craniofacial changes during rapid maxillary expansion. *Medical Engineering and Physics.* 2007;29:566-579.
 6. Herring SW. Mechanical influences on suture development and patency. *Frontiers of Oral Biology.* 2008;12:41-56.
 7. Romanyk DL, Collins CR, Lagravere MO, Toogood RW, Major PW, Carey JP. Role of the midpalatal suture in FEA simulations of maxillary expansion treatment for adolescents: A review. *International Orthodontics.* 2013;11:119-138.
 8. Tanaka E, Miyawaki Y, Tanaka M, Watanabe M, Lee K, de Pozo R, Tanne K. Effects of tensile forces on the expression of type III collagen in rat interparietal suture. *Archives of Oral Biology.* 2000;45:1049-1057.
 9. Fung YC. Chapter 7: Bioviscoelastic Solids. In: *Biomechanics: Mechanical Properties of Living Tissues.* 2nd ed. New York, NY: Springer-Verlag; 1993a. p. 277-287.
 10. Yoo L, Kim H, Shin A, Gupta V, Demer JL. Creep behavior of passive bovine extraocular muscle. *Journal of Biomedicine and Biotechnology.* 2011;2011:526705.
 11. Findley WN, Lai JS, Onaran K. Chapter 9: Nonlinear Creep (or Relaxation) Under Variable Stress (or Strain). In: *Creep and Relaxation of Nonlinear Viscoelastic Materials.* New York, NY: North-Holland Publishing Company. 1976a. p. 229-233.
 12. Delgadillo R, Bahia HU, Lakes R. A nonlinear constitutive relationship for asphalt binders. *Materials and Structures.* 2012;45:457-473.
 13. Findley WN, Lai JS, Onaran K. Chapter 7: Multiple Integral Representation. In: *Creep and Relaxation of Nonlinear Viscoelastic Materials.* New York, NY: North-Holland Publishing Company; 1976b. p. 172-175.
 14. Schapery RA. An engineering theory of nonlinear viscoelasticity with applications. *International Journal of Solids and Structures.* 1966;2:407-425.

15. Derombise G, Chailleux E, Forest B, Riou L, Lacotte N, Vouyovitch Van Schoors L, Davies P. Long-term mechanical behavior of Aramid fibers in seawater. *Polymer Engineering and Science*. 2011;51:1366-1375.
16. Findley WN, Lai JS, Onaran K. Chapter 5: Linear Viscoelastic Constitutive Equations. In: *Creep and Relaxation of Nonlinear Viscoelastic Materials*. New York, NY: North-Holland Publishing Company; 1976c. p. 52-69.
17. Fung YC. Chapter 7: The Meaning of the Constitutive Equation. In: *Biomechanics: Mechanical Properties of Living Tissue*. 2nd ed. New York, NY: Springer-Verlag; 1993b. p. 277-287.
18. Liu SS, Opperman LA, Kyung HM, Buschang PH, Is there an optimal force level for sutural expansion? *American Journal of Orthodontics and Dentofacial Orthopedics*. 2011;139:446-455.
19. Burrows AM, Richtsmeier JT, Mooney MP, Smith TD, Losken HW, Siegel MI. Three-dimensional analysis of craniofacial form in a familial rabbit model of nonsyndromic coronal suture synostosis using Euclidean distance matrix analysis. *Cleft Palate-Craniofacial Journal*. 1999;36:196-206.
20. Manhartsberger C, Seidenbusch W, Force delivery of Ni-Ti coil springs. *American Journal of Dentofacial Orthopedics*. 1996;109:8-21.
21. von Fraunhofer JA, Bonds PW, Johnson BE. Force generation by orthodontic coil springs. *Angle Orthodontist*. 1993;63:145-148.
22. Fung YC. Chapter 12: Bone and cartilage. In: *Biomechanics: Mechanical Properties of Living Tissues*. 2nd ed. New York, NY: Springer-Verlag; 1993c. p. 510-513.
23. Radhakrishnan P, Mao JJ. Nanomechanical properties of facial sutures and sutural mineralization front. *Journal of Dental Research*. 2004;83:470-475.
24. Persson M. The role of sutures in normal and abnormal craniofacial growth. *Acta Odontologica Scandinavica*. 1995;53:152-161.
25. Lu YT, Zhu HX, Richmond S, Middleton J. A visco-hyperelastic model for skeletal muscle tissue under high strain rates. *Journal of Biomechanics*. 2010;43:2629-2632.

26. Wysocki M, Kobus K, Szotek S, Kobielarz M, Kuroпка P, Będzіński R. Biomechanical effect of rapid mucoperiosteal palatal tissue expansion with the use of osmotic expanders. *Journal of Biomechanics*. 2011;44:1313-1320.
27. Coleman TF, Li Y. On the convergence of interior-reflective Newton methods for nonlinear minimization subject to bounds. *Mathematical Programming*. 1994;67:189-224.
28. Coleman TF, Li Y. A reflective Newton method for minimizing a quadratic function subject to bounds on some of the variables. *SIAM Journal on Optimization*. 1996;6:1040-1058.

5. Creep Modeling of Suture Behavior using a Nonlinear Burgers Model

Chapter 5 is an extension of Chapter 4 which considers the use of a nonlinear Burgers model to replicate suture behavior in creep. Two nonlinear formulations of the Burgers model are compared to the previously developed linear Burgers and MST methods. A version of this chapter has been published as:

Romanyk DL, Liu SS, Lipsett MG, Lagravere MO, Toogood RW, Major PW, Carey JP. Incorporation of stress-dependency in the modeling of midpalatal suture behavior during maxillary expansion treatment. *Proceedings of the ASME 2013 Summer Bioengineering Conference*. 2013;2013:SBC2013-14034.

5.1. INTRODUCTION

In order to widen a patient's upper jaw, or maxilla, orthodontists will make use of a maxillary expansion (ME) appliance. This procedure is typically used in adolescents having a narrow maxillary complex. Widening the jaw may be achieved through a variety of means such as expansion screws or springs [1]; however, they are all utilized to generate additional space allowing for correction of various tooth misalignments. An example of a common appliance is provided in Figure 5-1a.

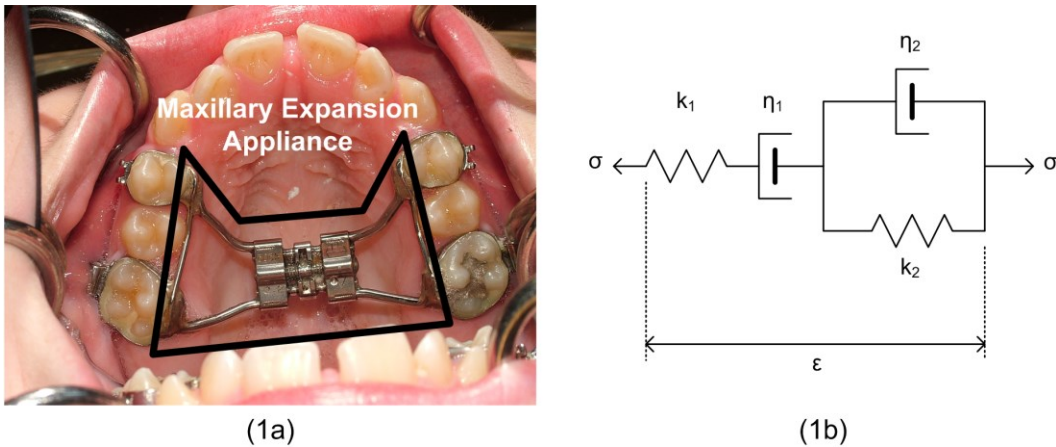


Figure 5-1: (a) Typical maxillary expansion appliance; (b) Spring-damper schematic of the Burgers model

As maxilla bones separate during ME treatment, strain will be imposed upon the cranial suture joining them. When unfused, this soft connective tissue, known as the midpalatal suture, will behave as a viscoelastic material [2]. Even though this fact is well understood, few attempts have been made in the literature to model this behavior. There is a substantial amount of debate surrounding ME treatment protocol, including optimal expansion force range and the suture's influence on treatment results. Further investigation of this tissue as a viscoelastic material will allow for insight into such questions, which will in turn guide future research and clinical practice.

This particular study focuses on evaluating the Burgers model's ability to represent experimental creep data (i.e. continual deformation under a constant stress application), with and without stress-dependent spring-damper coefficients.

Previous work has resulted in the development of a suitable model based on modified superposition theory (MST) [3], but further investigation of the Burgers model was necessary. While the MST model was found to provide a good fit to experimental data in past work, the Burgers model is a simple approach easily transferable between creep, relaxation, and general loading scenarios making it attractive.

5.2. METHODOLOGY

Raw data from a study published by Liu *et al.* (2011) was used for determination of model constants and validation [4]. The midsagittal suture of 6-week old male New Zealand white rabbits was exposed to constant force application through Sentalloy (GAC International, Bohemia, NY) NiTi open-coil springs. Force levels of 50g (0.49N), 100g (0.98N), and 200g (1.96N) were used, and subsequent suture expansion was measured using radiographs in two-week intervals up to week six. A total of eight, nine, and nine rabbits were used at the 0.49N, 0.98N, and 1.96N force levels, respectively. From this, four 0.49N specimens and five 0.98N and 1.96N specimens were randomly assigned to be used in model constant determination. The balance of specimens in each load-set was saved for model validation purposes.

Burgers and MST modeling approaches were both considered in this study. The Burgers model is described by a spring and damper in series with a parallel spring and damper, as highlighted in Figure 5-1b [5]. This configuration results in the governing equation illustrated in eq. (1). Both constant and stress-dependent parameters were considered. Quadratic, eq. (2), and linearly behaving, eq. (3) springs were used with two-term exponential, eq. (4) dampers. The default 'lsqcurvefit' command in MATLAB® (MathWorks®, Natick, Massachusetts, U.S.A.) which utilizes a trust-region-reflective algorithm, was incorporated to determine model constant values. These constants are denoted as a, b, and c in eq. (2)-(4).

$$\sigma + \left(\frac{\eta_1}{k_1} + \frac{\eta_1}{k_2} + \frac{\eta_2}{k_2} \right) \dot{\sigma} + \frac{\eta_1 \eta_2}{k_1 k_2} \ddot{\sigma} = \eta_1 \dot{\varepsilon} + \frac{\eta_1 \eta_2}{k_2} \ddot{\varepsilon} \quad (1)$$

$$k_i = a_i \sigma^2 + b_i \sigma + c_i \quad (2)$$

$$k_i = a_i \sigma + b_i \quad (3)$$

$$\eta_j = e^{a_j \sigma + b_j} \quad (4)$$

5.3. RESULTS

Model constants were determined at each load set and then averaged to obtain one single set of constants to be used in validation. The results of each model are presented in Figure 5-2 through Figure 5-4. Range bars associated with experimental data from Liu *et al.* (2011) [4] represents the standard deviation of data left over for model validation.

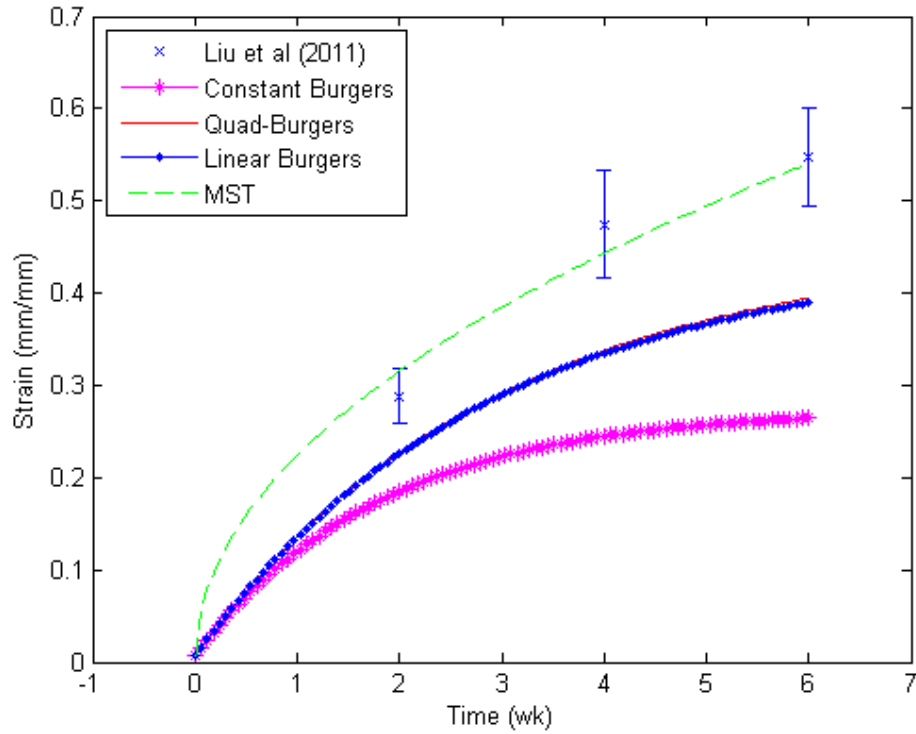


Figure 5-2: Model comparison at 0.49N of spring force

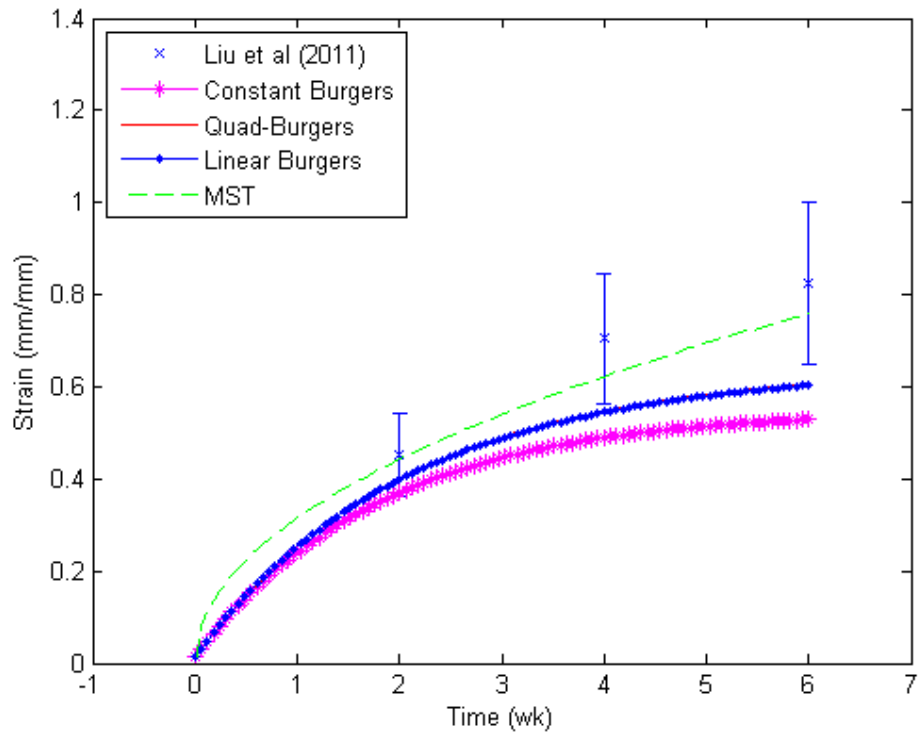


Figure 5-3: Model comparison at 0.98N of spring force

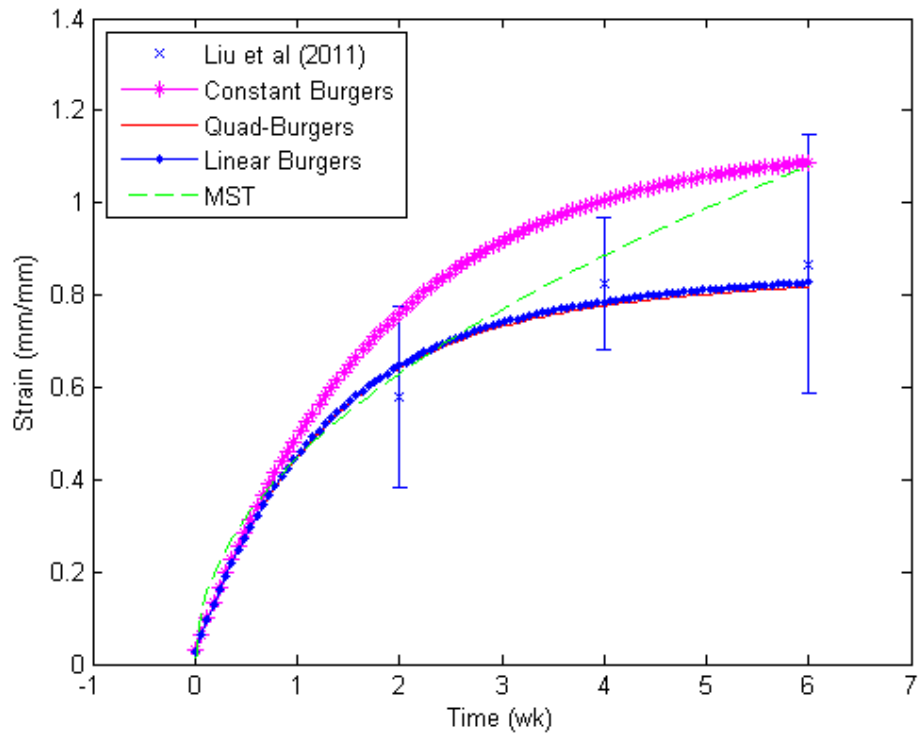


Figure 5-4: Model comparison at 1.96N of spring force

5.4. DISCUSSION AND CONCLUSIONS

In analyzing both linear and quadratic springs for the Burgers model, there was no difference between model predictions. That is, both spring representations provided the same results as seen in Figure 5-2 to Figure 5-4. Also, from this comparison it was noted that incorporating stress-dependency in the parameters did indeed change the predicted tissue response; however, no form of the Burgers model was able to predict suture response accurately at all applied load levels. This is to say that the physical description of initial elastic response, viscous flow, and delayed elasticity suggested by the Burgers model is not an accurate description of suture behavior, or other stress-dependent relationships describing spring and/or damper behavior are required. Thus, the MST model is still the optimal choice for predicting suture creep behavior during ME treatment.

While this particular spring-damper configuration did not represent suture behavior accurately over a range of loads, it is possible other frameworks may be more suitable. By moving towards a generalized model, and introducing various retardation times, it is suggested that a better fit to data may be achieved [5]. Future work in this area will surround studying other spring-damper models, such as the 5-parameter model, and using the MST method to predict suture response for different expansion appliance loads.

5.5. REFERENCES

1. Romanyk DL, Lagravere MO, Toogood RW, Major PW, Carey JP. Review of maxillary expansion appliance activation methods: Engineering and clinical perspectives. *Journal of Dental Biomechanics*. 2010;2010:496906.
2. Herring, SW. Mechanical influences on suture development and patency. *Frontiers of Oral Biology*. 2008;12:41-56.
3. Romanyk DL, Liu SS, Lipsett MG, Toogood RW, Lagravere MO, Major PW, Carey JP. Towards a viscoelastic model for the midpalatal suture: Development and validation using the midsagittal suture in New Zealand white rabbits. *Journal of Biomechanics*. 2013;46:1618-1625.

4. Liu SS, Opperman LA, Kyung HM, Buschang PH. Is there an optimal force level for sutural expansion? *American Journal of Orthodontics and Dentofacial Orthopedics*. 2011;139:446-455.
5. Findley WN, Lai JS, Onaran K. Chapter 5: Linear Viscoelastic Constitutive Equations. In: *Creep and Relaxation of Nonlinear Viscoelastic Materials*. New York, NY: North-Holland Publishing Company; 1976. p. 52-69.

6. Interrelating Creep and Suture Models for Suture Viscoelastic Behavior

The focus of Chapter 6 is the interrelation between creep and relaxation viscoelastic models. In this instance the creep model is determined using the rabbit midsagittal suture data also used in Chapters 4 and 5. Relaxation models are then determined from the known creep formulation using integral equations. A version of this chapter has been submitted to a peer-reviewed journal as:

Romanyk DL, Liu SS, Long R, Carey JP. Considerations for determining relaxation constants from creep modeling of nonlinear suture tissue. *International Journal of Mechanical Sciences*. 14-page manuscript submitted September 4, 2013.

6.1. INTRODUCTION

The study of a materials viscoelastic behavior has long been of interest to researchers in a variety of fields including polymers and biological tissues. It is common to only be interested in either creep, continual deformation under a constant applied stress, or relaxation, stress reduction under a constant deformation, depending on the application. Conversely, in certain instances it may be necessary to understand both the creep and relaxation response of a material. It is in these instances where the modeling of a material may become challenging in the theoretical interrelation between creep and relaxation models [1].

When the theoretical framework of a model is considered, relationships between creep, $\varepsilon(t)$, and relaxation, $\sigma(t)$, formulations can be generated. For instance, in the case of a modified superposition theory (MST) approach [1-5], models will take the form:

$$\varepsilon_c(t) = \int_0^t J(t-\tau, \sigma) \frac{\partial \sigma(\tau)}{\partial \tau} d\tau = \sigma_0 J(t, \sigma_0) \quad (1)$$

$$\sigma_r(t) = \int_0^t G(t-\tau, \varepsilon) \frac{\partial \varepsilon(\tau)}{\partial \tau} d\tau = \varepsilon_0 G(t, \varepsilon_0) \quad (2)$$

where $J(t, \sigma)$, $G(t, \varepsilon)$, t , σ_0 , and ε_0 are the creep compliance function, relaxation function, time, constant applied stress, and constant applied strain, respectively. It has been illustrated previously [1,6] that the two functions can be related through the integral equation:

$$1 = J(0, \sigma_0) G(t, \sigma_0 J(0, \sigma_0)) + \int_0^t G(t-\tau, \sigma_0 J(\tau, \sigma_0)) \frac{\partial J(\tau, \sigma)}{\partial \tau} d\tau \quad (3)$$

In special instances, known as quasilinear viscoelastic (QLV) theory, the strain history may take a form whereby it can be separated into its stress and time components leading to [7,8]:

$$\varepsilon(t) = \int_0^t J(t-\tau) \frac{d\varepsilon^e[\sigma(\tau)]}{d\sigma} \frac{d\sigma(\tau)}{d\tau} d\tau \quad (4)$$

where $J'(t)$ is the reduced creep function and $\varepsilon^e(\sigma)$ is known as the elastic strain response. It has been previously shown for a separable relaxation function that an alternative approach to eq. (3) may be used to interrelate creep and relaxation [7,8]. Using an analogous procedure, the reverse relationship may be derived to predict relaxation response when the creep behavior is known. In isolating for the elastic creep response, eq. (4) may be rewritten as:

$$\varepsilon^e[\sigma(t)] = \int_0^t G'(t-\tau) \frac{d\varepsilon}{d\tau} d\tau \quad (5)$$

where $G'(t)$ is the reduced relaxation function. As it is known that ε^e is solely a function of stress, $\varepsilon^e = F(\sigma)$, it follows that the inverse will yield a relationship for the stress response, $\sigma = F^{-1}(\varepsilon^e)$. Thus, if a step input in strain is applied and held constant, eq. (5) reduces to the following relationship for stress-relaxation:

$$\sigma_r(t) = F^{-1}[\varepsilon_0 G'(t)] \quad (6)$$

Furthermore, it was also shown for this framework [7,8] that the reduced relaxation and creep functions may be interrelated using linear viscoelasticity theory:

$$\int_0^t J'(t-\tau) G'(\tau) d\tau = \int_0^t G'(t-\tau) J'(\tau) d\tau = t \quad (7)$$

Thus, it should be expected that if one function is known, the other could be determined from either eq. (3) or (7). While this should theoretically be feasible, findings in the literature indicate that interrelating creep and relaxation functions is an intricate and complex process requiring detailed investigation [9-11].

As illustrated by Oza *et al.* (2003) [9], there are various creep and relaxation functions that may be used in eq. (1) and (2), generating different kernels, which are able to satisfy eq. (3). Selection of appropriate $J(t,\sigma)$ and subsequent $G(t,\varepsilon)$, or vice versa depending on the scenario, should be based on both the physics of the problem and ensuring that eq. (3) is satisfied. This is to say that depending on the assumption of eq. (1) or (2) there may not necessarily be a unique solution to eq. (3). As a result, it is absolutely imperative to

investigate a creep-to-relaxation transformation in great detail, and likely explore multiple function combinations [9].

Maxillary expansion (ME) treatment is a procedure used in orthodontics that widens the upper jaw (maxilla) of a patient to generate more room for tooth movement. An appliance is utilized in the palate to generate the outward force or displacement causing expansion. These appliances commonly incorporate compressed springs or expansion screws as the active element, and the choice of which method is used will dictate the treatment's mechanics [12]. In the case of springs, the system can be considered load-controlled since the spring applies a known force to the maxilla depending on its compression. Conversely, in the case of an expansion screw the problem becomes displacement-controlled as every turn of the screw applies a known displacement to the maxilla. As the upper jaw widens during treatment, the midpalatal suture will be primarily exposed to tensile loading [13]. This suture is a viscoelastically behaving soft tissue connecting the maxilla bones [14,15]. In an ideal scenario the midpalatal suture would widen during ME but would not be damaged allowing for physiological expansion. Furthermore, it has been suggested that an optimum force level exists to best promote bone growth during treatment [16,17]; however, this optimal range has not yet clearly been identified making further correlation between internal suture stress and resulting bone growth necessary. In light of the various methods that may be used for expansion, when studying suture behavior during ME it becomes necessary to understand both creep and relaxation behavior for use of spring and screw appliances, respectively.

The goal of this study is to further investigate the transformation of a creep model into its related relaxation formulation. Four different functional forms will be considered, and the results of each transformation presented. Specifically, all four models will be fit to the same set of nonlinear creep data using the midsagittal suture in New Zealand white rabbits and then transformed into their subsequent relaxation form. The aim is to identify a creep function that accurately represents the data and can provide a good representation of relaxation behavior.

6.2. METHODOLOGY

6.2.1. Modeling Methods

As early seminal works in the area, models previously developed by Lakes and Vanderby (1999) [6] and Oza *et al.* [1,9] were considered. Such models were selected based on their ability to include stress and strain dependency in the creep and relaxation response, respectively, while remaining relatively simple. Also, these studies consider in great detail a derivation allowing for the interrelation between creep and relaxation behavior. While this work contributes tremendously to the literature, it is possible that an error exists in application of the theory to modeling. As illustrated in eq. (3), the creep function inside the integral is defined at τ ; however, in the previous studies, it appears the authors have used the definition of $t-\tau$ which contradicts the form in eq. (3). That is, the derivation of eq. (3) appears entirely valid, it is only in implementation of models into the integral equation that there appears to be an error in substitution. Such a discrepancy would not change the validity of the derivation, and is not likely to have a tremendous impact on the results, but this is a point that should be addressed further. The scope of the current study is to determine an elementary creep-relaxation model not yet established for suture tissue. As there is no subsequent relaxation data available from the samples used, and suture modeling work is in a primitive stage, investigation of such a fact in the current study is not logical and considered outside the scope of study. Yet, this discrepancy between definition and model substitution should be investigated further with more complete data sets in well understood tissues.

6.2.1.1. Two-Term Inseparable (2TI) Method

A total of four creep-relaxation models will be considered in this study. Three of these were proposed in the literature while the fourth used a creep model previously developed by the authors to generate a new relaxation function. In a study by Oza *et al.* (2003) [9] the authors proposed a two-term creep-relaxation model taking the form:

$$J(t, \sigma) = g_1 t^n + g_2 \sigma^m \quad (8)$$

$$G(t, \varepsilon) = f_1 t^{-n} + f_2 [\varepsilon(t)] t^{-q} \quad (9)$$

where $g_1, g_2, n,$ and m are constants to be determined from creep data and $f_1, f_2,$ and q are stress-relaxation constants. Since eq. (8) is inseparable, the integral equation defined by eq. (3) must be used to determine relaxation constants in terms of creep constants. As previously reported [9], the relationships between the constants are given as:

$$q = 3n - m \quad (10)$$

$$f_1 = \frac{\sin(n\pi)}{g_1 n \pi} \quad (11)$$

$$f_2 = \frac{-f_1 g_2 m \Gamma(-n+1) \Gamma(m)}{n g_1^2 \Gamma(-2n+m+1) \Gamma(n)} \quad (12)$$

where [18]:

$$\Gamma(x) = \int_0^{\infty} e^{-t} t^{x-1} dt \quad (12a)$$

6.2.1.2. Three-Term Inseparable (3TI) Method

In a more general case, Oza *et al.* (2006) [1] suggested that the creep and relaxation forms be represented using a power law expansion. Expanding both the creep and relaxation functions to three terms yields:

$$J(t, \sigma) = g_1 t^n + g_2 \sigma^a t^m + g_3 \sigma^{2a} t^p \quad (13)$$

$$G(t, \varepsilon) = f_1 t^{-n} + f_2 [\varepsilon(t)]^a t^{-x} + f_3 [\varepsilon(t)]^{2a} t^{-q} \quad (14)$$

where $g_1, g_2, g_3, n, m, p,$ and a are creep constants and $f_1, f_2, f_3, x,$ and q are relaxation constants. The notable difference between eq. (8,9) and (13,14), other than the former including more terms, is the fact that the stress and strain terms are raised to an exponent, a , which is to be determined through experimental data. By again using eq. (3), it was determined [1]:

$$f_1 = \frac{\sin(n\pi)}{g_1 n \pi} \quad (15)$$

$$f_2 = \frac{-f_1 g_2 m \Gamma(-n+1) \Gamma(m)}{n g_1^{a+1} \Gamma(-2n+m+1) \Gamma(n)} \quad (16)$$

$$f_3 = \frac{\left[-f_1 g_3 (2m-n) \Gamma(-n+1) \Gamma(2m-n) - f_2 g_2 g_1^a m \Gamma(m) \Gamma(m-2n+1) - \frac{\Gamma(a+1)}{\Gamma(a)} f_2 g_2 g_1^a n \Gamma(n) \Gamma(2m-3n+1) \right]}{g_1^{(2a+1)} n \Gamma(n) \Gamma(2m-3n+1)} \quad (17)$$

$$x = (2+a)n - m \quad (18)$$

$$q = (2a+3)n - 2m \quad (19)$$

6.2.1.3. Three-Term Separable (3TS) Creep Function

A third creep-relaxation model selected for this study was proposed by Lakes and Vanderby (1999) [6] in which they suggested:

$$J(t, \sigma) = (g_1 + g_2 \sigma + g_3 \sigma^2) t^n \quad (20)$$

$$G(t, \varepsilon) = f_1 t^{-n} + f_2 [\varepsilon(t)] t^{-2n} + f_3 [\varepsilon(t)]^2 t^{-3n} \quad (21)$$

where g, f , and n terms represent model constants. In comparing eq. (20,21) to the models given in eq. (8,9) and eq. (13,14), it is noted that the creep function, eq. (20), is actually in a separable form. That is, it takes the form illustrated in eq. (4) where the stress and time components of $J(t, \sigma)$ may be separated entirely; however, eq. (21), the relaxation function, cannot be separated into its strain and time components. As previously illustrated [6], the stress constants may be written in terms of the relaxation constants as:

$$f_1 = \frac{\sin(n\pi)}{g_1 n \pi} \quad (22)$$

$$f_2 = \frac{-g_2 \sin(n\pi)}{g_1^3 n \pi} \quad (23)$$

$$f_3 = \frac{(2g_2^2 - g_1 g_3) \sin(n\pi)}{g_1^5 n \pi} \quad (24)$$

6.2.1.4. Single-Term (ST) Method

Finally, a new creep-relaxation model was generated based on a creep function previously validated by the authors [15]. This model was developed to predict creep of the midsagittal suture in New Zealand white rabbits for the purpose of simulating patient response to maxillary expansion treatment. As such, it is desirable to extend this creep model to a stress-relaxation form and

evaluate if it may be used to accurately predict both types of viscoelastic behavior. The strain response was found to take the form:

$$\varepsilon_c(t) = \sigma_0 (g_1 t^n \sigma_0^a + g_2 t^m \sigma_0^b) = \sigma_0 (2g_1 t^n \sigma_0^a) \quad (25)$$

Upon fitting eq. (25) to the data, which is the same data to be used in this study, it was found that $g_1 = g_2$, $n = m$, and $a = b$. As such, the original assumed form reduced to a single term expansion. In doing so, it can also be observed that eq. (25) now reduces to a separable form as in eq. (4) where:

$$J'(t) = 2g_1 t^n \quad (26)$$

$$\frac{d\varepsilon^e[\sigma(t)]}{d\sigma} = \sigma^a \quad (27)$$

Using the aforementioned QLV framework, the creep formulation described in eq. (26) and (27) can be related to subsequent stress-relaxation behavior. Firstly, the reduced creep and relaxation functions may be related using eq. (7):

$$\int_0^t [2g_1 (t-\tau)^n] G(\tau) d\tau = t \quad (28)$$

Or, using Laplace Transforms for a convolution integral, eq. (28) can be written as:

$$G'(s) 2g_1 s^{-n-1} \Gamma(n+1) = \frac{1}{s^2} \quad (29)$$

In solving eq. (29) for $G'(t)$ it is found that:

$$G'(t) = \frac{t^{-n} \sin(n\pi)}{2\pi g_1 n} \quad (30)$$

As per eq. (6), the stress-relaxation behavior can be determined by finding the inverse of the elastic strain response as a function of $\varepsilon_0 G'(t)$. Integrating eq. (27) to obtain the elastic strain response, eq. (31), and inverting the function yields the stress response, eq. (32):

$$\varepsilon^e(\sigma) = \int \sigma^a d\sigma = \frac{1}{a+1} \sigma^{a+1} \quad (31)$$

$$\sigma_r(t) = (a+1) \left[\varepsilon_0 \frac{t^{-n} \sin(n\pi)}{2\pi g_1 n} \right]^{1/a+1} \quad (32)$$

6.2.2. Experimental Data and Model Evaluation

Data from Liu *et al.* (2011) [16] for the midsagittal suture in New Zealand white rabbits was used to determine creep model constants. A detailed discussion of the experimental procedure will not be considered here, however, readers are encouraged to reference Liu *et al.* (2011) [16] and Romanyk *et al.* (2013) [15] for further information regarding experiments and data analysis, respectively. In brief, constant force coil-springs were attached to mini-screw implants (MISs) across the midsagittal suture of the rabbits. Three different loads were considered in the study being 0.49N (0.009MPa), 0.98N (0.018MPa), and 1.96N (0.037MPa) with eight, nine, and nine specimens being used at each load, respectively. Approximate cross-sectional dimensions were used to calculate the applied constant stress at each load level while the measured change in suture width allowed for calculation of strain. Four specimens at 0.49N and five at 0.98N and 1.96N were randomly selected to determine creep constants using the default ‘lsqcurvefit’ command in MATLAB[®] (MathWorkss, Natick, Massachusetts, USA.). Remaining specimens were used for validation purposes(0.49N, n=4; 0.98N, n=4; 1.96N, n=4). The average and standard deviation values of this data for weeks 2-6 are report in Table 1. From the control specimens in Liu *et al.* (2011) [16], it is noted that continual displacement occurs during the study as a result of growth. As in a previous study [15], this growth is considered minimal with respect to the overall suture strain and is neglected from the analysis.

Table 6-1: Average Values of Strain at each Measured Data Point for the Constant Determination and Validation Data (± 1 SD)

Week	0.49N Spring		0.98N Spring		1.96N Spring	
	Det. Average [n=4] (mm/mm)	Valid. Average [n=4] (mm/mm)	Det. Average [n=5] (mm/mm)	Valid. Average [n=4] (mm/mm)	Det. Average [n=5] (mm/mm)	Valid. Average [n=4] (mm/mm)
2	0.27 (0.07)	0.29 (0.03)	0.47 (0.09)	0.45 (0.09)	0.61 (0.10)	0.58 (0.20)
4	0.43 (0.10)	0.47 (0.06)	0.76 (0.15)	0.70 (0.14)	0.80 (0.15)	0.82 (0.14)
6	0.52 (0.13)	0.55 (0.05)	0.84 (0.16)	0.82 (0.18)	0.93 (0.17)	0.87 (0.28)

Upon determining creep constants at each load set, the values were averaged across the loads to obtain one single set of constants. During ME treatment patients may be exposed to a wide range of loads, thus it is important that a selected model be able to accurately predict suture response over an array of loads using a single set of constants. All models were plotted against the validation data to observe their fit.

Lastly, the subsequent relaxation form of each model will be determined and plotted. Though there is no corresponding data to compare these results to, a basic comparison of the model trends will be discussed along with any unexpected behavior (e.g. a physically unreasonable initial stress). Relaxation models were subjected to a displacement of 0.25mm which is a common ME appliance displacement corresponding to one turn of an expansion screw [19]. By averaging the initial MSI width for all specimens utilized for creep data, 9.72mm, and applying the 0.25mm displacement, the constant strain used for relaxation curves here was 0.0257.

Since detailed experimental data for the suture, relating creep and relaxation, is lacking from the literature, an additional study will be utilized to aid in evaluating any valid creep-relaxation models. Thornton et al [10] considered both the creep and relaxation of medial collateral ligaments (MCL) from New Zealand white rabbits. Data from this study will be used to further evaluate selected creep-relaxation models and their ability to fit both types of data. It is acknowledged that the MCL and suture vary in the constituents; however, this

additional analysis will still provide valid insight into the ability of a model to represent creep-relaxation behavior.

6.3. RESULTS

The determined model constants and average values, as determined from the determination data (Table 6-1), are recorded in Table 6-2. Figure 6-1 shows the four models plotted against validation data at all three of the load levels tested. It should be noted that in Figure 6-1 the three-term separable (3TS) and two-term inseparable (2TI) models overlap one another while the remaining two models, three-term inseparable (3TI) and single-term (ST), also overlap.

Table 6-2: Creep Model Constants for Each Load Set and their Corresponding Average (± 1 SD)

Two-Term Inseparable Function (2TI)							
	g_1	g_2	n	m			
Average	17.5625	5.9434	0.4904	0.7116			
(SD)	(4.4245)	(8.0906)	(0.0970)	(0.1901)			
0.49N	20.9384	1.1654	0.5777	0.8856			
0.98N	19.1955	15.2848	0.5076	0.5086			
1.96N	12.5536	1.3800	0.3860	0.7407			
Three-Term Inseparable Function (3TI)							
	g_1	g_2	g_3	n	m	p	a
Average	1.0229	1.2111	0.9624	0.4946	0.4911	0.4894	-0.6101
(SD)	(0.0158)	(0.0370)	(0.0069)	(0.0850)	(0.0960)	(0.0998)	(0.0295)
0.49N	1.0109	1.1768	0.9658	0.5722	0.5778	0.5788	-0.5782
0.98N	1.0169	1.2063	0.9670	0.5078	0.5076	0.9670	-0.6365
1.96N	1.0408	1.2503	0.9545	0.4037	0.3880	0.9545	-0.6155
Three-Term Separable Function (3TS)							
	g_1	g_2	g_3	n			
Average	17.6449	1.3129	1.0078	0.4912			
(SD)	(4.4815)	(0.1249)	(0.0073)	(0.0958)			
0.49N	20.9462	1.1795	1.0016	0.5777			
0.98N	19.4453	1.3320	1.0060	0.5077			
1.96N	12.5431	1.4271	1.0158	0.3883			
Single-Term Function (ST)							
	g_1	n	a				
Average	1.1246	0.4912	-0.5106				
(SD)	(0.0251)	(0.0958)	(0.0293)				
0.49N	1.0981	0.5777	-0.4789				
0.98N	1.1275	0.5077	-0.5366				
1.96N	1.1481	0.3883	-0.5163				

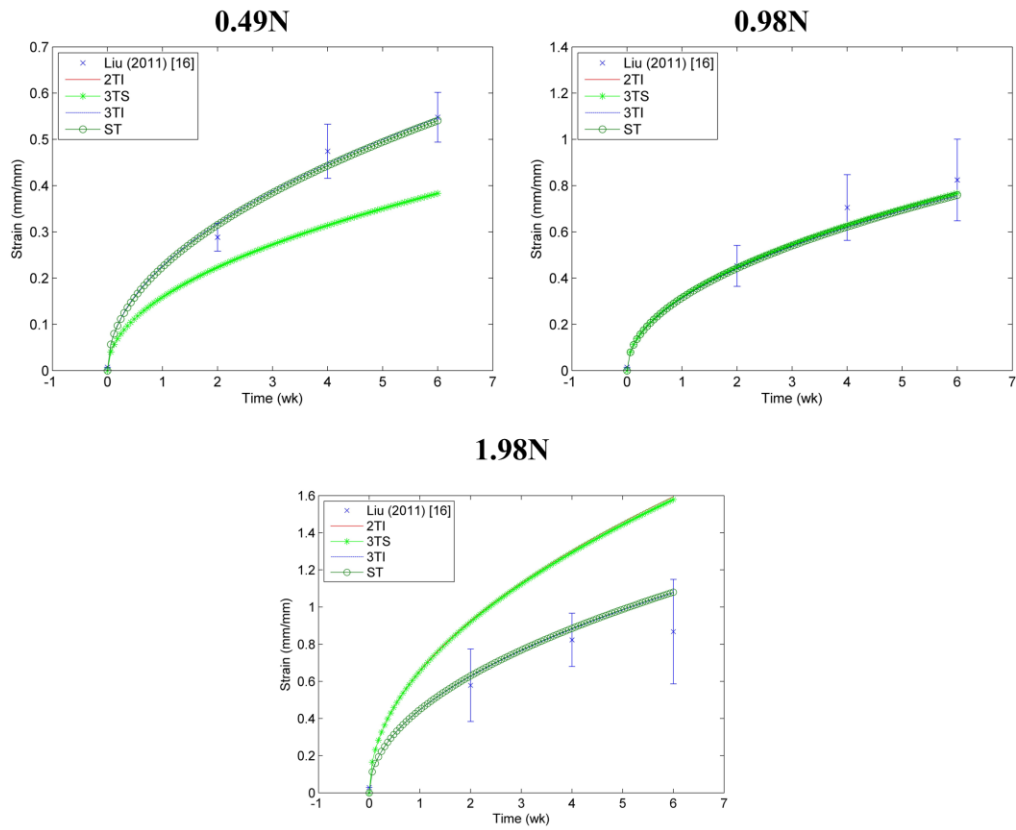


Figure 6-1: Model validation plots at 0.49N, 0.98N, and 1.96N load levels using the validation creep data from Liu et al. (2011) [16]

From values in Table 6-2, the relaxation constants for each model were determined using relationships from Section 6.2.1 and recorded in Table 6-3. It must be noted that “Average Creep Constants” does not refer to an average of the relaxation constants presented in Table 6-3; rather, it refers to the relaxation constants determined using the average creep constants from Table 6-2. Plots of the resulting relaxation curves using the averaged creep constants from Table 6-2 have been provided in Figure 6-2.

Table 6-3: Relaxation Function Model Constants Determined using the Creep Constants from Each Load Set as well as the Average Creep Constants

Two-Term Inseparable Function (2TI)							
	f_1	f_2	n	q			
Average Creep Constants	0.0369	-0.0010	0.4904	0.7596			
0.49N	0.0255	-0.0001	0.5777	0.8475			
0.98N	0.0327	-0.0014	0.5076	1.0142			
1.96N	0.0615	-0.0008	0.3860	0.4173			
Three-Term Inseparable Function (3TI)							
	f_1	f_2	f_3	n	x	q	a
Average Creep Constants	0.6291	-0.7500	-0.2504	0.4946	0.1963	-0.1019	-0.6101
0.49N	0.5362	0.6368	-0.2083	0.5722	0.2358	-0.1007	-0.5782
0.98N	0.6162	0.7386	-0.2766	0.5078	0.1848	-0.1382	-0.6365
1.96N	0.7232	0.8694	-0.2784	0.4037	0.1709	-0.0619	-0.6155
Three-Term Separable Function (3TS)							
	f_1	f_2	f_3	n			
Average Creep Constants	0.0367	-0.0001	0.0000	0.4912			
0.49N	0.0255	-0.0001	0.0000	0.5777			
0.98N	0.0322	-0.0001	0.0000	0.5077			
1.96N	0.0614	-0.0006	0.0000	0.3883			
Single-Term Function (ST)							
	g_1	n	a				
Average Creep Constants	1.1246	0.4912	-0.5106				
0.49N	1.0981	0.5777	-0.4789				
0.98N	1.1275	0.5077	-0.5366				
1.96N	1.1481	0.3883	-0.5163				

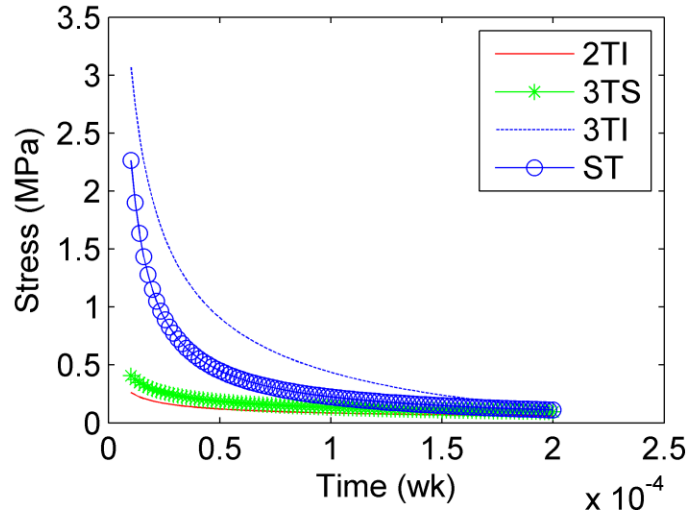


Figure 6-2: Relaxation plots for the 2TI, 3TS, 3TI, and ST models using the averaged creep constant values as described in Table 6-2 (Note: 1 hour $\approx 600 \cdot 10^{-5}$ weeks)

6.4. DISCUSSION

Firstly, inspecting the creep data, Figure 6-1 and Table 6-2, it is apparent that two of the approaches can be ruled out immediately. The 3TS and 2TI creep functions were unable to accurately replicate data using a single set of parameters at all load levels considered. As previously mentioned, it is necessary that a chosen function be able to replicate data accurately over a wide range of applied loads. Since these creep functions were unable to do so, they are not ideal candidates for this purpose. Conversely, the 3TI and ST creep functions were able to replicate the creep data within one standard deviation at all loads using a single set of constants. Thus, from the creep response, only the 3TI and ST functions could be potential candidates for an overall viscoelastic suture model.

It was shown previously that, in general, models with linear separable creep compliance functions were unable to represent this data accurately [15]. The inability of the 3TS function to predict suture creep response over a range of applied loads further illustrates and supports this point through its separable form; however, the ST separable approach was indeed found to provide accurate fit to creep data over several applied loads. Though the 2TI function proposed by Oza *et al.* (2003) [9] is of an inseparable form, it does not allow for an independent exponent to be assigned to the stress term. When inspecting other functional

forms it can be seen that the stress-exponent is not prescribed, and is determined through fitting of the data. As reported in Table 6-2 it was found that the stress-exponent, α , of the 3TI and ST functions were similar having values of -0.6101 and -0.5106, respectively; however, the 2TI function has a prescribed value of 1 for the stress-dependent term. When utilizing creep compliance functions in the creep-strain response, these exponent values would increase by a value of one as described in eq. (1). These results suggest that suture creep-strain is best related to stress through an experimentally determined stress exponent, and that separability/inseparability is not the most important factor when selecting an appropriate creep function.

All relaxation curves followed the expected trend and predicted reasonable stress values. Since all of the models are undefined at zero, the initial time was taken at approximately 5s, 0.00001 weeks, after load application. From Figure 6-2 it is noted that the 2TI and 3TS functions predicted similar relaxation behavior differing only slightly in their initial stress prediction. The remaining functions showed substantial deviation from these two. The 3TI function predicted an initial stress of approximately 3MPa while the ST approach was close to 2.3MPa. Work by Radhakrishnan and Mao (2004) [20] found the elastic moduli of cranial sutures in New Zealand white rabbits ranged from 1.16MPa – 1.46MPa. Furthermore, it is known that full suture ossification can range over a wide spectrum of ages [23] which would cause an increase in tissue stiffness. The periodontal ligament (PDL) is a tissue cited as being similar to the midpalatal suture in terms of connective tissue structure [13,21], and has been explored in much greater detail [22]. Experimental studies of the PDL have found elastic moduli values exceeding 1000MPa [22]. Of course, the sutures' rate-dependent response will generate a larger initial stress when exposed to a step-displacement than would be expected for a quasi-static condition; however, using these reported elastic moduli as a reference, it can be conjectured that the predicted initial stresses are within physically realistic bounds. That is, the initial stresses are larger than in a simple elastic scenario, but are not unreasonably large.

In all cases it could be stated that stresses decayed to 0.1MPa or below within minutes of strain application. In terms of maxillary expansion this is significant in that every model predicted rapid stress decay of the suture to near-negligible values providing confidence in the results. This would suggest that in typical treatment protocols of 2-3 expansions per day, one could likely expect stresses to decay to negligible amounts between expansions.

The difference in timeframe studied between stress-relaxation, minutes, and creep, weeks, is a consequence of their relation to ME treatment mechanics. Due to the nature of ME treatment with a spring, it is necessary to study suture behavior over the entire treatment to fully understand how much strain, or expansion, is generated as a result of the force application. When considering screw activated expansion, the key variable in question is the suture stress and, more specifically, if there is any stress accumulation between activations. That is, if the stress does not decay to a negligible amount prior to the next activation, there will be a superposition of stress leading to a larger initial stress from the previous activation. As illustrated here, the activation stress decays rapidly within minutes and the accumulation of stress would not occur with added activations during typical treatment protocols; thus, study of behavior beyond this initial activation would not provide any added information.

When considering all of the creep-relaxation models evaluated here, it was determined that the ST and 3TI functions would be most fitting for prediction of suture viscoelastic behavior. They were able to replicate creep data using a single set of constants over a wide range of loads and also predicted physically reasonable stress-relaxation behavior. The 2TI and 3TS functions were both unable to predict creep behavior accurately over all of the loads tested in this chapter. As such, they were eliminated as potential candidates for future modeling work.

Acknowledging the lack of relaxation data to fully validate any particular model, a creep-relaxation dataset for one specimen from Thornton *et al.* (1997) [10] was utilized to further investigate the 3TI and ST functions. While this data is not for a cranial suture, the rabbit MCL behaves in a nonlinear viscoelastic

manner similar to the suture [1,9]. Incorporating this in the present study will aid in further investigating the developed ST model with respect to interrelated creep and relaxation prediction. Creep and relaxation data was collected using the MCL's from female New Zealand white rabbits which is beneficial since this was the species used to collect suture data. Estimated data points from a sample creep-relaxation plot in allowed for the determination of creep constants and subsequent evaluation of the interrelated stress-relaxation curves.

Data presented in Thornton *et al.* (1997) had been normalized based on the initial values of the creep and relaxation functions they considered; however, since the creep functions are zero when time is zero, the data was transformed into strain and stress using average initial values presented in their study. That is, the applied constant stress during creep was taken as 14.9MPa and the constant strain applied during relaxation was 0.043. Also, since the ST and 3TI creep functions are both identically zero when $t=0$, the initial data-point in creep was removed from the analysis as models would be incapable of replicating this initial response. Considering the application of studying ME treatment, the initial response of the material is of much less importance than the long-term predictability of a creep model. Figure 6-3 shows a plot of the fitted creep functions and resulting relaxation predictions compared to experimental data.

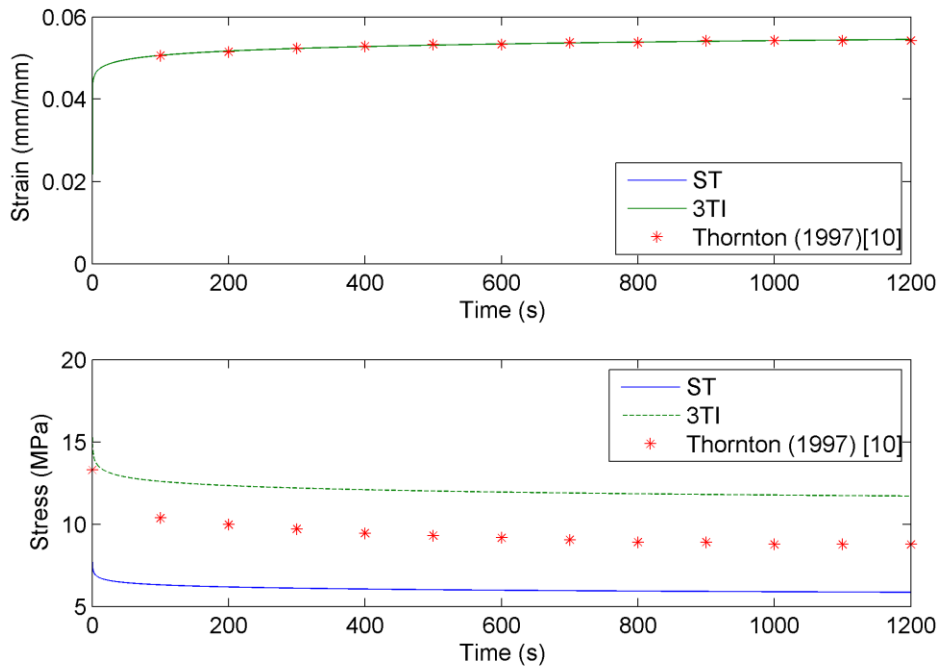


Figure 6-3: Creep and relaxation predictions using the single-term and three-term inseparable functions for data from Thornton et al [10]

Inspecting the results from Figure 6-3 it is evident that the creep formulations were able to fit the data well. When considering relaxation curves, the ST and 3TI functions under- and over-predicted empirical data, respectively; however, there are several additional factors that must be considered when discussing this analysis. Firstly, the experimental data used was only for one specimen and does not include data variance. Given that biological tissue related data can vary widely [22,24,25], it is entirely possible that a model will not necessarily fit a single specimen. As a result of tissue property variance and the multitude of protocols that may be used [26], it can be said that ME treatment results on the whole will vary widely between patients and/or samples. Thus, considering only one specimen was used and the desired application shows large variability, a highly precise model is not essential here. In general, both models followed the trend of data well and provided good agreement. More specifically, the ST model developed here was found to again replicate creep and relaxation

behavior well. Though there are acknowledged limitations in this added analysis, it provides added confidence that the ST model is a valid and robust approach for replicating creep-relaxation behavior. Future detailed investigation of this approach is required which incorporates a more comprehensive experimental dataset.

6.5. CONCLUSIONS

This study found that a single-term and three-term inseparable approach to modeling the viscoelastic behavior of the suture during ME treatment provided reasonable approximations. They were able to replicate creep data using a single set of constants across a range of applied loads and give physically reasonable predictions of relaxation behavior. Additionally, when these approaches were used for data from Thornton *et al.* (1997) [10], they were able to replicate viscoelastic behavior within the scope of this study. It is certainly acknowledged that additional creep-relaxation data for the suture needs to be studied in the future; however, considering the data currently available in the literature, the ST and 3TI approaches will allow for a good approximation of suture response to treatment.

The work conducted here regarding creep-relaxation prediction has further illustrated the necessity to investigate viscoelasticity in great detail. Two models, one inseparable and one separable, were unable to predict creep response over a range of loads using a single set of parameters. Results presented here further enforce that when researching creep-relaxation behavior of a material, it is crucial that various approaches are investigated to find the optimal model. Moreover, work here illustrated that separability/inseparability of the creep function is not as important as including experimentally determined stress-exponents for suture tissue. The four models tested predicted a range of relaxation behavior based on a single set of creep data. More specifically, the initial predicted stress points varied greatly while the overall decay of the models indicated negligible stress within minutes of strain application.

6.6. REFERENCES

1. Oza A, Vanderby Jr R, Lakes RS. Generalized solution for predicting relaxation from creep in soft tissue: Application to ligament. *International Journal of Mechanical Sciences*. 2006;48:662-673.
2. Green AE, Rivlin RS. The mechanics of non-linear materials with memory: Part 1. *Archives of Rational Mechanics and Analysis* 1957;1:1-21.
3. Ward IM, Onat ET. Non-linear mechanical behavior of oriented polypropylene. *Journal of Mechanics and Physics of Solids*. 196:11;217-229.
4. Findley WN, Lai JS, Onaran K. Chapter 9: Nonlinear Creep (or Relaxation) Under Variable Stress (or Strain). In: *Creep and Relaxation of Nonlinear Viscoelastic Materials*. New York, NY: North-Holland Publishing Company. 1976. p. 229-233.
5. Provenzano PP, Lakes RS, Corr DT, Vanderby Jr R. Application of nonlinear viscoelastic models to describe ligament behavior. *Biomechanics and Modeling in Mechanobiology*. 2002;1:45-57.
6. Lakes RS, Vanderby R. Interrelation of creep and relaxation: A modeling approach for ligaments, *Journal of Biomechanical Engineering*. 1999;121:612-615.
7. Fung YC. Chapter 7: Bioviscoelastic Solids. In: *Biomechanics: Mechanical Properties of Living Tissues*. 2nd ed. New York, NY: Springer-Verlag; 1993a. p. 277-287.
8. Dortmans LJMG, van de Ven AAF, Sauren AAHJ. A note on the reduced creep function corresponding to the quasi-linear visco-elastic model proposed by Fung. *Journal of Biomechanical Engineering*. 1994;116:373-375.
9. Oza A, Vanderby Jr R, Lakes RS. Interrelation of creep and relaxation for nonlinearly viscoelastic materials: Application to ligament and metal. *Rheologica Acta*. 2003;42:557-568.
10. Thornton GM, Oliynyk A, Frank CB, Shrive NG. Ligament creep cannot be predicted from stress relaxation at low stress: A biomechanical study of the rabbit medial collateral ligament. *Journal of Orthopaedic Research*. 1997;15:652-656.

11. Anderssen RS, Davies AR, de Hoog FR. On the sensitivity of interconversion between relaxation and creep. *Rheologica Acta*. 2008;47:159-167.
12. Romanyk DL, Lagravere MO, Toogood RW, Major PW, Carey JP. Review of maxillary expansion appliance activation methods: Engineering and clinical perspectives. *Journal of Dental Biomechanics*. 2010;2010: 496906.
13. Lee H, Ting K, Nelson M, Sun N, Sung SJ. Maxillary expansion in customized finite element method models. *American Journal of Orthodontics and Dentofacial Orthopedics*. 2009;136:367-374.
14. Herring SW. Mechanical influences on suture development and patency. *Frontiers of Oral Biology*. 2008;12:41-56.
15. Romanyk DL, Liu SS, Lipsett MG, Toogood RW, Lagravere MO, Major PW, Carey JP. Towards a viscoelastic model for the unfused midpalatal suture: Development and validation using the midsagittal suture in New Zealand white rabbits. *Journal of Biomechanics*. 2013;46:1618-1625.
16. Liu SS, Opperman LA, Kyung H, Buschang PH. Is there an optimal force level for sutural expansion? *American Journal of Orthodontics and Dentofacial Orthopedics*. 2011;139:446-455.
17. Zahrowski JJ, Turley PK. Force magnitude effects upon osteoprogenitor cells during premaxillary expansion in rats. *Angle Orthodontist*. 1992;62:197-202.
18. E. Kreyszig. Appendix 3: Auxiliary Material. In: *Advanced Engineering Mathematics*. 8th ed. New York NY: John Wiley & Sons Inc.; 1999. p. A51-57.
19. Lagravere MO, Carey JP, Heo G, Toogood RW, Major PW. Transverse, vertical, and anteroposterior changes from bone-anchored maxillary expansion vs traditional rapid maxillary expansion: A randomized clinical trial. *American Journal of Orthodontics and Dentofacial Orthopedics*. 2010;137:304.e1-304.e12.
20. Radhakrishnan P, Mao JJ. Nanomechanical properties of facial sutures and sutural mineralization front. *Journal of Dental Research*. 2004;83:470-475.

21. Pirelli P, Ragazzoni E, Botti F, Arcuri C, Cocchia D. A comparative light microscopic study of human midpalatal suture and periodontal ligament, *Minerva Stomatologica*. 1997;46:429-433.
22. Fill TS, Carey JP, Toogood RW, Major PW. Experimentally determined mechanical properties of, and models for, the periodontal ligament: Critical review of current literature. *Journal of Dental Biomechanics*. 2011;2011:312980.
23. Persson M. The role of sutures in normal and abnormal craniofacial growth, *Acta Odontologica Scandinavica*. 1995;53:152-161.
24. Tanaka E, Miyawaki Y, del Pozo R, Tanne K. Changes in the biomechanical properties of the rat interparietal suture incident to continuous tensile force application. *Archives of Oral Biology*. 2000;45:1059-1064.
25. Komatsu K, Sanctuary C, Shibata T, Shimada A, Botsis J. Stress-relaxation and microscopic dynamics of rabbit periodontal ligament. *Journal of Biomechanics*. 2007;40:634-644.
26. Lagravere MO, Major PW, Flores-Mir C. Long-term dental arch changes after rapid maxillary expansion treatment: A systematic review. *Angle Orthodontist*. 2005;75:155-161.

7. Simulating Suture Response to Screw and Spring Activated Maxillary Expansion Appliances

In the final analysis chapter of this thesis, Chapter 7 utilizes the models developed in Chapters 4-6 for prediction of suture response to expansion appliance loads. Screw appliances are simulated as a stress-relaxation scenario while spring and magnetic appliances are considered to impose a constant or decaying force application. Overall, Chapter 7 presents the clinical of the theoretical modeling work conducted in this thesis.

7.1. INTRODUCTION

Biomechanical analysis of orthodontic procedures is critical to understanding and predicting patient response. One such treatment, maxillary expansion (ME), has received some consideration in the literature [1-3]; however, substantial work remains in fully understanding the influence of expansion appliances on treatment outcome. One such area of interest is the unfused midpalatal suture's behavior resulting from ME appliance activations [4]. Clinical studies have been conducted to observe suture opening [5,6], yet such experiments are unable to assess stresses/strains induced in the suture; furthermore, the suture's viscoelastic nature must be incorporated in simulations to capture its time- and rate-dependency during ME [4].

Finite element analysis (FEA) studies including viscoelasticity were conducted with the goal of better understanding adolescent response to ME. Tanaka *et al.* (2000) [7] modeled the interparietal suture in rats using a Kelvin spring-damper model. This was then implemented in a small-scale FEA study including only the suture and local surrounding bone. In a full-skull FEA study, Provatidis *et al.* [8] set all stress values in the model to zero between screw appliance activations. Both works provided insight into tissue viscoelasticity during ME treatment; however, they are primitive with respect to material models and methods.

This study's focus is to use previously developed analytical suture models to investigate the influence screw and spring ME appliances and protocols have on its response. Additionally, characteristics specific to each type of activation method will be explored. The initial stress and rate of decay will be considered for screw activated appliances, and the applied force from a spring will be studied as both constant and decaying. In doing so, this study will provide quantitative insight to debates that currently surround ME treatment and its impact on the suture.

7.2. METHODOLOGY

Models from previous studies were utilized when simulating suture response to ME appliances. Experimental data using the midsagittal suture in

New Zealand white rabbits [9] allowed for the determination of creep-strain model constants and subsequent validation [3]. Another study considered the development of a related stress-relaxation model [10]. Detailed discussion is provided in these studies, and thus will not be restated here.

7.2.1. Screw Activated Appliances

During screw appliance ME treatment, the maxillary complex is exposed to a step increase in displacement held constant until the next activation. This leads to a stress-relaxation scenario where engaged tissues are initially strained and then allowed to relax between activations; thus, a stress-relaxation model is used in simulating midpalatal suture response to screw activation.

The amount of suture opening from a single activation will depend on a large number of variables such as maxilla bone structure/dimensions, location of the appliance, and attachment methods. In this study, an appliance expansion of 0.25mm will be assumed for activations. Since the amount of suture strain is unknown and will be variable between patients, four levels of displacement will be simulated: 0.25, 0.20, 0.15, and 0.10mm. The true amount of suture displacement is likely not to equal the appliance expansion because of palatal bone articulation/tipping [11]; however, this will provide a “worst case scenario” during ME treatment.

Models from Lakes and Vanderby (1999) [12] (3TS), Oza *et al.* (2003) [13] (2TI), Oza *et al.* (2006) [14] (3TI), and Romanyk *et al.* (unpublished) [10] (ST) were used in a previous study that interrelated creep models to a subsequent relaxation form. The 3TI and ST models were found to best replicate creep-strain data; however, due to a lack of corresponding stress-relaxation data for the rabbit midsagittal suture, definitive conclusions could not be made regarding stress-relaxation model accuracy. As such, all four will be considered to provide a range of stress values over which the suture can be expected to act. The models are given as:

$$3TI \quad \sigma_r(t) = 0.6291\varepsilon_0 t^{-0.4946} - 0.75\varepsilon_0^{0.3899} t^{-0.1963} - 0.2553\varepsilon_0^{0.7798} t^{0.1019} \quad (1)$$

$$\text{ST} \quad \sigma_r(t) = 0.4894(0.2880\varepsilon_0 t^{-0.4912})^{1/0.4894} \quad (2)$$

$$\text{2TI} \quad \sigma_r(t) = 0.0369\varepsilon_0 t^{-0.4904} - 0.0014\varepsilon_0^2 t^{-0.7596} \quad (3)$$

$$\text{3TS} \quad \sigma_r(t) = 0.0567\varepsilon_0 t^{-0.4912} - 0.0002\varepsilon_0^2 t^{-0.9824} \quad (4)$$

where t is the time in weeks, ε_0 is the constant strain applied to the suture, and $\sigma_r(t)$ is the stress-relaxation as a function of time. In this study, strain has been defined as:

$$\varepsilon = \frac{SutureWidth_{new} - SutureWidth_{old}}{SutureWidth_{old}} \quad (5)$$

In the experimental data used, the average mini-screw implant width of specimens was 9.72mm prior to expansion, and was used for $SutureWidth_{old}$. All other coefficients are model constants determined using the aforementioned experimental data. It must be noted that at $t=0$ the stress determined by each model approaches infinity which is not physically possible. As such, simulations will begin at approximately $t=5s=0.00001weeks$ to account for this singularity. Considering the timeframe of interest is over hours, and that activation of a screw will take several seconds, 5s was considered a reasonable time to begin simulations.

7.2.2. Spring Activated Appliances – Constant Force

In contrast to screw appliances, the spring element will apply a known, or determinable, force to the maxilla complex. If the spring force remains constant, the complex is in a state of creep-strain. That is, the applied force, or stress, remains constant while the tissue continuously deforms.

The creep-strain response of the rabbit midsagittal suture was previously determined as [3]:

$$\varepsilon_c(t) = 2.2492\sigma_0^{0.4894} t^{0.4912} \quad (6)$$

where σ_0 is a constant applied stress and $\varepsilon_c(t)$ is the resulting creep-strain. Again, all other numerical values are experimentally determined constants. A constant applied spring force of 0.98N (100g), equating to an applied stresses of

0.018MPa, is considered for simulations. As done previously [3], the response will be simulated over a six-week period.

7.2.3. Spring Activated Appliances – Decaying Force

Simulating suture response to a spring with decaying force provides insight to the importance of applying a constant force during ME. Three different decay functions have been studied since it is not known how stress in the suture would decay during ME treatment:

$$\text{Linear:} \quad \sigma_L(t) = \sigma_i - \alpha t \quad (7)$$

$$\text{Exponential:} \quad \sigma_E(t) = \sigma_i \exp(-\beta t) \quad (8)$$

$$\text{Inverse:} \quad \sigma_I(t) = \frac{\sigma_i}{(t+1)^\gamma} \quad (9)$$

where α , β , and γ are time-constants that dictate the amount of decay over time for each respective type of function, and σ_i is the initial stress.

The creep model defined by eq. (6) is no longer valid as stress is not constant. To predict suture response to a decaying stress, the modified superposition theory definition, eq. (10) [14], was altered to obtain the relationship given in eq. (11):

$$\varepsilon(t) = \int_0^t J[t-\tau, \sigma(\tau)] \frac{d\sigma}{d\tau} d\tau \quad (10)$$

$$\varepsilon(t) = \sigma_i \left[2.2492 \{\sigma(t)\}^{-0.5106} t^{0.4912} \right] + \int_0^t \left[2.2492 \{\sigma(t)\}^{-0.5106} t^{0.4912} \right] \frac{d\sigma(t)}{d\tau} d\tau \quad (11)$$

where $2.2492 \{\sigma(t)\}^{-0.5106} t^{0.4912}$ represents the creep compliance function, $J(t, \sigma)$, and is the same as that used to generate eq. (6). Equations (7)-(9) are used in eq. (11) to simulate a stress that decays 30% and 10% of the original applied stress, 0.018MPa, over a six-week period.

7.3. RESULTS

Figure 7-1a plots the initial stresses for each of the four stress-relaxation models against suture displacements, and Table 7-1 provides associated numerical values. From Table 7-1 it is apparent that the Oza *et al.* (2006) model predicts the largest initial stresses, ranging from 0.71-3.08MPa, over other models.

Considering the other three models, at 0.25mm of activation the stresses ranged from 0.41-2.27MPa, and from 0.11-0.35MPa at 0.10mm.

In Figure 7-1b sample stress-relaxation curves are shown using the 2TI and 3TI models for a 0.25mm activation. The 3TI model illustrates the “worst case scenario”, largest initial stress, at this activation while the 2TI model is the “best case scenario”, lowest initial stress, of the four models considered.

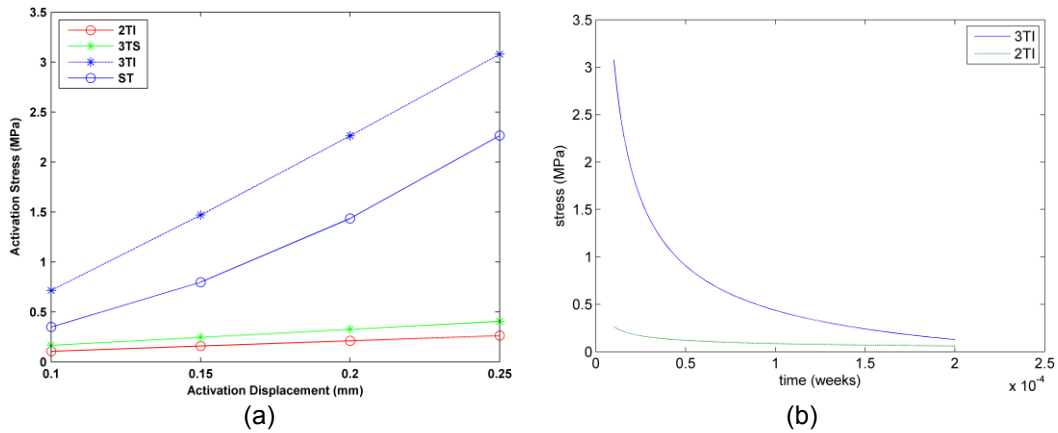


Figure 7-1: (a) Plot of initial stress at varying levels of activation displacement; (b) Sample plot of stress-decay for the worst and best case scenarios (1 hour ≈ 0.006 weeks)

Table 7-1: Activation Stress Values at Varying Levels of Initial Displacement

Stress at Each Activation (MPa)				
	0.25mm	0.20mm	0.15mm	0.10mm
ST	2.27	1.44	0.80	0.35
3TI	3.08	2.26	1.47	0.71
2TI	0.26	0.21	0.16	0.11
3TS	0.41	0.33	0.25	0.17

Suture strain response to a spring activated appliance was plotted in Figure 7-2 for exponential, linear, and inverse decay. Decay to 30% of the initial force is plotted in Figure 7-2a, and a decay of 10% in Figure 7-2b. The constant force response is included in both instances. Recorded in Table 7-2 are the final strain values for all decaying curves and the constant case. It was found that for a decay of 30%, the decrease in obtained suture strain, defined as the ratio of strain from a

decaying spring to that of a constant force, ranged from 75.86%-79.90%. For 10% decay, the resulting strain was 92.91%-97.04% of the constant force case.

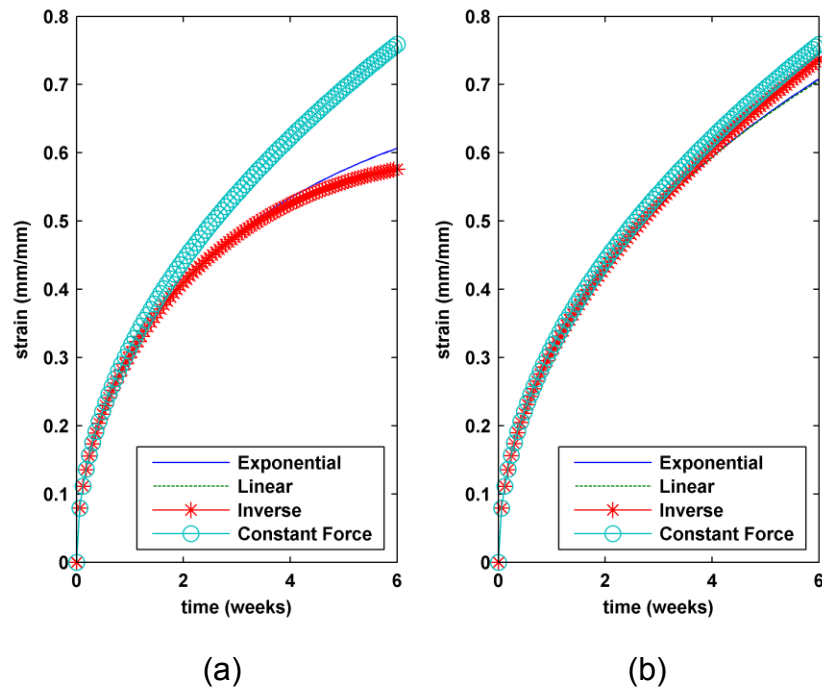


Figure 7-2: Suture strain response to exponentially, linearly, and inversely decaying springs and a constant force spring for: (a) 30% decrease in force; (b) 10% decrease in force

Table 7-2: Comparison of Decaying Functions to 70% and 90% to a Constant Force Spring

		Final Strain (mm/mm)	% of Constant Force Expansion
Constant Force Spring		0.7593	N/A
30% Decay	Exponential Decay	0.6067	79.90
	Linear Decay	0.5760	75.86
	Inverse Decay	0.5760	75.86
10% Decay	Exponential Decay	0.7083	93.28
	Linear Decay	0.7055	92.91
	Inverse Decay	0.7368	97.04

7.4. DISCUSSION

Inspecting Figure 7-1 curves and Table 7-1 values, it is apparent that the 3TI model predicts the largest stress values of all models tested. The lack of complimentary stress-relaxation data for suture failure prevents the formation of definitive conclusions; however, other existing work can be used to discuss numerical findings. Work by Genna *et al.* (2008) [15] noted failure of the periodontal ligament (PDL) due to tensile stresses in the range of 3-4MPa using a loading rate of 1mm/min. While this experiment was not conducted for stress-relaxation behavior, and there are slight differences between the PDL and suture [16], it can be conjectured that suture soft tissue failure would result in a similar range. Additionally, since the suture may be at variable levels of ossification [17], this would increase its stiffness and failure strength over the PDL.

Considering stresses (Table 7-1) predicted at upper, 0.25mm, and lower, 0.10mm, bound displacements, and the aforementioned failure range, it is suggested that suture failure is improbable based on a single screw activation. While the predicted stresses for 0.25mm of activation approach the failure window observed for the PDL, it is unlikely that all screw displacement would be transferred to the suture tissue due to bone articulation [11]. Though, if a series of screw activations were made rapidly in series, it is possible that stresses would superimpose to reach a point of failure. From the ranges of displacements and

models studied here, as few as two-three subsequent screw activations could result in suture soft tissue failure. This finding highlights the importance of maintaining a moderate activation schedule during ME treatment to avoid superimposing stresses in the suture.

Perhaps the most interesting result is the rate of suture stress-decay resulting from a step input in displacement. From Figure 7-1b it can be seen that both models decay to minimal stresses within 0.0002weeks, or approximately 2 minutes. This result highlights that regardless of the deviation in predicted initial stress between models, the stress in suture tissue decays rapidly. The impact of this is both advantageous as well as detrimental. On the one hand, if stresses have decayed to negligible amounts prior to the next activation, then there will be no superimposition of stresses. This is beneficial in avoiding suture failure. Conversely, research has shown that maintaining traction, inside an optimal range, on the suture facilitates bone growth throughout treatment [9,18]. Increasing the amount of bone development during ME is critical for reducing the retention phase, and thus overall treatment time.

When considering suture response to spring activation, it was apparent that the path in which the force decayed had little effect on results. There was only a 4.04% difference in strain-decay between tested functions at 30%, and a 3.76% difference at 10% force-decay. The significance of this finding is that regardless of how a spring decays (e.g. linearly, inversely, exponentially, etc.), the amount of decay is the important factor in appliance design.

In comparing the decaying spring force to that of the constant force, there was certainly a decrease in overall expansion. In both the 30% and 10% decay scenarios, the fraction of achieved strain compared to the constant force case was within 5% of the fractional decay in applied force. Due to the sutures viscoelastic nature, specifically its creep behavior, it was previously unknown as to how much a decrease in spring-force would influence suture expansion. From these simulations, it is now evident that suture expansion will closely follow spring-force decay; thus, it is necessary to maintain a constant spring-force to reduce ME treatment time.

Results suggest that spring activation can provide more physiologic suture expansion over screw activation. Springs are able to provide a continuous, and predictable, force/stress on the suture throughout treatment. Conversely, screw activation results in a large jump in initial stress followed by rapid stress-decay. This type of behavior is adverse to bone development during ME and may result in suture failure in as few as two-three rapid activations. Despite this evidence, there is an adverse factor that prevents the simple implementation of a spring appliance: tooth movement. The low levels of force that would ideally be applied to the suture must be transferred through the tooth and PDL. This will generate unwanted tooth movement during ME when only the palatal bone movement is desired.

One solution to avoiding tooth movement is anchoring the ME appliance to the maxilla bones; however, this requires much more invasive techniques. Another potential alternative would be combining spring and screw activation, similar to an approach used by Wichelhaus *et al.* (2004) [19]. Utilization of the screw in the initial phase of treatment could generate PDL necrosis, creating a more rigid connection between the ME appliance and maxilla. Afterwards, the compressed spring would then apply continuous low-magnitude force to the palate, providing more physiologic suture expansion. While further investigation would be required to study patient response to this protocol, it certainly provides another viable option.

It is recognized that there are limitations to this study. The previously validated creep model required various assumptions as described by Romanyk *et al.* (2013a) [3]. Also, the lack of subsequent relaxation data prevents detailed evaluation of the stress-relaxation models considered. Notwithstanding these limitations, this study is still significant in that it presents physically relevant quantitative data for the suture during ME treatment. The comparison between spring and screw appliances, and their impact on the suture during treatment, is the first of its kind and allows for a clinically relevant discussion regarding the advantages and disadvantages of each method.

7.5. CONCLUSIONS

The presented analysis clearly highlights suture response to a constant force application as well as the impact that 30% and 90% decay over a six-week period would have. Additionally, a range of expected initial suture stresses in response to screw activation have been suggested, and the rate of stress-decay was studied. It was found that screw activation could potentially lead to suture failure in as few as two-three subsequent activations, and that stress in the suture decayed rapidly within hours. While the spring activation method could theoretically provide more physiologic expansion, it presents problems with generation of unwanted tooth movement.

7.6. REFERENCES

1. Provatidis CG, Georgiopoulos B, Kotinas A, McDonald JP. On the FEM modeling of craniofacial changes during rapid maxillary expansion. *Medical Engineering and Physics*. 2007;29:566-579.
2. Lee H, Ting K, Nelson M, Sun N, Sung SJ. Maxillary expansion in customized finite element method models. *American Journal of Orthodontics and Dentofacial Orthopedics*. 2009;136:367-374.
3. Romanyk DL, Liu SS, Lipset MG, Toogood RW, Lagravere MO, Major PW, Carey JP. Towards a viscoelastic model for the unfused midpalatal suture: Development and validation using the midsagittal suture in New Zealand White rabbits. *Journal of Biomechanics*. 2013a;46:1618-1625.
4. Romanyk DL, Collins CR, Lagravere MO, Toogood RW, Major PW, Carey JP. Role of the midpalatal suture in FEA simulations of maxillary expansion treatment for adolescents: A review. *International Orthodontics*. 2013b;11:119-138.
5. Ghoneima A, Abdel-Fattah E, Hartsfield J, El-Bedwehi A, Kamel A, Kula K. Effects of rapid maxillary expansion on the cranial and circummaxillary sutures. *American Journal of Orthodontics and Dentofacial Orthopedics*. 2011;140:510-519.

6. Leonardi R, Sicurezza E, Cutrera A, Barbato E. Early post-treatment changes of circumaxillary sutures in young patients treated with rapid maxillary expansion. *Angle Orthodontist*. 2011;81:36-41.
7. Tanaka E, Miyawaki Y, Tanaka M, Watanabe M, Lee K, del Pozo R, Tanne K. Effects of tensile forces on the expression of type III collagen in rat interparietal suture. *Archives of Oral Biology*. 2000;45:1049-1057.
8. Provatidis CG, Georgiopoulos B, Kotinas A, McDonald JP. On the FEM modeling of craniofacial changes during rapid maxillary expansion. *Medical Engineering and Physics*. 2007;29:566-579.
9. Liu SS, Opperman LA, Kyung HM, Buschang PH. Is there an optimal force level for sutural expansion? *American Journal Orthodontics and Dentofacial Orthopedics* 2011;139:446-455.
10. Romanyk DL, Liu SS, Long R, Carey JP. Considerations for determining relaxation constants from creep modeling. 14-page manuscript submitted to *International Journal of Mechanical Sciences* September 4, 2013.
11. Braun S, Bottrel JA, Lee KG, Lunazzi JJ, Legan HL. The biomechanics of rapid maxillary sutural expansion. *American Journal Orthodontics and Dentofacial Orthopedics*. 2000;118:257-261.
12. Lakes RS, Vanderby R. Interrelation of creep and relaxation: A modeling approach for ligaments. *Journal of Biomechanical Engineering*. 1999;121:612-615.
13. Oza A, Vandery R, Lakes RS. Interrelation of creep and relaxation for nonlinearly viscoelastic materials: Application to ligament and metal. *Rheologica Acta*. 2003;42:557-568.
14. Oza A, Vandery R, Lakes RS. Generalized solution for predicting relaxation from creep in soft tissue: Application to ligament. *International Journal of Mechanical Sciences*. 2006;48:662-673.
15. Genna F, Annovazzi L, Bonesi C, Fogazzi P, Paganelli C. On the experimental determination of some mechanical properties of porcine periodontal ligament. *Meccanica*. 2008;43:55-73.

16. Pirelli P, Ragazzoni E, Botti F, Arcuri C, Cocchia D. A comparative light microscopic study of human midpalatal suture and periodontal ligament. *Minerva Stomatologica*. 1997;46:429-433.
17. Persson M. The role of sutures in normal and abnormal craniofacial growth. *Acta Odontologica Scandinavica*. 1995;53:152-161.
18. Herring SW. Mechanical influences on suture development and patency. *Frontiers of Oral Biology*. 2008;12:41-56.
19. Wichelhaus A, Geserick M, Ball J. A new nickel titanium rapid maxillary expansion screw. *Journal of Clinical Orthodontics*. 2004;38:677-680.

8. Conclusions and Future Work

8.1. CONCLUSIONS

The research presented in this thesis was conducted in a logical manner as to properly study the midpalatal suture's viscoelastic behavior during ME treatment. A review of the literature surrounding current expansion appliances and ME simulation techniques has been provided in Chapter's 2 and 3, respectively. These reviews in turn dictated the necessity to model the suture's viscoelastic behavior to better understand patient response and improve upon existing appliances. Thus, the subsequent modeling work, Chapter's 4-6, focused on developing accurate creep-strain, stress-relaxation, and general strain viscoelastic models. Finally, these models were utilized in Chapter 7 to investigate current expansion appliances and their impact on the suture.

There are a number of significant contributions that have been made to the literature as a result of the thesis research. Firstly, reviewing the literature surrounding existing ME appliance designs and simulation techniques highlighted strengths and weaknesses of current practices. It was found that existing appliances could be grouped in four major categories based on their activation methods: screw, spring, magnet, and shape memory alloy. Synthesizing the types of mechanics used in practice, specifically their force-displacement behavior, guided the modeling work towards replicating their influence on the midpalatal suture. Current ME appliances either produce step-wise increases in displacement (screw), continuous decaying forces (spring, magnet), or nearly constant forces (spring, shape memory alloys). Notwithstanding its popularity amongst clinicians due to its simplicity, screw activated appliances were noted as having the most significant disadvantages resulting from their mechanics and requirement of patient activation.

The second portion of the literature review discussed the state of ME treatment simulation and midpalatal suture modeling. To date, little work has been conducted towards viscoelastic modeling of the midpalatal suture. In addition, FEA simulations have either neglected the suture or have assumed linear

elastic properties for bone or related soft tissue (e.g. PDL). In order to make observations regarding response of the suture or local surrounding bone, especially for transient response or in cases of rapidly applied loads, the sutures' viscoelastic behavior should be incorporated. In light of the variation in ME treatment appliances and protocols, along with the lack of advanced models and simulations, it became apparent that further investigation was required.

In order to improve upon the predictive literature surrounding ME, a creep model was developed that could predict New Zealand white rabbit midsagittal suture response to ME level forces. As a range of loads may be applied in ME treatment, it was necessary that the selected model be able to replicate creep strain accurately over several load sets using a single set of experimentally determined constants. In testing a total of seven models it was found that nonlinear approaches with experimentally determined stress exponents were able to meet these requirements. In light of this, it can be said that suture tissue behaves in a nonlinear fashion. Additionally, since both separable and inseparable creep functions were successful in representing experimental data, this indicates that inseparability of the creep function is not necessary in predicting suture creep.

In transforming creep models into their subsequent relaxation form, and altering the creep formulation to predict strain resulting from a decaying force, simulation of existing ME appliances was possible. Simulation of screw activated appliances illustrated that it is unlikely a single activation would generate tissue failure; however, as few as 2-3 rapid activations could generate stresses in a potential failure range. When considering suture response to constant force and decaying springs, results showed that suture expansion was strongly dependent on force decay. Even in light of this fact, it was found that the type of decay (e.g. linear, inverse, or exponential) had little influence on the strain. That is, all three tested decay functions predicted very similar results.

As a result of the research presented in this thesis, it can be suggested that expansion using a constant force spring would be the ideal method for ME treatment. It could provide timely expansion in the active phase of treatment while maintaining low levels of force. Additionally, by subjecting the suture to a

constant traction, conditions favorable for bone generation are facilitated. Such conditions can decrease the retention phase, and as a result the overall time required for treatment. Work remains in the investigation of anchoring a low-force appliance such that it would not generate tooth movement; however, it is apparent that low force expansion is ideal when considering suture response.

8.2. FUTURE WORK

While the research conducted in this thesis has significantly contributed to the literature surrounding ME treatment, as previously mentioned there are indeed limitations to this work. The method of obtaining force-displacement data for the suture could be improved upon. Data was collected through using constant force expansion springs attached to the rabbit skull using mini-screw implants approximately 4mm on either side of the suture. Ideally, experimental data would strictly isolate for the suture and the cross-sectional dimensions would be accurately measured. This would then allow for a more precise calculation of stress and strain, as opposed to an approximation. In the future it would be ideal to conduct more precise experiments leading to more confidence in the determined constants, and hence subsequent predictions. Additionally, collection of subsequent relaxation data would aid in the investigation of combined creep and relaxation behavior as well as their theoretical interrelation.

Beyond the improvement of experimental data for model refinement, there are a number of projects that could serve as logical extensions to this work. Firstly, the implementation of these viscoelastic models in FEA simulations are of great interest. Such research will allow for investigation of suture expansion over time, the impact of loading rate and magnitude on suture stresses and strains, and the overall load-bearing contribution of the suture during ME treatment. As discussed in the literature review of this thesis, current FEA studies do not incorporate the suture's viscoelastic nature, and thus are incapable of accurate transient simulations. Incorporating viscoelastic suture properties into full-skull FEA simulations can provide significant contributions towards studying the impact of ME treatment protocols on patient response.

A second future study that would significantly advance the orthodontic literature includes a histological investigation relating suture stresses and strains to tissue remodeling. It has been noted by various authors in the literature that an optimal load exists in terms of generating bone during ME treatment; however, this range has not been clearly identified. By combining *in-vivo* experiments, likely animal-based, with the analytical models developed here, it is suggested that a correlation between suture stress and bone formation could be developed. In doing so, this work would elucidate debate regarding the range of forces that facilitate the largest amount of bone formation, and hence reducing the amount of retention phase required during treatment.

Finally, research into the failure criteria of suture tissue is necessary for a thorough understanding of ME treatment. By conducting experiments to investigate this failure range, which has yet to be clearly defined, it will allow for more definitive conclusions to be made regarding the impact of a given appliance or protocol on patient response. This would include investigating a variety of loading rates as well as quasi-static testing to determine stress and strain regimes resulting in tissue disruption or tearing. The viscoelastic models developed here may then be used in conjunction with this knowledge to better understand which appliance(s) can achieve optimal physiologic expansion.

Complete List of References

Anderssen RS, Davies AR, de Hoog FR. On the sensitivity of interconversion between relaxation and creep. *Rheologica Acta*. 2008;47:159-167.

Angell EH. Treatment of irregularity of the permanent or adult teeth. Part 1. *Dental Cosmos*. 1860;1:540-544.

Angell EH. Treatment of irregularity of the permanent or adult teeth. Part 2. *Dental Cosmos*. 1860;1:599-560.

Bell RA. A review of maxillary expansion in relation to rate of expansion and patient's age. *American Journal of Orthodontics*. 1982;81:32-37.

Biederman W. A hygienic appliance for rapid expansion. *Journal of Practical Orthodontics*. 1968;2:67-70.

Braun S, Bottrel JA, Lee KG, Lunazzi JJ, Legan HL. The biomechanics of rapid maxillary sutural expansion. *American Journal of Orthodontics and Dentofacial Orthopedics*. 2000;118:257-261.

Burrows AM, Richtsmeier JT, Mooney MP, Smith TD, Losken HW, Siegel MI. Three-dimensional analysis of craniofacial form in a familial rabbit model of nonsyndromic coronal suture synostosis using Euclidean distance matrix analysis. *Cleft Palate-Craniofacial Journal*. 1999;36:196-206.

Callister WD. Mechanical properties of metals. In: *Materials Science and Engineering: an introduction*. 6th ed. Hoboken, NJ: John Wiley & Sons Inc.; 2003. p. 121-123.

Coleman TF, Li Y. On the convergence of interior-reflective Newton methods for nonlinear minimization subject to bounds. *Mathematical Programming*. 1994;67:189-224.

Coleman TF, Li Y. A reflective Newton method for minimizing a quadratic function subject to bounds on some of the variables. *SIAM Journal on Optimization*. 1996;6:1040-1058.

Corbett MC. Slow and continuous maxillary expansion, molar rotation, and molar distalization. *Journal of Clinical Orthodontics*. 1997;31:253-263.

Culea L, Bratu C. Stress analysis of the human skull due to the insertion of rapid palatal expander with finite element analysis (FEA). *Key Engineering Materials*. 2009;399:211-218.

Darendeliler MA, Strahm C, Joho JP. Light maxillary expansion forces with the magnetic expansion device. A preliminary investigation. *European Journal of Orthodontics*. 1994;16:479-490.

Darendeliler MA, Lorenzon C. Maxillary expander using light, continuous force and autoblocking. *Journal of Clinical Orthodontics*. 1996;30:212-216.

Defraia E, Marinelli A, Baroni G, Tollaro I. Dentoskeletal effects of a removable appliance for expansion of the maxillary arch: a postero-anterior cephalometric study. *European Journal of Orthodontics*. 2008;30: 57-60.

Delgadillo R, Bahia HU, Lakes R. A nonlinear constitutive relationship for asphalt binders. *Materials and Structures*. 2012;45:457-473.

Derombise G, Chailleux E, Forest B, Riou L, Lacotte N, Vouyovitch Van Schoors L, Davies P. Long-term mechanical behavior of Aramid fibers in seawater. *Polymer Engineering and Science*. 2011;51:1366-1375.

Dortmans LJMG, van de Ven AAF, Sauren AAHJ. A note on the reduced creep function corresponding to the quasi-linear visco-elastic model proposed by Fung. *Journal of Biomechanical Engineering*. 1994;116:373-375.

Fang Y, Lagravere MO, Carey JPR, Major PW, Toogood RR. Maxillary expansion treatment using bone anchors: development and validation of a 3D finite element model. *Computation Methods in Biomechanics and Biomedical Engineering*. 2007;10:137-149.

Fill TS, Carey JP, Toogood RW, Major PW. Experimentally determined mechanical properties of, and models for, the periodontal ligament: critical review of current literature. *Journal of Dental Biomechanics*. 2011;2011: 312980.

Findley WN, Lai JS, Onaran K. Chapter 5: Linear Viscoelastic Constitutive Equations. In: *Creep and Relaxation of Nonlinear Viscoelastic Materials*. New York, NY: North-Holland Publishing Company; 1976 p. 52-69.

Findley WN, Lai JS, Onaran K. Chapter 7: Multiple Integral Representation. In: *Creep and Relaxation of Nonlinear Viscoelastic Materials*. New York, NY: North-Holland Publishing Company; 1976 p. 172-175.

Findley WN, Lai JS, Onaran K. Chapter 9: Nonlinear Creep (or Relaxation) Under Variable Stress (or Strain). In: *Creep and Relaxation of Nonlinear Viscoelastic Materials*. New York, NY: North-Holland Publishing Company. 1976 p. 229-233.

Fok J, Toogood RW, Badawi H, Carey JP, Major PW. Analysis of maxillary arch force/couple systems for a simulated high canine malocclusion: Part 1. Passive ligation. *Angle Orthodontist*. 2011;81:953-959.

Fung YC. Chapter 2: The meaning of the constitutive equation. In: *Biomechanics: mechanical properties of living tissues*. 2nd ed. New York NY: Springer Science+Business Media Inc.; 1993. p. 43-46.

Fung YC. Chapter 7: Bioviscoelastic Solids. In: *Biomechanics: Mechanical Properties of Living Tissues*. 2nd ed. New York, NY: Springer-Verlag; 1993 p. 277-287.

Fung YC. Chapter 12: Bone and cartilage. In: *Biomechanics: Mechanical properties of living tissues*. 2nd ed. New York, NY: Springer-Verlag; 1993.p. 510-513.

Gautam P, Valiathan A, Adhikari R. Stress and displacement patterns in the craniofacial skeleton with rapid maxillary expansion: a finite element method study. *American Journal of Orthodontics and Dentofacial Orthopedics*. 2007;132:5 e1-11.

Genna F, Annovazzi L, Bonesi C, Fogazzi P, Paganelli C. On the experimental determination of some mechanical properties of porcine periodontal ligament. *Meccanica*. 2008;43:55-73.

Ghoneima A, Abdel-Fattah E, Hartsfield J, El-Bedwehi A, Kamel A, Kula K. Effects of rapid maxillary expansion on the cranial and circummaxillary sutures. *American Journal of Orthodontics and Dentofacial Orthopedics*. 2011;140:510-519.

Green AE, Rivlin RS. The mechanics of non-linear materials with memory: Part 1. Archives of Rational Mechanics and Analysis 1957;1:1-21.

Haas AJ. Rapid expansion of the maxillary dental arch and nasal cavity by opening the midpalatal suture. Angle Orthodontist. 1961;31:73-90.

Herring SW. Mechanical influences on suture development and patency. Frontiers of Oral Biology. 2008;12:41-56.

Hibbeler RC. Strain transformation. In: Mechanics of materials. SI Edition. Singapore: Prentice Hall Inc.; 2004. p. 512-515.

Holberg C. Effects of rapid maxillary expansion on the cranial base--an FEM-analysis. Journal of Orofacial Orthopedics. 2005;66:54-66.

Holberg C, Rudzki-Janson I. Stresses at the cranial base induced by rapid maxillary expansion. Angle Orthodontist. 2006;76:543-550.

Holberg C, Holberg N, Schwenzer K, Wichelhaus A, Rudzki-Janson I. Biomechanical analysis of maxillary expansion in CLP patients. Angle Orthodontist. 2007;77:280-287.

Isaacson RJ, Wood JL, Ingram AH. Forces produced by rapid maxillary expansion: Part 1. Design of the force measuring system. Angle Orthodontist. 1964;34:256-260.

Isaacson RJ, Ingram AH. Forces produced by rapid maxillary expansion: Part 2. Forces present during treatment. Angle Orthodontist. 1964;34:261-270.

Iseri H, Tekkaya AE, Oztan O, Bilgic S. Biomechanical effects of rapid maxillary expansion on the craniofacial skeleton, studied by the finite element method. *European Journal of Orthodontics*. 1998;20:347-356.

Jafari A, Shetty KS, Kumar M. Study of stress distribution and displacement of various craniofacial structures following application of transverse orthopedic forces--a three-dimensional FEM study. *Angle Orthodontist*. 2003;73:12-20.

Jayade V, Annigeri S, Jayade C, Thawani P. Biomechanics of torque from twisted rectangular archwires: A finite element investigation. *Angle Orthodontist*. 2007;77:214-220.

Johnson TP, Socrate S, Boyce MC. A viscoelastic, viscoplastic model of cortical bone valid at low and high strain rates. *Acta Biomaterialia*. 2010;6:4073-4080.

Jutte CV, Kota S. Design of nonlinear springs for prescribed load-displacement functions. *Journal of Mechanical Design*. 2008; 130: 081403-1-081403-10.

Kilic N, Oktay H. Effects of rapid maxillary expansion on nasal breathing and some naso-respiratory and breathing problems in growing children: A literature review. *International Journal of Pediatric Otorhinolaryngology*. 2008;72:1595-1601.

Knaup B, Yildizhan F, Wehrbein H. Age-related changes in the midpalatal suture. A histomorphometric study. *Journal of Orofacial Orthopedics*. 2004;65:467-474.

Komatsu K, Sanctuary C, Shibata T, Shimada A, Botsis J. Stress-relaxation and microscopic dynamics of rabbit periodontal ligament. *Journal of Biomechanics*. 2007;40:634-644.

Koudstaal MJ, van der Wal KG, Wolvius EB, Schulten AJ. The Rotterdam Palatal Distractor: introduction of the new bone-borne device and report of the pilot study. *International Journal of Oral and Maxillofacial Surgery*. 2006;35:31-45.

Kreyszig E. Appendix 3: Auxiliary Material. In: *Advanced Engineering Mathematics*. 8th ed. New York NY: John Wiley & Sons Inc.; 1999. p. A51-57.

Lagravere MO, Major PW, Flores-Mir C, Orth C. Long-term dental arch changes after rapid maxillary expansion treatment: a systematic review. *Angle Orthodontist*. 2005;75:155-161.

Lagravere MO, Carey JP, Heo G, Toogood RW, Major PW. Transverse, vertical, and anteroposterior changes from bone-anchored maxillary expansion vs traditional rapid maxillary expansion: A randomized clinical trial. *American Journal of Orthodontics and Dentofacial Orthopedics*. 2010;137:304.e1-304.e12.

Lakes RS, Vanderby R. Interrelation of creep and relaxation: A modeling approach for ligaments, *Journal of Biomechanical Engineering*. 1999;121:612-615.

Lee H, Ting K, Nelson M, Sun N, Sung SJ. Maxillary expansion in customized finite element method models. *American Journal of Orthodontics and Dentofacial Orthopedics*. 2009;136:367-374.

Leonardi R, Sicurezza E, Cutrera A, Barbato E. Early post-treatment changes of circumaxillary sutures in young patients treated with rapid maxillary expansion. *Angle Orthodontist*. 2011;81:36-41.

Liu SS, Opperman LA, Kyung H, Buschang PH. Is there an optimal force level for sutural expansion? *American Journal of Orthodontics and Dentofacial Orthopedics*. 2011;139:446-455.

Lu YT, Zhu HX, Richmond S, Middleton J. A visco-hyperelastic model for skeletal muscle tissue under high strain rates. *Journal of Biomechanics*. 2010;43:2629-2632.

Manhartsberger C, Seidenbusch W, Force delivery of Ni-Ti coil springs. *American Journal of Dentofacial Orthopedics*. 1996;109:8-21.

Mommaerts MY. Transpalatal distraction as a method of maxillary expansion. *British Journal of Oral and Maxillofacial Surgery*. 1999; 37:268-272.

Norton RL. Load determination. In: *Machine design: an integrated approach*. 3rd ed. Upper Saddle River, NJ: Pearson Prentice Hall; 2006. p. 73-126.

Norton RL. Appendix C: Material Properties. In: *Machine Design: an integrated approach*. 3rd ed. Upper Saddle River, NJ: Pearson Prentice Hall; 2006. p. 943-950.

Oza A, Vanderby Jr R, Lakes RS. Interrelation of creep and relaxation for nonlinearly viscoelastic materials: Application to ligament and metal. *Rheologica Acta*. 2003;42:557-568.

Oza A, Vanderby Jr R, Lakes RS. Generalized solution for predicting relaxation from creep in soft tissue: Application to ligament. *International Journal of Mechanical Sciences*. 2006;48:662-673.

Persson M. The role of sutures in normal and abnormal craniofacial growth. *Acta Odontologica Scandinavica*. 1995;53:152-161.

Pirelli P, Ragazzoni E, Botti F, Arcuri C, Cocchia D. A comparative light microscopic study of human midpalatal suture and periodontal ligament, *Minerva Stomatologica*. 1997;46:429-433.

Popov EP, Balan TA. Chapter 2: Strain. In: *Engineering Mechanics of Solids*. 2nd ed. Upper Saddle River NJ: Prentice-Hall Inc.; 1998. p. 60-68.

Popov EP, Balan TA. Beam statics. In: *Engineering mechanics of solids*. 2nd ed. Upper Saddle River, NJ: Prentice Hall; 1998. p. 267-313.

Popov EP, Balan TA. Symmetric beam bending. In: *Engineering Mechanics of Solids*. 2nd ed. Upper Saddle River, NJ: Prentice Hall; 1998. p. 325-367.

Popowics TE, Herring SW. Load transmission in the nasofrontal suture of the pig, *Sus scrofa*. *Journal of Biomechanics*. 2007;40:837-844.

Provatidis C, Georgiopoulos B, Kotinas A, McDonald JP. In-vitro validation of a FEM model for craniofacial effects during rapid maxillary expansion *Proceedings of the IASTED International Conference on Biomechanics; 2003 June 30-July 2; Rhodes, Greece: Acta Press; 2003: p. 68-73.*

Provatidis C, Georgiopoulos B, Kotinas A, MacDonald JP. In vitro validated finite element method model for a human skull and related craniofacial effects during rapid maxillary expansion. *Proceedings of the Institution of Mechanical Engineers. Part H: Journal of Engineering in Medicine*. 2006;220:897-907.

Provatidis C, Georgiopoulos B, Kotinas A, McDonald JP. On the FEM modeling of craniofacial changes during rapid maxillary expansion. *Medical Engineering and Physics*. 2007;29:566-579.

Provatidis CG, Georgiopoulos B, Kotinas A, McDonald JP. Evaluation of craniofacial effects during rapid maxillary expansion through combined in vivo/in vitro and finite element studies. *European Journal of Orthodontics*. 2008;30:437-448.

Provenzano PP, Lakes RS, Corr DT, Vanderby Jr R. Application of nonlinear viscoelastic models to describe ligament behavior. *Biomechanics and Modeling in Mechanobiology*. 2002;1:45-57.

Radhakrishnan P, Mao JJ. Nanomechanical properties of facial sutures and sutural mineralization front. *Journal of Dental Research*. 2004;83:470-475.

Reed-Hill RE, Abbaschian R. Chapter 17: Deformation twinning and martensite reactions. In: *Physical metallurgy principles*. 3rd ed. Boston, MA: PWS Publishing Company; 1994. p. 584-585.

Romanyk DL, Lagravère MO, Toogood RW, Major PW, Carey JP. Review of maxillary expansion appliance activation methods: engineering and clinical perspectives. *Journal of Dental Biomechanics*. 2010;2010:496906.

Romanyk DL, Liu SS, Lipsett MG, Toogood RW, Lagravere MO, Major PW, Carey JP. Towards a viscoelastic model for the unfused midpalatal suture: Development and validation using the midsagittal suture in New Zealand white rabbits. *Journal of Biomechanics*. 2013;46:1618-1625.

Romanyk DL, Melenka GW, Carey JP. Modeling stress-relaxation behavior of the periodontal ligament during the initial phase of orthodontic treatment. *Journal of Biomechanical Engineering*. 2013;135:0910071-8.

Romanyk DL, Liu SS, Long R, Carey JP. Considerations for determining relaxation constants from creep modeling. 14-page manuscript submitted to International Journal of Mechanical Sciences September 4, 2013.

Sander C, Huffmeier S, Sander FM, Sander FG. Initial results regarding force exertion during rapid maxillary expansion in children. Journal of Orofacial Orthopedics. 2006;67:19-26

Schapery RA. An engineering theory of nonlinear viscoelasticity with applications. International Journal of Solids and Structures. 1966;2:407-425.

Shahar R, Zaslansky P, Barak M, Friesem AA, Currey JD, Weiner S. Anisotropic Poisson's ratio and compression modulus of cortical bone determined by speckle interferometry. Journal of Biomechanics. 2007;40:252-264.

Sia S, Koga Y, Yoshida N. Determining the center of resistance of maxillary anterior teeth subjected to retraction forces in sliding mechanics: An in vivo study. Angle Orthodontist. 2007;77:999-1003.

Storey E. Tissue response to the movement of bones. American Journal of Orthodontics. 1973;64:229-247.

Tanaka E, Miyawaki Y, Tanaka M, Watanabe M, Lee K, de Pozo R, Tanne K. Effects of tensile forces on the expression of type III collagen in rat interparietal suture. Archives of Oral Biology. 2000;45:1049-1057.

Tanaka E, Miyawaki Y, de Pozo R, Tanne K. Changes in the biomechanical properties of the rat interparietal suture incident to continuous tensile force application. Archives of Oral Biology. 2000;45:1059-1064.

Thornton GM, Oliynyk A, Frank CB, Shrive NG. Ligament creep cannot be predicted from stress relaxation at low stress: A biomechanical study of the rabbit medial collateral ligament. *Journal of Orthopaedic Research*. 1997;15:652-656.

Trindade IEK, Castilho RL, Sampaio-Teixeira ACM, Trindade-Suedam IK, Silva-Filho OG. Effects of orthopedic rapid maxillary expansion on internal nasal dimensions in children with cleft lip and palate assessed by acoustic rhinometry. *Journal of Craniofacial Surgery*. 2010;21:306-311.

Verrue V, Dermaut L, Verheghe B. Three-dimensional finite element modelling of a dog skull for the simulation of initial orthopaedic displacements. *European Journal of Orthodontics*. 2001;23:517-527.

Viazis AD, Vadiakis G, Zelos L, Gallagher RW. Designs and applications of palatal expansion appliances. *Journal of Clinical Orthodontics*. 1992;26: 239-243.

von Fraunhofer JA, Bonds PW, Johnson BE. Force generation by orthodontic coil springs. *Angle Orthodontist*. 1993;63:145-148.

Ward IM, Onat ET. Non-linear mechanical behavior of oriented polypropylene. *Journal of Mechanics and Physics of Solids*. 196:11;217-229.

Wichelhaus A, Geserick M, Ball J. A new nickel titanium rapid maxillary expansion screw. *Journal of Clinical Orthodontics*. 2004;38:677-680.

Wysocki M, Kobus K, Szotek S, Kobielarz M, Kuropka P, Będziński R. Biomechanical effect of rapid mucoperiosteal palatal tissue expansion with the use of osmotic expanders. *Journal of Biomechanics*. 2011;44:1313-1320.

Xia Z, Chen J. Biomechanical validation of an artificial tooth-periodontal ligament-bone complex for in vitro orthodontic load measurement. *Angle Orthodontist*. 2013;83:410-417.

Yang CJ, Pan XG, Qian YF, Wang GM. Impact of rapid maxillary expansion in unilateral cleft lip and palate patients after secondary alveolar bone grafting: Review and case report. *Oral Surgery, Oral Medicine, Oral Pathology and Oral Radiology*. 2012;114:e428-430.

Yoo L, Kim H, Shin A, Gupta V, Demer JL. Creep behavior of passive bovine extraocular muscle. *Journal of Biomedicine and Biotechnology*. 2011;2011:526705.

Young HD, Freedman RA. Chapter 21: Electric charge and electric field. *University Physics 11th ed*. San Fransisco CA: Pearson Education Inc.; 2004. p. 801.

Zahrowski JJ, Turley PK. Force magnitude effects upon osteoprogenitor cells during premaxillary expansion in rats. *Angle Orthodontist*. 1992;62:197-202.

Zimring JF, Isaacson RJ. Forces produced by rapid maxillary expansion. Part 3. Forces present during retention. *Angle Orthodontist*. 1965;35:178-186.